



The  
University  
Of  
Sheffield.

# **Multiple Parallel Concatenated Gallager Codes and Their Applications**

By

Ahmed Obaid Aftan

Thesis submitted for the Degree of Doctor of Philosophy

Department of Electronic & Electrical Engineering

The University of Sheffield

June 2018

## **Acknowledgement**

I would like to express my sincere gratitude to my supervisor, Dr. Mohammed Benaissa, for his highly guidance and continuous encourage were very helpful to the success of my research. I also wish to thank my second supervisor Dr. Wei Liu.

I appreciate the kind efforts and excellent guidance from Professor Hatim M. Behairy and his unconditional support has contributed extremely to the progress of my work on the research.

I am grateful to all colleagues and staffs in communications research group for their help and support. Special thanks are due to my friends Dr, Abdelrahman Arbi, Ibrahim Ali Kh. Shati and Di Fan for their friendly support.

I would like to thank my lovely wife and my wonderful sons who have been with my at each step, bringing so much help, joy and happiness into my life.

I give my final words of gratitude to my mother, brothers and sisters for being as they are. Thank you so much.

I am very thankful to Mrs. Hilary J Levesley for her quick response for all the queries and friendly support during every phase of my research work at the University of Sheffield.

This thesis is dedicated to the soul of my beloved father Obaid may Allah have a mercy on him.

## **Abstract**

Due to the increasing demand of high data rate of modern wireless communications, there is a significant interest in error control coding. It now plays a significant role in digital communication systems in order to overcome the weaknesses in communication channels. This thesis presents a comprehensive investigation of a class of error control codes known as Multiple Parallel Concatenated Gallager Codes (MPCGCs) obtained by the parallel concatenation of well designed LDPC codes. MPCGCs are constructed by breaking a long and high complexity of conventional single LDPC code into three or four smaller and lower complexity LDPC codes. This design of MPCGCs is simplified as the option of selecting the component codes completely at random based on a single parameter of Mean Column Weight (MCW).

MPCGCs offer flexibility and scope for improving coding performance in theoretical and practical implementation. The performance of MPCGCs is explored by evaluating these codes for both AWGN and flat Rayleigh fading channels and investigating the puncturing of these codes by a proposed novel and efficient puncturing methods for improving the coding performance.

Another investigating in the deployment of MPCGCs by enhancing the performance of WiMAX system. The bit error performances are compared and the results confirm that the proposed MPCGCs-WiMAX based IEEE 802.16 standard physical layer system provides better gain compared to the single conventional LDPC-WiMAX system.

The incorporation of Quasi Cyclic QC-LDPC codes in the MPCGC structure (called QC-MPCGC) is shown to improve the overall BER performance of MPCGCs with reduced overall decoding complexity and improved flexibility by using Layered belief propagation decoding instead of the sum product algorithm (SPA).

A proposed MIMO-MPCGC structure with both a 2X2 MIMO and 2X4 MIMO configurations is developed in this thesis and shown to improve the BER performance over fading channels over the conventional LDPC structure.

# Table of Contents

1.1 ACKNOWLEDGEMENT .....	II
1.1 ABSTRACT .....	III
<b>CHAPTER 1: INTRODUCTION .....</b>	<b>1</b>
1.1 OVERVIEW.....	2
1.2 RESEARCH AIM .....	2
1.3 MOTIVATION .....	2
1.4 OBJECTIVES.....	3
1.5 ORIGINAL CONTRIBUTIONS .....	4
1.6 THESIS OUTLINE .....	5
1.7 PUBLISHED PAPERS.....	8
<b>CHAPTER 2: BACKGROUND AND LITERATURE REVIEW.....</b>	<b>9</b>
2.1 INTRODUCTION.....	9
2.2 CHANNEL CODING .....	10
2.2.1 <i>General coding communication overview</i> .....	10
2.3 CHANNEL CAPACITY FOR COMMUNICATION SYSTEM.....	10
2.4 FUNDAMENTAL OF LDPC CODES .....	13
2.5 REPRESENTATIONS OF LDPC CODES .....	14
2.5.1 <i>Matrix Representation</i> .....	14
2.5.2 Graphical representation.....	15
2.6 LDPC CODE CONSTRUCTION .....	16
2.6.1 Gallager codes .....	16
2.6.2 Mackay codes .....	17
2.6.3 Quasi-cyclic LDPC (QC-LDPC) codes.....	17
2.7 ENCODING OF LDPC .....	18
2.8 LDPC DECODING ALGORITHMS.....	18
2.8.1 Iterative Message-Passing Algorithms .....	18
2.9 SOFT AND HARD DECODING.....	19
2.10 EXIT CHARTS AND DENSITY EVOLUTION .....	21
2.11 WORLDWIDE INTEROPERABILITY FOR MICROWAVE ACCESS WiMAX-IEEE802.16	21
2.12 QUADRATIC AMPLITUDE MODULATION (QAM).....	22
2.13 MULTIPLE INPUT MULTIPLE OUTPUT (MIMO) .....	23
2.14 HISTORY OF THE PARALLEL CONCATENATION GALLAGER CODES (PCGC).....	24

<b>CHAPTER 3: CONSTRUCTION OF MODIFIED STRUCTURED OF MULTIPLE PARALLEL CONCATENATED GALLAGER CODES (MPCGC).....</b>	<b>28</b>
3.1 INTRODUCTION.....	28
3.2 ENCODING OF MPCGC .....	29
3.3 PROPOSED SYSTEM MODEL OF MPCGC ENCODER .....	31
3.4 PROPOSED MPCGC SERIAL DECODER .....	33
3.5 PROPOSED MPCGC PARALLEL DECODER .....	35
3.6 THE SUM PRODUCT ALGORITHM (SPA).....	37
3.7 ITERATIVE DECODING OF MPCGC .....	39
3.8 MCW COMBINATION AND CODE DESIGN.....	45
3.9 SIMULATION AND ANALYSIS.....	49
3.9.1 BER performance analysis .....	49
3.9.2 MPCGC complexity analysis .....	55
3.10 SUMMARY .....	59
<b>CHAPTER 4: EFFICIENT PUNCTURING METHOD FOR MULTIPLE PARALLEL CONCATENATED GALLAGER CODES .....</b>	<b>60</b>
4.1 INTRODUCTION.....	60
4.2 PUNCTURED MPCGC CODES.....	61
4.3 MPCGC PARALLEL ENCODER .....	65
4.4 PUNCTURED MPCGC PARALLEL DECODER .....	66
4.5 SIMULATION RESULTS AND DISCUSSION .....	67
4.5.1 BER performance analysis .....	67
4.5.2 MPCGC complexity analysis .....	73
4.6 SUMMARY .....	75
<b>CHAPTER 5: PERFORMANCE ANALYSIS OF MULTIPLE PARALLEL CONCATENATED GALLAGER CODES FOR WiMAX APPLICATIONS .....</b>	<b>76</b>
5.1 INTRODUCTION.....	76
5.2 WiMAX SCENARIO.....	77
5.3 WiMAX PHYSICAL LAYER MODEL.....	78
5.4 THE ASSUMPTIONS.....	81
5.4.1 MPCGC Encoder/Decoder .....	81
5.4.2 Interleaving.....	81
5.4.3 BPSK modulator.....	82
5.4.4 Serial to parallel transformation .....	82

5.4.5 Inverse Fast Fourier Transform (IFFT) .....	82
5.4.6 Additive white Gaussian noise (AWGN) .....	83
5.5 SIMULATION RESULTS AND DISCUSSION .....	84
5.5.1 Girth removable analysis .....	84
5.5.2 BER performance analysis .....	86
5.6 SUMMARY .....	91
<b>CHAPTER 6: PERFORMANCES ANALYSIS OF MPCGC WITH QC-LDPC CODES AND MIMO APPLICATION.....</b>	<b>92</b>
6.1 INTRODUCTION.....	92
6.2 PROPOSED QC-MPCGC SYSTEM MODEL .....	93
6.2.1 QC-LDPC Encoder.....	94
6.3 LAYERED DECODING.....	95
6.4 MULTIPLE INPUT MULTIPLE OUTPUT (MIMO) .....	96
6.5 PROPOSED MIMO-MPCGC SYSTEM MODEL .....	98
6.5.1 The Channel of the proposed MIMO-MPCGC .....	99
6.5.2 The Channel equalizer of the proposed MIMO-MPCGC .....	100
6.6 SIMULATION RESULTS AND DISCUSSION .....	100
6.6.1 BER performance analysis .....	102
6.6.2 QC-MPCGC complexity analysis .....	105
6.7 SUMMARY .....	109
<b>CHAPTER 7: CONCLUSION AND FUTURE WORK .....</b>	<b>110</b>
7.1 CONCLUSION .....	110
7.2 FUTURE WORK.....	112
APPENDIX A.....	114
REFERENCES .....	115

## List of Figures

Figure 2.1 Digital communication system .....	11
Figure 2.2 Channel capacity of AWGN channel [8] .....	13
Figure 2.3 Tanner graph of the parity check matrix H .....	15
Figure 2.4 WiMAX equipment .....	22
Figure 2.5 MIMO channel for M transmitter antennas and N receiver antennas .....	24
Figure 3.1 Block diagram of MPCGC Encoder of M LDPC component .....	33
Figure 3.2 Serial decoding mode .....	34
Figure 3.3 Block diagram of MPCGC serial decoder .....	35
Figure 3.4 Block diagram of MPCGC decoder .....	36
Figure 3.5 MPCGC decoding flow chart .....	43
Figure 3.6 Flow chart of BER calculation according to the Monte Carlo method .....	44
Figure 3.7 Decoding algorithm of two component decoders for MPCGC .....	45
Figure 3.8 Design effect of MCW on the extrinsic information quality at $E_b/N_0=0$ dB .....	47
Figure 3.9 Design effect of MCW on the extrinsic information quality at $E_b/N_0=0.5$ dB .....	48
Figure 3.10 Design effect of MCW on the extrinsic information quality at $E_b/N_0=1.3$ dB .....	48
Figure 3.11 Design of four components decoder .....	49
Figure 3.12 BER comparison for different LDPC coding model over AWGN channel .....	50
Figure 3.13 Effect of MCW on the different LDPC coding model over AWGN channel .....	51
Figure 3.14 Design of three component decoder .....	51
Figure 3.15 BER comparison for different LDPC coding model over AWGN channel .....	52
Figure 3.16 BER comparison for different parallel concatenation LDPC coding model over AWGN channel .....	53
Figure 3.17 BER comparison for different LDPC coding model over AWGN channel .....	54
Figure 3.18 Capacity achieved for different coding model over AWGN channel .....	54
Figure 3.19 Capacity achieved for different coding model over AWGN channel .....	55
Figure 3.20 Complexity and performance comparison between LDPC and MPCGC .....	56
Figure 3.21 Complexity and performance comparison between LDPC and MPCGC .....	57
Figure 3.22 Complexity and performance comparison between different components of MPCGC .....	58
Figure 3.23 Complexity and performance comparison between different components of MPCGC .....	58
Figure 4.1 Block diagram of the proposed efficient punctured MPCGC system .....	64

Figure 4.2 Methods of MPCGC puncturing after MPCGC encoder .....	64
Figure 4.3 Block diagram of MPCGC encoder .....	66
Figure 4.4 BER comparison for different LDPC coding model over AWGN channel .....	68
Figure 4.5 BER comparison of MPCGC with LDPC over flat fading Rayleigh channel .....	68
Figure 4.6 PER comparison of MPCGC with LDPC over flat fading Rayleigh channel .....	69
Figure 4.7 BER performance of different punctured MPCGC over AWGN channel .....	70
Figure 4.8 PER performance of different punctured MPCGC over AWGN channel .....	71
Figure 4.9 BER comparison of punctured MPCGC with LDPC over flat Rayleigh fading channel .....	71
Figure 4.10 PER comparison of punctured MPCGC with LDPC over flat Rayleigh fading channel .....	72
Figure 4.11 Complexity and performance comparison between punctured MPCGCs and conventional MPCGC .....	73
Figure 4.12 Complexity and performance comparison between punctured MPCGCs and conventional MPCGC .....	74
Figure 5.1 WiMAX system .....	78
Figure 5.2 Block diagram of WiMAX-OFDM physical layer model .....	80
Figure 5.3 Structure of the parity check matrix of WiMAX IEEE 802.16 standard with $\frac{1}{2}$ code rate and 768 code length .....	80
Figure 5.4 Entries of standard LDPC-WiMAX parity check matrix with girth 4 .....	84
Figure 5.5 Entries of standard LDPC-WiMAX parity check matrix with free girth 4 .....	85
Figure 5.6 Entries of MPCGC-WiMAX parity check matrix with girth .....	85
Figure 5.7 Entries of MPCGC-WiMAX parity check matrix with free girth 4 .....	86
Figure 5.8 BER comparison for different LDPC coding model .....	88
Figure 5.9 BER comparison of WiMAX physical layer model .....	88
Figure 5.10 PER comparison for MPCGC-WiMAX system and single LDPC-OFDM .....	89
Figure 5.11 BER comparison of WiMAX physical layer model over AWGN channel .....	90
Figure 5.12 BER comparison of WiMAX physical layer model over flat fading channel .....	90

---

Figure 6.1 QC-MPCGC System Model .....	93
Figure 6.2 Layered schedule between check and variable nodes of the example graph .....	96
Figure 6.3 MIMO Channel .....	97
Figure 6.4 MIMO-MPCGC system model .....	98
Figure 6.5 Equalizer model .....	100
Figure 6.6 BER comparison of QC-MPCGC and different coding model over AWGN channel .....	103
Figure 6.7 BER comparison of Layered QC-MPCGC and different coding model over AWGN channel .....	103
Figure 6.8 BER comparison of 2X2 MIMO-LDPC over fading channel .....	104
Figure 6.9 BER comparison of 2X4 MIMO-LDPC over fading channel .....	104
Figure 6.10 BER comparison of MIMO-LDPC over fading channel .....	105
Figure 6.11 Complexity and performance comparison between QC- MPCGC and conventional MPCGC .....	106
Figure 6.12 Complexity and performance comparison between QC- MPCGC and conventional MPCGC .....	106
Figure 6.13 Entries of the base matrix (64x64) of the QC-MPCGC .....	107
Figure 6.14 Entries of the parity check matrix (192x384) of the QC-MPCGC .....	107
Figure 6. 15 Complexity and performance comparison between Layered BP QC- MPCGC and conventional MPCGC .....	108
Figure 6.16 Complexity and performance comparison between Layered BP QC- MPCGC and conventional MPCGC .....	109

---

## List of Tables

Table 3.1 Complexity comparisons results .....	57
Table 5.1 WiMAX simulation Parameter .....	81

---

## List of Abbreviations

ASK	Amplitude Shift Keying
AWGN	Additive White Gaussian Noise
BEC	Binary Erasure Channel
BER	Bit Error Rate
BPSK	Binary Phase Shift Keying
BSC	Binary Symmetric Channel
BW	Bandwidth
b/s/Hz	Bits per second per Hertz
CDMA	Code Division Multiple Access
CP	Cyclic Prefix
CSI	Channel State Information
dB	Decibel
DE	Density Evolution
dmin	Minimum Distance
Eb/N0	Energy per bit to noise power spectral density ratio
EXIT	Extrinsic Information Transfer Chart
FDMA	Frequency Division Multiple Access
FEC	Forward Error Correction
FFT	Fast Fourier Transform
$GF(q)$	Galois Finite Fields
IEEE	Institute of Electrical and Electronics Engineers
ISI	Inter-Symbol Interference
Layered BP	Layered belief propagation
LDPC	Low-Density Parity Check

---

LLR	Log-Likelihood Ratio
LOS	Line-Of-Sight
MAP	Maximum A Posteriori Probability
MIMO	Multiple-Input-Multiple-Output
MISO	Multiple-Input-Single-Output
ML	Maximum Likelihood
MPCGC	Multiple Concatenated Gallager Codes
MCW	Mean Column Weight
NB-LDPC	Non-binary Low Density Parity Check Codes
NLOS	Non-Line-of-Sight
OFDM	Orthogonal Frequency Division Multiplexing
OFDMA	Orthogonal Frequency Division Multiple Access
PDF	Probability Distribution Function
PER	Packet Error Rate
PSD	Power Spectral Density
PHY	Physical Layer Network
QAM	Quadrature Amplitude Modulation
QC-LDPC	Quasi Cyclic Low Density Parity Check
QC-MPCGC	Quasi Cyclic Multiple Concatenated Gallager Codes
SIMO	Single-Input-Multiple-Output
SISO	Single-Input-Single-Output
SNR	Signal-to-Noise-Ratio
SOFDMA	Scalable Orthogonal Frequency Division Multiple Access
SPA	Sum Product Algorithm
STC	Space-Time-Code
TDMA	Time Division Multiple Access
TG	Tanner Graph
WiMAX	Worldwide Interoperability for Microwave Access
ZF	Zero Forcing

# Chapter 1

## Introduction

### 1.1 Overview

Channel coding in digital wireless communication systems is very important because it enables a measure of controlling the errors in data transmission over unreliable communication channels. Low-density parity check (LDPC) codes have played an important role in error correction for achieving reliable data transmission in a communication system over a noisy channel because of their performance that is very close to the Shannon limit. LDPC is based on linear block codes and can be considered as a better error-correcting scheme when compared with other codes. LDPC was first introduced by Gallager five decades ago and then remained largely forgotten for over 50 years [1]. The only distinguished work was by Michael Tanner in 1981 when he introduced diagrammatic representations of the codes subsequently called the Tanner graph [2]. Since the invention of Turbo codes in 1993[3], researchers started to focus on finding low complexity codes that have a performance approaching the Shannon channel capacity. Finally, LDPC was rediscovered again by Mackay and Neal in 1995 [4][5]. Most research has focused on the single LDPC component to overcome the high decoding complexity and implementation bottlenecks for longer code lengths due to the number of connections in the bipartite Tanner graph.

MPCGC is a new class of parallel-concatenated codes designed from the parallel concatenation of LDPC codes. It is a concatenation of three or more LDPC codes built in parallel concatenation [6]. A benefit from applying concatenated small codes instead of a single long code is to achieve a low error rate with an overall encoding and decoding complexity that is lower than what is required for a conventional single long LDPC code. The lower complexity of the MPCGC codes can be achieved by encoding and decoding each component code separately. Furthermore, the MPCGC structure offers improved flexibility in terms of matching the coding performance and code complexity to a channel's condition (choice of component codes). The reason for applying LDPC codes in the well-known turbo code structure of the concatenated codes is to conquer the fairly complex encoding and decoding of a long code length into multi steps, while maintaining the information flow among the LDPC component decoders and reducing any information loss between the

decoding steps. The attractive properties of LDPC codes have led them to be considered even better than the best-known turbo code [7-9].

The work in this thesis further investigates Multiple Parallel Concatenated Gallager Codes (MPCGC) and their evaluation under a range of configurations and channels.

Further explorations for MPCGCs in this thesis are concerned with the capacity achieved for different communication models.

The thesis includes the study of punctured MPCGCs and their application to the improving a communication's system performance over AWGN and flat Rayleigh fading channels. The advantages of using QC-LDPC with MPCGC are investigated in this thesis for enhancing coding performance and reducing decoding complexity.

Application of MPCGC in WiMAX and MIMO are presented with detailed analysis and shown to yield improved performance in each case.

## **1.2 Research aim**

The main aim of the research is a further investigation into the design of efficient coding models based on the MPCGC structure to achieve a low error rate with an overall encoding and decoding complexity that is lower than what is required for a conventional single equivalent long LDPC code.

The key idea is to exploit the advantages of using smaller LDPC codes in a turbo code structure in an active approach, to achieve an optimal trade-off between excellent performance and encoder/decoder complexity. In addition, attractive applications for MPCGCs that benefit from the flexibility of the such codes while maintaining/improving coding performance with reduced implementation overheads will be evaluated via extensive simulation models.

## **1.3 Motivation**

Reliable channel coding is very efficient in wireless digital communication when it comes to improve system performance and to provide capacity achievement. LDPC codes have been considered a top research topic since the end of the 90s and in the 2000s; and are used in wide applications in deep space communication, next-generation networks and data storage. The foundation of this thesis based on the improvement the system performance with low

complexity in encoder/decoder components by investigated an efficient structure for LDPC codes based on multiple parallel concatenations codes called MPCGCs.

The another was motivated to explore the advantage of using concatenated smaller LDPC codes as alternative approach of conventional single long LDPC code to achieve excellent performance while maintaining/improving coding performance with reduced implementation overheads. Moreover, the MPCGC structure is more amenable to flexible when using with another application such WiMAX and MIMO applications. Furthermore, MPCGC is useful with applications that required throughput achieved to enhance the system performance.

Another motivation of MPCGC for compatible code rate application where some application required puncturing technique to let the code rate variable and flexible to use in this applications such WiMAX network.

The using of QC-LDPC codes with MPCGC structure has reduced the decoding complexity of the communication system in terms of the number of iterations and edges compared to the conventional MPCGC.

Finally, the incorporated of the MPCGC structure with MIMO technique has added a flexible improvement and enhanced the system performance of these applications.

## **1.4 Objectives**

In order to achieve the research aims, the following objectives have been set.

1. Investigating and developing an MPCGC structure with three and four LDPC component codes with different modulations over AWGN and flat Rayleigh fading channel. The crucial design of the mean column weight (MCW) is investigated and selected for optimum performance.
2. Evaluating the complexity of the proposed structures and proposing a metric in terms of the number of iterations and edges in addition to calculating the resulting capacity.
3. Proposing a novel and efficient puncturing method for Multiple Parallel Concatenated Gallager Codes (MPCGC).
4. Further exploration of the MPCGC structure by incorporating a powerful MPCGC in the IEEE 802.16/WiMAX standard.
5. Further investigation for MPCGC by incorporating the efficient QC-LDPC based on the circular permutation matrices. The QC-MPCGC offers an improvement to the

system performance by reducing the decoding complexity compared to the original long LDPC codes.

6. Exploring different decoding algorithms to reduce the MPCGC complexity. The Layered belief propagation (BP) decoder instead of the sum-product algorithm (SPA) decoder leading to a Layered BP QC-MPCGC, reducing the overall decoding complexity compared to the conventional MPCGC.
7. Applying the MIMO technique with MPCGC to enhance the system performance.

## 1.5 Original Contributions

The thesis delivers important contributions to MPCGCs and their application as listed below:

1. Further exploration of the SISO MPCGCs by evaluating these codes for both AWGN and flat Rayleigh fading channels. The BER performance was improved when compared with the single LDPC component with the same parameters (see chapter 3).
2. A new MPCGC based on four LDPC component codes, where significant performance improvement was obtained with a higher complexity trade-off compared to the conventional MPCGC of three LDPC components (see chapter 3).
3. Designing the best MCW values of LDPC codes to get an excellent BER performance for MPCGC of three LDPC components. The suitable design of the MCW values has enhanced the system performance at low, medium and high  $E_b/N_0$  regions. Both modulations of MPCGC-BPSK and MPCGC-64 QAM are applied to enhance the system performance. Formulation of capacity achieved proposed (see chapter 3).
4. Proposing a novel and efficient puncturing method for Multiple Parallel Concatenated Gallager Codes (MPCGC). Random, regular and irregular punctured MPCGC are proposed and applied to obtain a compatible suitable code rates ( $R$ ) for applications like WiMAX. The proposed efficient punctured MPCGCs system is analysed over AWGN and flat Rayleigh fading channels. Simulation results show improved performance when compared to a single long LDPC code with the same parameters before and after puncturing. (see chapter 4).
5. First to apply the MPCGC structure to the standard IEEE 802.16 WiMAX. Shown that MPCGC-WiMAX achieves better BER performance compared with the single LDPC-WiMAX. It was extended to study the girth effect which defines the length of the shortest cycle of the Tanner graph

6. On the designing of the suitable LDPC parties and how to remove the girth affects. The advantage of using irregular puncturing process was incorporated with the MPCGC-WiMAX to maximize the original code rate from  $\frac{1}{4}$  to  $\frac{1}{2}$ . (see chapter 5).
7. First to propose new QC-MPCGC scheme where the single QC-LDPC component is incorporated with two LDPC Gallager component codes. The QC-MPCGC shown to provide better performance compared to the single QC-LDPC component with the same parameters. The complexity of the QC-MPCG was evaluated and shown to be less than that of the conventional MPCGC system (see chapter 6).
8. A new Layered BP QC-MPCGC scheme by using layered BP decoder instead of the sum-product algorithm (SPA) decoder to enhance the system performance compared to the conventional LDPC component with the the same parameters. In addition, the proposed Layered BP QC-MPCGC has the advantage of reducing the decoding complexity when compared to the MPCGC system (see chapter 6).
9. More insights into the MIMO-MPCGC over fading channels were provided through the system analysis. Two MIMO approaches with zero forcing equalizer were applied. The 2x2 MIMO-MPCGC and 2x4 MIMO-MPCGC systems have been designed and analyzed (see chapter 6).

## 1.6 Thesis outline

The thesis is structured into seven chapters; is organized as follows.

**Chapter 1** provides an introduction to the research topic and highlights the benefit from applying MPCGC on the coding systems. The aim of the thesis, followed by the required objectives, thesis original contribution. Finally, the thesis layout and list of publication are presented.

**Chapter 2** presents background about the benefit of the channel coding and capacity of the communication system. Followed by the study of the fundamental and construction methods of LDPC codes. The encoding and decoding process is covered in details. Furthermore, the highlights of the WiMAX and MIMO applications will be used with MPCGCs have presented. Finally, a review of the history of the Parallel concatenation codes is presented in details.

**Chapter 3** the motivation for investigation and explore the proposed MPCGC structure is highlighted. The process of encoding and decoding the MPCGC system has been described in

detail, where a better design for the MCW values has been calculated. The BER performance has been enhanced according to the computer simulation of variable coding model. A competitive comparison for parallel and serial MPCGC coding has been made. In addition, MPCGC provides better performance compared with both the serial MPCGC and the single LDPC component.

At last, the achieved capacity has been improved and calculated for both MPCGC-BPSK and MPCGC- 64 QAM.

**Chapter 4** addresses the proposed punctured MPCGC system, where different puncturing methods has been presented. This chapter further investigated the punctured MPCGC performance, where a different puncturing method has analyzed to make an optimum competitive system performance. These three methods are explained such as random, regular and irregular punctured MPCGC and evaluated. Finally, the complexity analysis has been achieved and the benefit from punctured MPCGC has less complexity than conventional MPCGC.

**Chapter 5** presented a novel MPCGC-WiMAX system, where the MPCGC has incorporated with the standard IEEE 802.16/WiMAX to get the advantage from the flexibility of the MPCGC codes. This chapter is focused on improving the WiMAX performance by introducing the encoder and decoder process then the interleaving process has been used to make the transmitted data safety from errors and to ensure the FEC high robust and reliable. Moreover, the OFDM system has been designed and analyzed as it is based the WiMAX system.

The result shows the improvement of the MPCGC-WiMAX model when compared to the single LDPC-WiMAX. In addition, the effect of the girth removable has been addressed. Finally, the application of irregular punctured MPCGC-WiMAX has been applied to make the compatible code rate with a trade-off in system performance.

**Chapter 6** concentrates on evaluating the effect of the QC-LDPC on the MPCGC system. QC-MPCGC provides improvement compared to the conventional single QC-LDPC codes. Further, exploration to the MPCGC has applied by incorporating the Layered BP decoder instead of the sum-product algorithm. The Layered BP QC-MPCGC has less complexity compared to the conventional QC-MPCGC with a little trade-off in BER performance. Finally, The analysis is extended by evaluating the effect of the MIMO-MPCGC over fading

channel with zero forcing equalizer. Two scenarios are considered, the first scenario investigates the 2x2 MIMO-MPCGC performance and the second scenario investigates the 2x4 MIMO-MPCGC performance. Both two scenarios have analyzed and evaluated to achieve better system performance with good Eb/No improvements when compared both above two the conventional MIMO-MPCGC systems at the same parameter

**Chapter 7** concludes the research by summarising the outcomes of the thesis and listing the concluding remarks. Moreover, at the end of the chapter, the future work directions are given.

## **1.7 Published Papers**

1. Ahmed Aftan, Mohammed Benaissa and Hatim Behairy, “Efficient coding Method of Multiple Parallel Concatenated Gallager Codes for WiMAX,” (accepted) in the 9th IEEE WIAD conference, 26- 28 June 2018, at the Kings College London UK.
2. Ahmed Aftan, Mohammed Benaissa and Hatim Behairy, “Efficient Puncturing Method For Multiple Parallel Concatenated Gallager Codes,” submitted to the *Global Communications Conference (IEEE GLOBECOM), International Conference, Abu Dhabi on 9 Dec 2018*.

## Chapter 2

### Background and Literature Review

#### 2.1 Introduction

Reliable channel coding is very efficient in wireless digital communication when it comes to improve system performance and to provide capacity achievement. LDPC codes have been considered a top research topic since the end of the 90s and in the 2000s; and are used in wide applications in deep space communication, next-generation networks and data storage.

It was determined by Richardson that there is similarity between the performance of LDPC codes and the Shannon limit in 2001. LDPC codes of block length  $10^7$  approaching the Shannon limit within 0.0045dB have been shown by simulations [8]. There is a direct proportional relationship between the block length and their excellent forward error correction properties, their minimum distance ( $d_{min}$ ). A parity check matrix which is sparse characterizes LDPC codes, as suggested by the name. Thus, a matrix wherein the number of 1's is much less than the number of 0's is a sparse matrix. An increase in the number of 1's is not necessary for an increase in the size of the matrix because of the sparse property of the matrix. This implies that the decoding complexity does not have to be increased for it to gain better distance properties.

This chapter includes an introduction and literature review to the keywords that considered in this thesis, first a literature review is provided, including the fundamental of channel coding of LDPC codes particularly the general coding overview then explaining the concept of the channel capacity for communication systems. In addition, the LDPC code representation and construction have introduced with the concept of the encoding and decoding system. Also considered here the effect of exit chart on designing of good LDPC codes that provides perfect performance. Moreover, an application of the multiple parallel concatenation in WiMAX and MIMO systems have been introduced. At the end, review of the parallel concatenation LDPC codes is given.

## 2.2 Channel coding

The purpose of channel coding is to protect the transmitted data through a noisy medium channel by finding perfect codes that can improve the reliability of the communication system. This is achieved by adding parity information bits to transmit the data through a noisy channel securely. At the receiver side, apart from the parity of the transmitted message might be incorporated with the main information data for error correction, which might have been added to the main information through the channel. Further advantages from error correction codes focused on error detection, as at least if no error correction happen the errors should be detectable [9].

### 2.2.1 General coding communication overview

In 1940, R. Hamming pioneered the principle of forwarding error correction (FEC), and he made this first contribution in this field by invented the Hamming (7, 4) code in 1950 [10]. A different point between Hamming code and LDPC code that the parity check for an LDPC can be written as sparse; only a few one's bits compared to the zero's bits in the array. While, Hamming has full-length code  $2^m-1$  columns, where columns are binary numbers and (m) represents the number of rows through the parity check matrix. In addition, LDPC code depend on the construction of the parity matrix on the transmitted data, while Hamming code is related to algebraic and cyclic coding theory. However, the concerning with how to create a reliable, practical encoding and decoding communication systems is called channel coding [11][12].

## 2.3 Channel Capacity for communication system

In 1948, Claude E Shannon presented in his paper the concept of information theory. He determined the limits on the reliable transmission of data over noisy channels and how they can be calculated. Shannon proved that for a known communication channel such as that shown in Figure 2.1, there is a limit called capacity beyond which reliable transmission of data is not possible. Reliable transfer of data is applicable at rates, which are close to the channel capacity theoretically. The general Shannon theorem presented the relationship between the ability of the channel to transport error-free information, compared with the signal to noise ratio that affected the channel and the bandwidth used for information transmission [11].

$$C = W \log_2 \left( 1 + \frac{S}{N} \right) \quad (2.1)$$

Where,

$C$ : Channel capacity in bit/sec

$W$ : Bandwidth in Hz

$S$ : Signal power in watt

$N$ : Noise power in watt

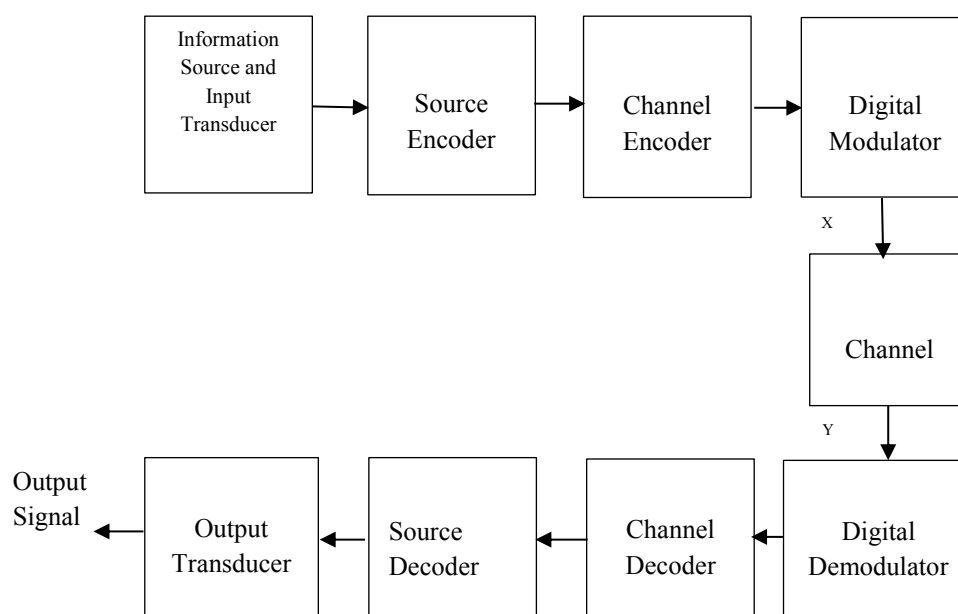


Figure 2.1 Digital communication system.

The additive white-Gaussian-noise (AWGN) channel is a commonly used memoryless channel among any other channels, like the binary symmetric channel (BSC) or the binary erasure channel (BEC). Therefore, we consider the AWGN channel in the codes design calculations.

Let  $X = [x_1, \dots, x_m]$ , and  $Y = [y_1, \dots, y_m]$  represent the random variables of the input and output of the channel, respectively, each bit from the ensemble can be represented as  $c_m \in \{0, 1\}$  to  $x_m$  where,  $x_m = 2(c_m - 1)$  as  $x_m \in \{\pm 1\}$ , In addition, the channel output can be

represented in time domain as  $y_m = x_m + w_m$ , where  $w_m$ , represents the real value from AWGN with zero mean and variance  $\sigma^2$ .

Let us describe the Gaussian probability density function (pdf) of the channel  $P(y_n \setminus x_n)$  as

$$P(y|x = \pm 1) = \frac{1}{\sqrt{2\pi}\sigma} e^{-\frac{(y \pm 1)^2}{2\sigma^2}}. \quad (2.2)$$

The source information probability  $P(x = +1) = P(x = -1) = \frac{1}{2}$

$$P(y) = 1/2 [P(y|x = +1) + P(y|x = -1)] \quad (2.3)$$

$$P(y|x) = \prod_m P(y_m|x_m). \quad (2.4)$$

The corrections process of the LDPC decoder depends on the two factors, firstly reducing the codeword error's probability, secondly the maximising of the posterior probability (MAP)  $P(x|y)$ . Before Turbo codes invention and rediscovery of LDPC codes, it was believed that practically were incredible to reach near Shannon limit. This invention considered that practically possible to find capacity approaching codes [12].

The system of achievable rates  $R$  can achieve a reliable communication at code rate  $R$  according to  $R < C$  [11]. The Capacity (bits per second)  $C$  is the ability of the channel to convey information, for example, 0.5 code rate that means each channel has to transfer a half bit of information per second. According to the derivation [13, 14], the capacity of the AWGN channel.

$$C = 0.5 \sum_{x=\pm 1} \int_{-\infty}^{\infty} P(y|x) \log_2 \frac{P(y|x)}{P(y)} dy \quad (2.5)$$

The integration of equation (2.6) can be summarized to the expectation  $E\{\cdot\}$ . This integral can be done according to Monte Carlo integration.

The relationship between the channel capacity  $C$  and signal to noise ratio (SNR) is illustrated in Figure 2.2 [14]. The SNR is represented by  $E_b/N_0$ , where  $E_b$  represents the average energy per bit and  $\sigma^2 = N_0/2$  is the power spectral density of the two-sided of the AWGN channel. At certain code rate  $R$ , the Shannon capacity provides a free error probability at the certain limit

for SNR. Only Turbo codes and LDPC have reached the Shannon limit within 0.5 dB by using long block length [12][15].

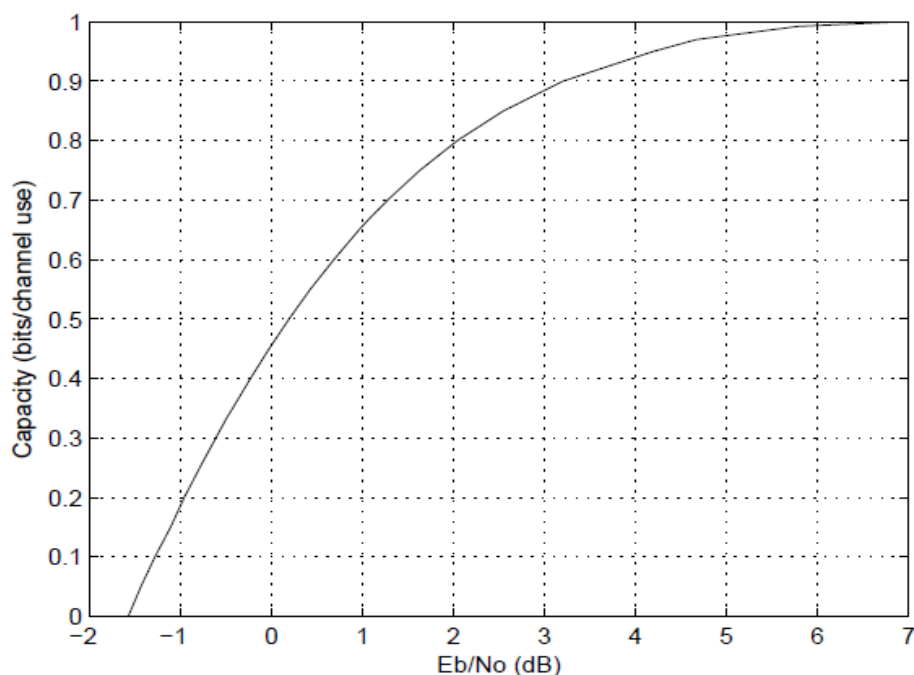


Figure 2.2 Channel capacity of AWGN channel.

## 2.4 Fundamental of LDPC codes

LDPC is considered a linear error correcting codes where the information bits are involved with redundancy bits to produce the codeword. At the receiver, the information will recover from the codeword. Let's consider the number of parity bits is  $M$ , while the length of the main information bits is  $K$  and  $N$  is the length of the block length or codeword. The LDPC parity can be defined over Galois finite fields  $GF(q)$  of order  $q > 2$ . The redundancy is introduced by the encoding process.

$$M = N - K \quad (2.6)$$

The LDPC code is considered the systematic coding scheme and the binary codes, which means the codeword is either 0 or 1. Moreover, for the systematic LDPC construction, the message bits  $m$  is multiplied with the redundant or the parity bits  $p$  to generate the codeword and is defined as.

$$c = [m \ p] \quad (2.7)$$

The error control code depends on the important parameter called code rate  $R$ , which represents the redundancy introduced by the LDPC code as in.

$$R = K/N = (N - M)/N \quad (2.8)$$

The parity check matrix of LDPC is linear block codes, which can be described by a binary  $K \times N$  generator matrix  $G$ . The codeword can be described as

$$c = mG \quad (2.9)$$

Also

$$cH^T = 0 \quad (2.10)$$

The modulo-2 arithmetic ( $\oplus$ ) is used to carry both the operation above [14].

## 2.5 Representations of LDPC codes

Two different methods can represent the LDPC codes. Firstly, by linear block codes, they can be represented by matrices; secondly by the graphical representation.

### 2.5.1 Matrix Representation

LDPC codes are a class of linear block codes which has parity check matrix  $H$  has a number of one equalling 1% or fewer. To give an example of a low-density parity-check matrix, the matrix defined in the equation (2.11) represents a parity check matrix with  $(m \times n)$  dimension for  $H(4, 8)$  code.

To describe these matrices, there are two numbers;  $W_r, W_c$  for the total number of 1's in each row and columns respectively.

There are two conditions  $W_r \ll m$  and  $W_c \ll n$  must be satisfied for a matrix to be called low density parity check. In order to apply this, the parity check matrix should usually be high sparse density and very large, so that the example matrix cannot be really called low-density [16].

$$H = \begin{bmatrix} 0 & 1 & 0 & 1 & 1 & 0 & 0 & 1 \\ 1 & 1 & 1 & 0 & 0 & 1 & 0 & 0 \\ 0 & 0 & 1 & 0 & 0 & 1 & 1 & 1 \\ 1 & 0 & 0 & 1 & 1 & 0 & 1 & 0 \end{bmatrix} \quad (2.11)$$

### 2.5.2 Graphical representation

Tanner introduced an active graphical representation of LDPC codes. He provided a complete representation for both encoder and decoder of LDPC codes.

The Tanner graphs are bipartite graphs, meaning that the all nodes of the graph are divided into two distinct sets, and the edges only comprise connecting nodes of two different types. In a Tanner graph, the two types of nodes are called check nodes (c-nodes) and variable nodes (v-nodes).

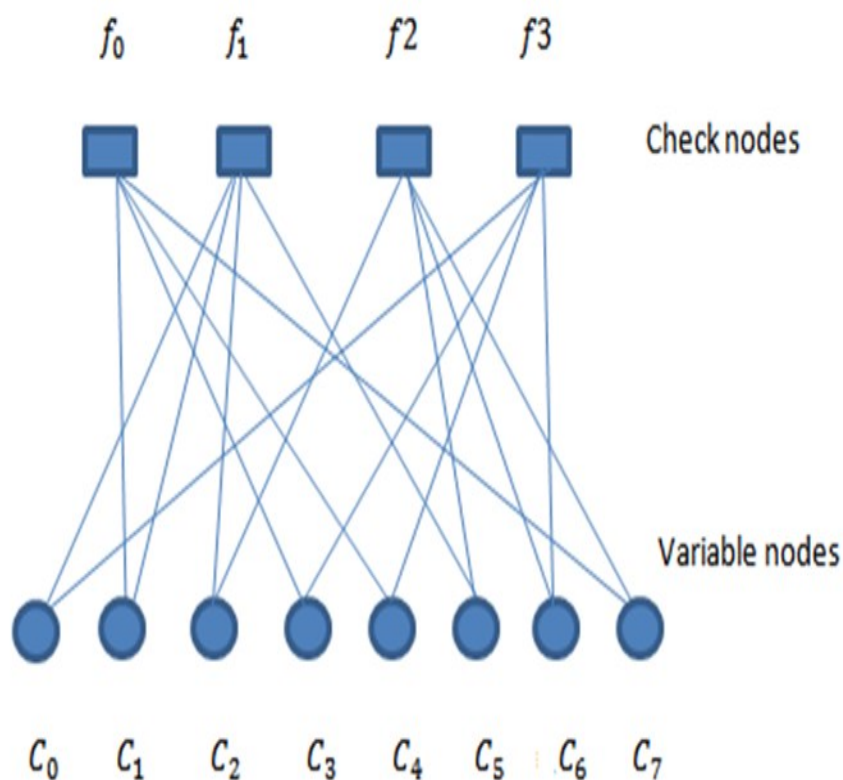


Figure 2.3 Tanner graph of the parity check matrix H.

Figure 2.3 is an example of a Tanner graph (TG), that was invented in 1981 by Tanner [2]. The figure represents the same code as the matrix in the equation (2.12). The creation of such a graph is rather straightforward. It consists from check nodes (the number of parity bits) and

variable nodes (the number of bits in a code word). The element to be called  $h_{ij}$  of  $H$  is a 1, when check node  $f_i$  is connected to variable node  $c_j$ .

Corresponding to the specified path,  $c2 \rightarrow f1 \rightarrow c5 \rightarrow f2 \rightarrow c2$  is an example of an unwanted short or small cycle, as shown in Fig (2.3). Those produced bad decoding performance and should usually be avoided since they require a long time [17].

## 2.6 LDPC code construction

Many algorithms have been used to design the parity check matrix of LDPC. These methods depend on the computer-based and the algebraic methods, where algebraic method depends on finite mathematics [18][19], combinational approaches [20] and circulant permutation matrices [21]. The high flexible codes are computer-based which is near to Shannon limit performance. However, there are some essential codes considered as the previous methods such following.

### 2.6.1 Gallager codes

LDPC codes were proposed by Gallager which contain three important parameters ( $N, W_c, W_r$ ) to represent the block length and the non-zero numbers in each column and row [22]. The random column permutation is considered when design the parity check matrix  $H$  of Gallager codes. It is obtained that the Gallager codes performed better with the increasing in the randomness of the parity check bits.

There are two types of Gallager codes depending on the number of 1s in each row or column. An LDPC code is called regular when  $W_c$  and  $W_r$  are constant for each column and row. Furthermore, it could be possible while looking to the graphical representation to see the regularity of the code, as there is the same number of incoming edges for every v-node as well as for all the c-nodes. The code is called irregular when the total number of 1's in each row or column is not constant. The construction of Gallager LDPC codes has three main steps:

1. Construction of the sparse parity check matrix  $H$  then splitting into  $W_c$  submatrices  $H = H_1, \dots, H_{W_c}$ , which each column has 1s as well every submatrices has  $\left\lfloor \frac{N-W_r}{W_c} \right\rfloor$ .
2. The submatrix  $H_1$  arranged 1s in the row elements in sloping style. In other words, the elements of 1 in the  $i$ th row ( $1 \leq i \leq W_r$ ) replaced with another place as  $(i-1)W_r$  to  $iW_r$ .
3. The remaining submatrices  $H_2, \dots, H_{W_c}$  are created by column permutations of  $H_1$ .

The example of Gallager parity check matrix  $H$  (20, 3, 4) as shown in equation (2.12).

$$H = \left[ \begin{array}{c}
 \begin{array}{l}
 11110000000000000000 \\
 00001111000000000000 \\
 00000000111100000000 \\
 00000000000011110000 \\
 00000000000000001111 \\
 \text{-----} \\
 10000100010001000000 \\
 01000100010000001000 \\
 00100010000001000100 \\
 00010000001000100010 \\
 00000001000100010001 \\
 \text{-----} \\
 10000100000100000100 \\
 01000010001000010000 \\
 00100001000010000010 \\
 00010000100001001000 \\
 00001000010000100001
 \end{array} \\
 \begin{array}{l}
 c1 \oplus c2 \oplus c3 \oplus c4 = 0 \\
 c5 \oplus c6 \oplus c7 \oplus c8 = 0 \\
 c9 \oplus c10 \oplus c11 \oplus c12 = 0 \\
 c13 \oplus c14 \oplus c15 \oplus c16 = 0 \\
 c17 \oplus c18 \oplus c19 \oplus c20 = 0 \\
 \text{-----} \\
 c1 \oplus c6 \oplus c10 \oplus c14 = 0 \\
 c2 \oplus c6 \oplus c10 \oplus c18 = 0 \\
 c3 \oplus c7 \oplus c14 \oplus c14 = 0 \\
 c4 \oplus c11 \oplus c15 \oplus c19 = 0 \\
 c8 \oplus c12 \oplus c16 \oplus c20 = 0 \\
 \text{-----} \\
 c1 \oplus c6 \oplus c12 \oplus c18 = 0 \\
 c2 \oplus c7 \oplus c11 \oplus c16 = 0 \\
 c3 \oplus c8 \oplus c13 \oplus c19 = 0 \\
 c4 \oplus c9 \oplus c14 \oplus c17 = 0 \\
 c5 \oplus c10 \oplus c15 \oplus c20 = 0
 \end{array}
 \end{array} \right. \quad (2.12)$$

### 2.6.2 Mackay codes

This type of LDPC codes was invented by Mackay [5], which illustrates the benefit of designing  $H$  sparse matrices. The parity check matrix structure contains constant numbers from 1s with random positions. In addition, the distribution of 1s in each row set uniformly. The effect of eliminating the short cycles called girth  $g$  of length 4 is considered in the designing the Mackay codes. The principle of this code is to reduce the number of 1s in each column of the  $H$  matrix by introducing a factor called low weight columns.

### 2.6.3 Quasi-cyclic LDPC (QC-LDPC) codes

Quasi-Cyclic LDPC (QC-LDPC) codes have submatrices with cyclic connections in the rows or columns. These codes offer excellent performance with efficient implementation. The encoding process can be done by using shift registers [19][20]. However, this code was applied to the single LDPC component with long codes. The identity shifting process of the row-columns of the submatrices are constructed and considered. In addition, at the decoder memory, the know locations of one row or column can conclude the remaining rows or columns in the original submatrix [25][26]. There are many methods for constructing the QC-

LDPC based on the arrangements shift values of the submatrices. Furthermore, the avoiding of the girth cycles have been considered and suggested by using finite geometry, algebraic design and special algorithms[23][24].

## 2.7 Encoding of LDPC

The reason for using the encoder to generate the codeword that consists of the message bits and some parity check bits. In addition, it is possible to include the information message bits in an LDPC encoded message. The encoding process is usually done by selecting appropriate variable nodes for placing the message bits, and in the next step to calculate the missing values of the remaining nodes [9].

The sparse generation of the parity check matrix  $H$  is considered when created the required parity check bits. Furthermore, the generation of the Generator matrix  $G = [P, I_K]$  with the order  $(K, N)$  depends on the parity check matrix  $H = [I_{n-K}, P^T]$  with the order  $(n - k, n)$ . The design of the parity check matrix should satisfy  $G \cdot H^T = 0$  as well as, the systematic parity check matrix  $H_1$  could be as  $[I_{n-K}, P^T]$ , where  $P$  represents the parity sub matrix while  $I_K$  represents the dimension of the identity matrix  $(k \times k)$ .

The syndrome equation of the LDPC code can be represented by  $C \cdot H^T$  which means  $[m \cdot G \cdot H^T = 0]$  where the code word  $C$  is calculated as  $C = m \cdot G$  and in the next step, the using of the syndrome vector in the decoding process [28].

## 2.8 LDPC Decoding Algorithms

### 2.8.1 Iterative Message-Passing Algorithms

The message passing algorithm, also called sum-product algorithm (SPA), is an efficient algorithm, where the inference problems can be solved in both statistical physics and error control coding.

The Sum-Product Algorithm (SPA) provides better coding performance with a trade off in the decoding complexity. For simplification of the algorithm operations of the SPA which is based on soft-decision decoding, multi modifications for both binary and non-binary Low Density Parity Check Codes (NB-LDPC) have been proposed, but still required high implementation in the decoding complexity. The min sum algorithm (MSA) is modified from

the check node operation of the SPA, but still require a high quantized message to be delivered between the nodes inside the decoding process [29].

For LDPC decoding the Sum-Product algorithm (SPA) decoding is a soft-decision message-passing algorithm that requires calculating the likelihood ratio (LLR intrinsic message) for variable node operations to apply the decoding decisions.

The decoding process starts by make the LLRs pass over to the variable nodes. The step sum' operations on the input LLRs were performed by variable nodes (V) as calculated in equation (2.13). Moreover, the computed extrinsic messages are delivered along the connected edges to the check nodes (C) [1][30].

The operation of the SPA variable node:

$$V_i = LLR_n + \sum_{j \neq i} C_j \quad (2.13)$$

Where,  $n = 1, 2, 3 \dots$  number of variable nodes

$i, j = 1, 2, 3 \dots$  degree of variable node

The check nodes (C) perform the parity check operation and computes the messages that are to be passed to the respective variable nodes (V), as in (2.14).

The operation of the SPA Check node:

$$C_k = 2 \tan^{-1}(\prod_{k \neq l} \tanh \frac{V_l}{2}) \quad (2.14)$$

Where,  $l, k = 1, 2 \dots$  degree of check node

The system repeats this process until the parity check is fulfilled or the maximum iterations are attained. We can observe that high precision extrinsic messages are required by the SPA to be forwarded between the nodes and the SPA contains non-linear function in the check node operation. As a result, high decoding complexity is observed. Nevertheless, desirable decoding performance can be achieved by the SPA [31].

## 2.9 Soft and Hard Decoding

The soft decoding means a multi-bit resolution and depends on the reliability of the transmission, since at this step not only do we receive the value of the signal from the receiver but also its probability to be true via extra bits that are added to the message. In this

form, the message is presented in a sign-magnitude format where the sign is the value of the message (0 or 1 as in hard decoding), and the magnitude is the probability of being correct. The received value when the magnitude is low is classified unreliable during assessment by the decoder, which can influence its algorithm [12].

Besides requiring the parity information, the propagation of reliability information is required by the soft decision decoding. Additional bits are required by this information to be propagated for each edge or message in the graph. To bring together the reliability of the other incoming messages, a reliability update along with the parity update is carried out by the nodes and an estimated reliability for each outgoing message is resultantly produced by this phenomenon.

As compared with the current estimate of the parity for that message or variable, the propagation of only one bit per message or graph edge is featured in hard decision decoding. The message update with an XOR network and the simple parity check is carried out by the check nodes. Besides the received bit and addition of the input messages, a weighted majority function is performed by the variable nodes. The current iterations estimate of the decoded bit is determined by summation or the sign of the majority. The sign of the majority or summation of all inputs except the current edges input is outgoing messaging from the variable nodes. This represents the inferred value for that variable message and all other connected checks [10][26].

At the receiver, the incoming message from the detector to the decoder can take many types. Hard decision decoding is satisfied when the incoming message from the detector consists of only one single bit. The value is decided using a threshold at the receiver. This threshold is computed based on channel properties, and the values above the threshold will be treated as 1 and 0 for values below since the hard decoding leads to hard decisions on the variables of each cycle.

The complexity of the decoder depends on the number of magnitudes even though it allows it to assess the incoming message better, giving it a better chance of successful decoding. The existence of reliability bits allows soft decoders to make better assumptions on data as compared with hard decision decoders that do not have any probability values to work with incoming bits that are equally treated [28].

## 2.10 EXIT Charts and Density Evolution

The extrinsic information transfer (EXIT) chart of LDPC code is a graphical method used to predict the decoding threshold of the received codeword. EXIT chart is working on the based on the iterative cooperation between check nodes and variable nodes to take the decoding decision with appropriate iterations [15][27]. EXIT chart is considered one solution to enhance the performance of the LDPC iterative decoding at the error floor region. Moreover, Richardson et al. [33] and Luby et al. [34] succeed to show how to make an optimisation to the pair of the degree distribution polynomial of the channels. However, their work was focused on the conventional single LDPC component, which suffered from high implementation in the decoding complexity.

The predicted decoding threshold based on EXIT chart is free-cycle Tanner graph. Likewise, the density evolution (DE) of LDPC can predict the channel conditions by predicting probability density functions (pdfs) of the iterative decoding. The DE can predict the decoding of BER when converging to zero. The probability of error relies on the channel parameters, example the standard deviation ( $\sigma$ ) of the AWGN channel [33].

## 2.11 Worldwide Interoperability for Microwave Access (WiMAX)-IEEE802.16

WiMAX is a telecommunication technology that produces a high data rate over large coverage areas to a large number of users as shown in Figure 2.4. The first introduced in 2005 to solve the weakness of Wi-Fi network. Moreover, the WiMAX antenna had a communication range up to 40 miles with data rate 70 Mbps [35].

The first version from WiMAX based IEEE802.16 standard covered the frequency band 10 - 66 GHz and needs line-of-sight (LOS) towers. After that, the designed standard has covered the frequency band 2-11 GHz at different physical (PHY) specifications, to enable non line of sight (NLOS) connections that require efficiently techniques to attenuate the effect of the multipath and fading. WiMAX technology is based on OFDM technique and it's possible to be potential replacement candidate for mobile communication network such code division multiple access (CDMA) and the global System for Mobile Communication (GSM), or to increase the system capacity [36][37].

The OFDM-based physical layer of the IEEE802.16 standard can be worked as a wireless backhaul technology for 2G, 3G and 4G networks. In 2005, the IEEE802.16-2004 was updated by 802.16e-2005 with uses Scalable Orthogonal Frequency Division Multiple Access (SOFDMA). More updated versions, including 802.16e with multiple antenna supported by Multiple Input Multiple Output (MIMO). To satisfy the high demands of the next generation data, the modulated is chosen as it is more efficient (more bits per OFDM/SOFDMA symbol) [21].

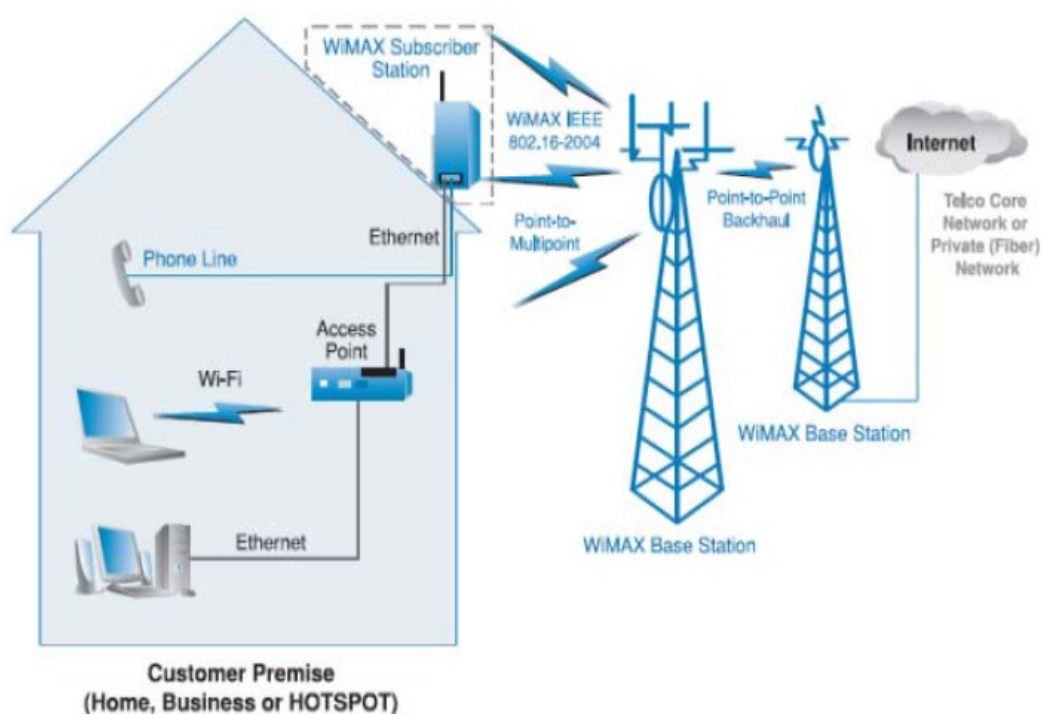


Figure 2.4 WiMAX equipment [38].

## 2.12 Quadratic amplitude modulation (QAM)

Both the phase and amplitude of signal are changed for the creation of Quadrature amplitude modulation (QAM). Through making changes in the amplitude and phase, the bits are mapped to two analogue signals. Afterwards, two analogue signals are orthogonal due to them being out of phase with each other by  $90^\circ$ . There are different kinds of QAM depending on structure of the constellation diagram. Rectangular-QAM represents the QAM with a rectangular structure and circular-QAM is the name given to circular symmetry constellations. Under dissimilar channel conditions, the performance of each constellation is different. Afterwards, modulation and demodulation of rectangular-QAM is rather simple

because of its regular structure which results from amplitude modulations in phase and Quadrature. However, channels influenced by phase noise are the most suitable for circular-QAM. Moreover, such schemes can be implemented now because of the assistance of digital signal processing. Henceforth, a combination of ASK and PSK can basically be considered to be Quadrature amplitude modulation (QAM) [39]. This implies that, in both the phase and amplitude of the carrier signal, the digital information is carried. In comparison to the desired transmission frequency, the modulator output frequency is frequently lower and the modulator frequency being up-converted to the appropriate radio frequency (RF) for transmission is essential.  $M=64$  for M-ary QAM is the condition for “64-QAM” to result. Afterwards, at the time of each symbol period,  $K = \log_2 M$  bits of information is transmitted by QAM. 64 possible symbols each having 6 bits are presented for 64-QAM. Different bit errors taking place for every symbol error are minimized as bits are mapped into symbol frequently according to the Gray codes. This code makes sure that a single bit in error is likely corresponded to by a single symbol in error as Gray-coding is a bit assignment where there difference in the bit patterns in adjacent symbol is only of one bit. Afterwards, rectangular constellation of a Gray-coded unfiltered 64-QAM [40][41].

### 2.14 Multiple Input Multiple Output (MIMO)

In recent years, research studies discussed the Multiple Input Multiple Output (MIMO) systems at length due to their possible attributes. Exploiting the multiple antennas at both receiver and transmitter sides is one of the conventional features of MIMO, which is described as transmit-receive diversity property. In addition, it is also observed in basic types, either at the receiver side SIMO, or at transmitter side MISO [42].

MIMO has the potential to uplift the capacity without reducing the transmitted power, by which we can infer that it is uniformly dispersed among its multiple antennas. The utilization of smart antennas leading to increase in total performance is the one of the appropriate solutions of Inter Symbol-Interference in MIMO [43]. The Diversity Spatial multiplexing gain, Array gain and Interference minimisation are the general benefits offered by the MIMO. For MIMO communication system as in Figure 2.5 with number of  $M$  transmitted and  $N$  received antennas, all of the sent signals are exposed by each of the received antennas so that the MIMO fading channel model could be clarified. Accordingly, the SISO channel is enabled to be illustrated as a  $M_T \times M_R$  matrix. The  $M_T \times M_R$  MIMO channel matrix at a

certain moment of time may be represented over the required bandwidth of frequency-flat fading [44][45].

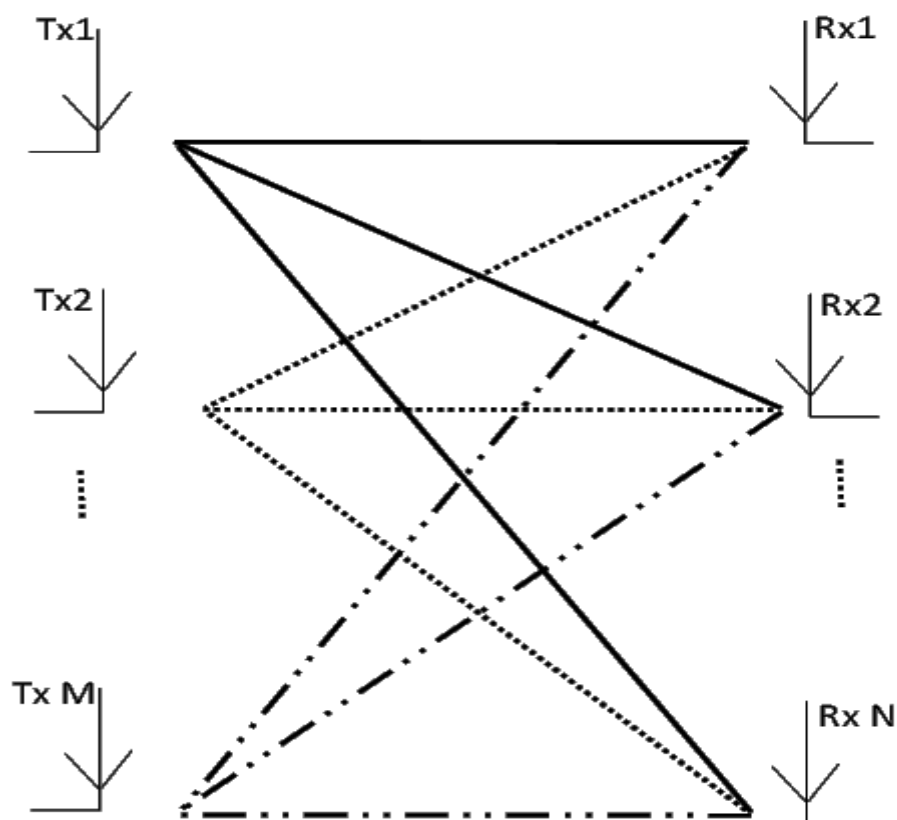


Figure 2.5 MIMO channel for M transmitter antennas and N receiver antennas.

### 2.15 History of the Parallel concatenation Gallager codes (PCGC)

LDPC is one of the more well-known error correcting codes designed in noisy communication channels to minimize the probability of information loss. This probability can be reduced to a minimum as desired by using LDPC, thus the data rate of transmission can be close to Shannon's limit as required. In 1993, Claude Berrou et al. presented a practical code suitable to approach the channel capacity at low (SNR) and called it Turbo codes; and with the invention of turbo codes, scholars switched their focus to the parallel concatenation for finding a low complexity code which can approach the Shannon channel's capacity [46]. The rediscovery of the LDPC followed the invention of turbo codes which were reinvented with the work of Mackay in 1995 [20][31].

The last years have observed the increasing research interests in parallel concatenation of LDPC codes instead of Turbo codes to improve system performance. The presented research is focused on the further studies of the parallel concatenation of LDPC codes.

Parallel Concatenated Gallager Code (PCGC) is a class of concatenated error correcting codes designed to reduce the encoding and decoding complexity of long block length LDPC codes. The complexity of the encoding and decoding of LDPC codes increases linearly with the code length ( $N$ ). In addition, the using of conventional single LDPC component means that one encoder in the transmitter and one decoder at the receiver are used in single input single output (SISO) system. In the conventional LDPC codes with long block length suffers from high decoding complexity and error floor problems at high SNR, where the reason for high complexity is the higher paths connectivity in the bipartite of the Tanner graph (TG). The first original work on Parallel Concatenated Gallager Codes introduced by H. Behairy and S. C. Chang in 2000. A new field from a concatenation of only two LDPC codes was revealed and presented a scheme to concatenate two LDPC codes using the turbo code principle. They got several benefits from considering this approach such as reducing complexity, delay, and memory required. This is in addition to the enhancement in the bit error rate BER performance when compared with a single LDPC code with the same parameter. Moreover, they used a different Mean Column Weights (MCWs) for each LDPC code  $MCW_1=2$  and  $MCW_2=2.66$  through a bipartite graph in the decoder as well as they used LDPC code rate  $\frac{1}{2}$  for both, and with the concatenation results in a  $\frac{1}{3}$  rate without used interleaver between the codes [48]. Moreover, the previous work is restricted to only two LDPC component code with overall code rate  $R=1/3$  concatenated in parallel using Turbo code structure and only used LDPC Gallager codes. Later another work in conventional serial and parallel concatenation PCGC [31], but the concatenation still limited to only two LDPC component and have not been most successful due to their limitation.

In 2000, irregular repeat-accumulate (RA) codes are devised by Jin et al as a competitive alternative to the parallel concatenation of LDPC code [49]. The main advantage of using irregular RA codes instead of irregular LDPC codes is that the encoding complexity is linear in the code length. The RA consists from an outer code that is a mixture of repetition codes and inner code that consists of parity check bits and an accumulator (a differential encoder) [50][51]. My investigations of MPCGCs research can be fully parallelized while an a posteriori probability (APP) iterative decoder cannot due to the accumulator.

In 2003, Zhao and Valenti presented a parallel concatenated convolutional code (PCCC) based on the Turbo code (TC) under quasi-static fading relay channel, which transmitted the encoded data twice using the interleaver. The classic turbo decoder is used to decode the received data [52]. In addition, the advantages from using LDPC codes by Mackay [33][20] instead of the turbo codes have offered an improvement in the BER performance and reducing in the error floor at the higher SNR region, which made the turbo codes suitable for only lower SNR region.

The better performance achieved when using turbo coding as an outer code and LDPC as an inner code in a serial concatenation [53], despite this concatenation has performed well in deep space communication but required a high computational complexity compared with the MPCGCs research. Further modification in serial concatenation codes, Damian A. Morero et al. [54] have reported a new approach to reduce the computational complexity and to improve the error floor region by combined both LDPC codes and turbo codes in serial.

The forward error corrections are essential in the multiple input multiple output (MIMO) channels for high-quality communication, in 2003, Futaki and Ohtsuki presented a system with iterative turbo decoding called (MIMO-LDPC-TD) using two LDPC encoders and decoders. Moreover, each LDPC codes have identical MCW. They improved the performance and reduced the complexity smaller than that in the conventional MIMO-LDPC [55]. However, my investigations in MIMO-MPCGCs provides better BER performance compared with the reported Futki and Ohtsuki results due to using three LDPC components.

In 2006, Serrato and Tim O'Farrell presented a new class from parallel concatenation by applying two different LDPC codes with different MCW values through using the Maximum A-Posteriori (MAP) of the SPA decoder. The result was obtained from the authors improving the system performance with a low complexity compared to the individual conventional LDPC codes, but they used only two LDPC codes concatenated in parallel with overall code rate  $1/3$  and  $1/2$  for each individual LDPC code rate. The presented research of the MPCGC structure is more flexible to utilizing three or four LDPC codes by modifications to using the a priori information calculated during the super iteration of the decoding process [56].

In 2013, Kumar and Kshetrimayum presented a methodology for parallel concatenation of the LDPC codes. They presented an efficient methodology for PCGC by utilizing one component of LDPC at high mean column weight (MCW)  $> 2.5$  and sending the parity bits of the

encoder twice. The performance of this methodology outperforms existing PCGC regarding BER performance in both AWGN and flat fading Rayleigh channels. It also showed that the proposed PCGC provides coding improvement compared to the conventional PCGC in terms of decoding complexity and decoding delay [52]. The current study in MPCGCs is more flexible to use three or more LDPC components with different MCW values. Furthermore, the MPCGCs provide superior improvements compared to the other conventional LDPC components.

At the end of 2013, presented a new class from parallel concatenation of multiple components of LDPC codes. Multiple Parallel Concatenated Gallager Codes (MPCGC) were used to reduce the long component from LDPC code into multiple small (lower-complexity) LDPC codes for improving performance in practical. The MPCGC structure with three LDPC components provided better system performance with low complexity compared to the single conventional LDPC [57]. However, the previous work from MPCGC obtained significant BER improvement but limited to the only Gallager LDPC codes and applied to the only SISO system. The presented study is more flexible compared to the previous work by the ability to use four LDPC components as well as the possibility to use different decoding method such Layered BP decoder. In addition, the presented study provides the advantage of applying MIMO technique with MPCGC structure to improve the system performance without exploiting high decoding complexity.

In 2017, a modified PCGC decoding scheme for combined LDPC and turbo convolutional code presented a modified practical extrinsic information and achieved a trade-off in the performance of the reducing error floor region, computational complexity and latency [58]. The presented research has good performance with a trade off in complexity compared to the previous combined LDPC with turbo convolutional code.

A new efficient technique in the non-zero syndrome of parallel concatenation proposed by using two-component LDPC code [59], one component used zero syndromes and the other used non zero syndromes. The result showed a better BER performance compared with the existing PCGC or the dedicated LDPC code for the same parameters of code rate and code length. However, the high computational complexity limitation has affected this work while in the current study, the using QC-MPCGCs provides better system performance with less complexity.

## Chapter 3

# Construction of Modified Structured of Multiple Parallel Concatenated Gallager Codes (MPCGC)

### 3.1 Introduction

This chapter focuses on the construction of structured MPCGC, where MPCGC are a new class of parallel-concatenated codes designed from parallel concatenation of three or four component Low-Density Parity-Check (LDPC) codes. MPCGC provides a better error-correcting procedure as compared with the turbo codes and the other codes. Moreover, the reason for using LDPC codes in the well-known turbo code structure is to conquer the fairly complex decoding of a long block length ( $N$ ) into steps. In MPCGC scheme, the component LDPC codes concatenated in parallel without using interleaver.

We intend to show that MPCGC have good error-correcting capabilities with high performance in both Additive White Gaussian Noise (AWGN) and flat fading channel, all the simulations were carried out in Matlab and C language because of the simulators are normally designed to scale and make it easier to produce accurate result.

Analysis of the proposed coding scheme using both iterative and Maximum Likelihood (ML) decoding is presented. The system model techniques used are based on the Gaussian approximation of the extrinsic information [48]. In addition, a good trade-off between coding gain and complexity can be carried out using the parallel concatenated codes proposed by Forney [60].

MPCGC is a concatenation of three or four LDPC with free interleaver, and the benefit of applying concatenated code instead of a single code is to provide better coding performance with an overall decoding complexity that is less than needed for a conventional single code. Furthermore, the reduced complexity can be achieved by individually decoding each component code.

The organization of this chapter as follows; in section 3.2 the MPCGC encoding has been explained in detail. In section 3.3 the proposed system model of the MPCGC encoder is presented. The proposed serial and parallel MPCGC structure has been done in section 3.4 and 3.5 respectively. Followed by the presentation and explanation the SPA decoder in

section 3.6. In section 3.7, we explain in detail the iterative decoding of the MPCGC structure. The MCW combination and code design has been done in section 3.8. The simulation results and discussion of the research is presented in section 3.9 as well the complexity analysis has been presented. Finally, the chapter summary is presented in section 3.10.

### 3.2 Encoding of MPCGC

MPCGC are a class of PCGC where  $M$  distinctive components with 3 component LDPC encoders are used, each of which is described by a generator matrix  $(k, n)$  with code rate  $R = 1/2$ . The concatenated in parallel method is used to build an overall length  $(N)$  and codeword rate  $R$ :

$$R = 1 / (M + 1) \quad (3.1)$$

An irregular code with different mean column weights (MCW) are used, which allows the codeword bits to participate in a different number of parity check equations.

A single LDPC parity checks that the matrix of dimensions  $(m, n)$  contains  $n$  column with Hamming weight  $C_n$  where  $1 \leq C_n \leq m$  and  $n \in \{1 \dots n\}$ . Also, each of weight  $w_l$ , where  $w_l \leq m, l \in \{1, \dots, m\}$ .

Where,

$$\lambda(x) = \sum_{i=1}^m \lambda_i x^i \quad (3.2)$$

Specifically, the distribution of the column weight has a highest column weight of  $M$ . In other words,  $\lambda_i$  represents in the matrix the fraction of columns weight  $i$ , while

$$\text{MCW} \cong \sum_{i=1}^m i \lambda_i \quad (3.3)$$

This can be introduced as the (MCW) of the matrix. MCW represents the symbol (left) node degree distribution of the Tanner graph[61]. Moreover, MCW has the ability to make the construction of structured MPCGC easier and flexible to achieve better performance when maximizing the value of the MCW in the LDPC parity, and many improvements can be achieved by blocking short cycles, while optimizing the bipartite graph depends on the better MCW found in the structure phase. When the codeword  $C$  is viewed as:

$$C = [P, \bar{S}]$$

Where,

$P$  is the parity sequence bits and  $S$  the information sequence e bits, the parity check matrix  $H$  can be viewed as:

$H = [H^P, H^S]$ . Then

$$(H^P, H^S) \begin{pmatrix} P \\ S \end{pmatrix} = 0 \quad (3.4)$$

The information bits  $S$  is involved with the codeword  $C$  when organizing the parity check matrix. Thus, the  $H^P$  part of the parity-check matrix has a lower density than the part  $H^S$ . This style from the columns is arranged in such a way that the information bits are associated with the high-weight columns, while the parity bits are associated with the lower-weight columns.

For example, let consider  $H$  ( $m = 4, n = 8$ ) LDPC parity check matrix is:

$$H = \begin{bmatrix} 1 & 1 & 0 & 1 & 1 & 1 & 0 & 1 \\ 0 & 0 & 1 & 0 & 1 & 0 & 1 & 0 \\ 1 & 1 & 0 & 0 & 1 & 0 & 1 & 1 \\ 1 & 1 & 1 & 1 & 0 & 1 & 1 & 1 \end{bmatrix}, H = [H^P, H^S] \quad (3.5)$$

The distribution of the column weight is:

$$\lambda(x) = 0.375x^2 + 0.625x^3$$

From equation (3.3), the MCW can be calculated as follow:

$$\text{MCW} = (2 \times 0.375) + (3 \times 0.625) = 2.625$$

From the above parity-check matrix, we can write out the set of parity-check equations:

$$x_0 + x_1 + x_3 + x_4 + x_5 + x_7 = 0$$

$$x_2 + x_4 + x_6 = 0$$

$$x_0 + x_1 + x_4 + x_6 + x_7 = 0$$

$$x_0 + x_1 + x_2 + x_3 + x_5 + x_6 + x_7 = 0$$

The equations above will be part of planning the Tanner graph in iterative decoding algorithms[51][52].

The generator matrix is based on a linear code and is used to organize all the possible codewords. A linear  $(n, k)$  code has  $k \times n$  generator matrix.

Given a message  $\bar{S}$ , the codeword will be the product of  $G$  and  $P$  with entries modulo 2:

$$C = G \cdot \bar{S} \quad (3.6)$$

Given the received codeword  $y$ , the syndrome vector is:

$$z = H \cdot y \quad (3.7)$$

When  $z = 0$ , it means that the received codeword is error-free, otherwise the position of the flipped bit takes the value of  $z$ .

The randomly generated parity check matrix  $H$  is not systematic, and the Gaussian elimination and reordering of columns are meant to derive an equivalent parity check matrix in systematic form.  $H$  is redefined as the original matrix with its column reordered as in the Gaussian elimination, so the generator matrix  $G$  of LDPC can be defined as:

$$G^T = \begin{pmatrix} P \\ I_k \end{pmatrix} \quad (3.8)$$

Where  $I_k$  is the  $(K \times K)$  identity matrix [63].

### **3.3 Proposed system model of MPCGC Encoder**

The system encoder is created by the parallel concatenation of four LDPC encoders that are concatenated directly. Figure 3.1 represents the MPCGC encoder where  $\underline{u}$  (of length  $k$ ) represents the vector of systematic information bits, while  $v^M$  (of length  $k$ ) are the parity bits generated by  $M^{\text{th}}$  encoder and  $M \in \{1, \dots, M\}$ .

The 4 LDPC encoders work on the same inputs as a result of the output stream code. Figure 3.1 illustrates the block diagram of the MPCGC encoder system with code rate 1/5 where  $\underline{e}$  represents the systematic information bits sequence of length  $K$  and  $b^1, b^2, b^3, b^4$  and  $b^M$  are the parity bits sequences of length  $K$  generated by first, second, third and fourth LDPC

encoders, respectively. By conquering the total encoding process into something less complex, a reduction in the overall encoding complexity is done.

We consider a code rate  $R=1/5$  and overall code length  $N=1000$ , of MPCGC as a result of the concatenation of four LDPC codes with the same code rate  $R=1/2$  whose parity check matrices  $H_1, H_2, H_3$  and  $H_4$  are of dimension  $(m \times n)$  where  $m=200, n=400$ ; also with the parameters of MPCGC in  $MCW1=2.04, MCW2=2.73, MCW3=2.79$  and  $MCW4=1.89, N=1000$  when using the parallel decoding process.

$$R = 1/(M + 1) = 1/(4 + 1) = 1/5$$

The parity check matrix of each LDPC code corresponding to the information part can be denoted by  $H_1^P, H_2^P, H_3^P$  and  $H_4^P$ .

To generate codeword  $C1$

$$[b^1 \cdot e][H_1^P \ H_1^S]^T = 0 \quad (3.9)$$

Also for codeword  $C2$

$$[b^2 \cdot e][H_2^P \ H_2^S]^T = 0 \quad (3.10)$$

Also for codeword  $C3$

$$[b^3 \cdot e][H_3^P \ H_3^S]^T = 0 \quad (3.11)$$

Also for codeword  $C4$

$$[b^4 \cdot e][H_4^P \ H_4^S]^T = 0 \quad (3.12)$$

In addition, the overall MPCGC codeword has the form:

$$C = [b^1 \ b^2 \ b^3 \ b^4 \ e] \quad (3.13)$$

Irregular LDPC codes have been used in all parity check matrix of MPCGC and it is known to outperform regular LDPC codes since the number of ones in each row and column is not constant, though always very small when compared with the whole size of the parity check matrix [57].

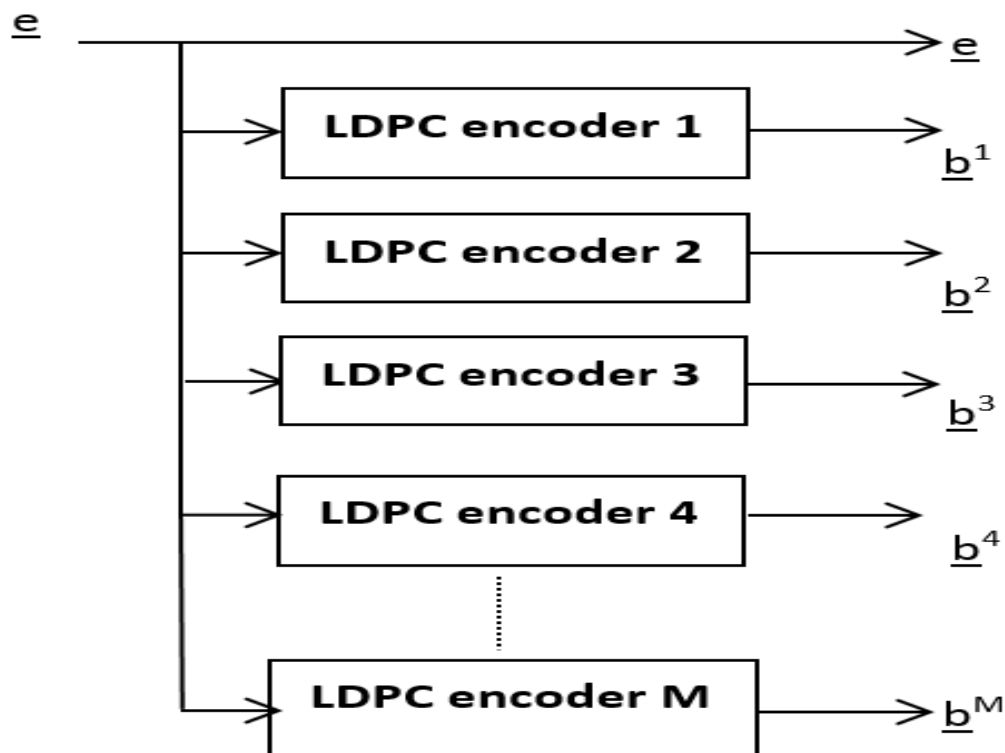


Figure 3.1 Block diagram of MPCGC Encoder of M LDPC component.

For further applications to the parallel concatenation of LDPC codes, we can use less complex MPCGC design, by choosing three LDPC components.

We can consider a code rate  $R=1/4$  and overall code length  $N=768$ , of MPCGC as a result of the concatenation of three LDPC codes with the same code rate  $R=1/2$  whose parity check matrices  $H_1$ ,  $H_2$  and  $H_3$  of dimensions  $(m \times n)$  where  $m=192$ ,  $n=384$ . Moreover, the remaining parameters of the MPCGC are  $MCW1=1.94$ ,  $MCW2=2.81$  and  $MCW3= 1.81$ ,  $N=768$  when using the parallel decoding process.

$$R = 1/(M + 1) = 1/(3 + 1) = 1/4$$

### 3.4 Proposed MPCGC Serial decoder

The output from the first LDPC decoder is directly passed on to the second component, while the output of the second decoder is passed on to the third decoder, then the output from the third decoder is passed on to the fourth component decoder, then the output of the fourth decoder is passed on to the first decoder and so on, as shown in Figure (3.2). This type of

decoding is called serial mode in which every LDPC decoder has to wait for the next decoder's output to start the decoding.

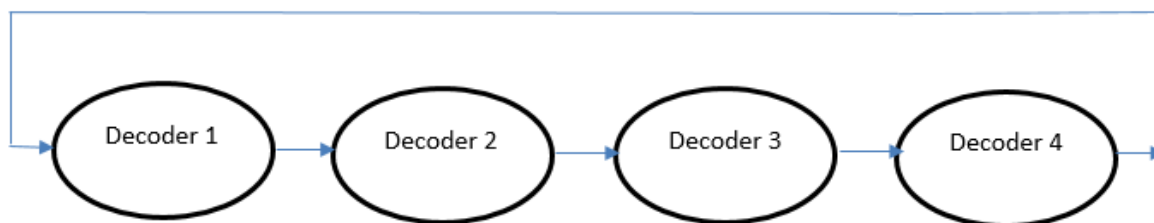


Figure 3.2 Serial decoding mode.

For less complexity from MPCGC design, we can also use 3 LDPC components at the decoder part.

During each super iteration, (M) component decoders, the serial decoder can be used as shown in Figure 3.3 below. All component decoders use the sum product algorithm as in the first super iteration; the a posteriori probabilities  $\underline{P}_1(\underline{u})$  of the (N) coded bits have been calculated using the received data ( $y^0$ ) and ( $y_1$ ) without applying information; also, the information data have been equally distributed as +1 or -1.

In the second LDPC component, the decoder calculates the second a posteriori probabilities  $\underline{P}_2(\underline{u})$  by using received sequences ( $y^0$ ) and ( $y_2$ ) alongside the a priori (extrinsic) information  $\underline{P}_{1e}(\underline{u})$  which is available from the first decoder. In addition, the decoder of the third LDPC component computes the third a posteriori probabilities  $\underline{P}_3(\underline{u})$  by using received sequences ( $y^0$ ) and ( $y_3$ ) along with the a priori (extrinsic) information  $\underline{P}_{2e}(\underline{u})$  available from the second decoder. Finally, in the fourth LDPC component, the decoder computes the fourth a posteriori probabilities  $\underline{P}_4(\underline{u})$  using received sequences ( $y^0$ ) and ( $y_4$ ) along with the a priori (extrinsic) information  $\underline{P}_{3e}(\underline{u})$  available from the third decoder.

The decoding process directly continues for the last decoder as well using received data ( $y^0$ ) and ( $y_M$ ) along with the a priori (extrinsic) information available from the previous component decoder  $\underline{P}_{m-1e}(\underline{u})$  in order to complete the calculation corresponding to the  $\underline{P}_2(\underline{u})$  for all M component decoders.

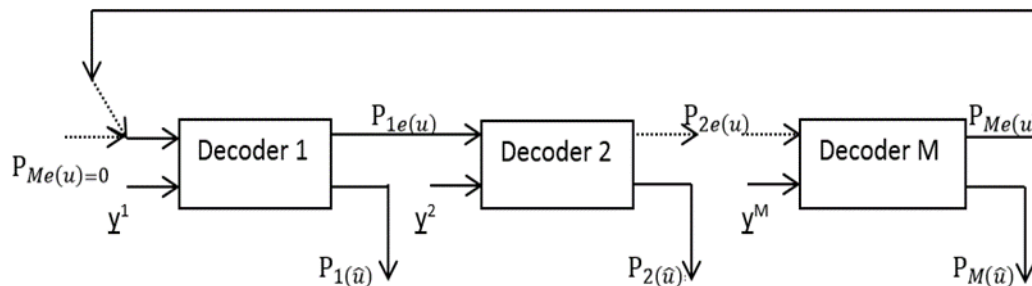


Figure 3.3 Block diagram of MPCGC serial decoder.

### 3.5 Proposed MPCGC Parallel decoder

During each super iteration, ( $M$ ) component decoders, the parallel decoder can be used as shown in Figure 3.4. All component decoders process information at the same time and use the sum product algorithm as in the first super iteration (all ( $M$ ) LDPC decoders launched simultaneously), each using the received sequence ( $y^0$ ) and ( $y^M$ ) without applying any a priori (extrinsic) since the information bit is equally  $+1$  or  $-1$ . Each LDPC component decoder computes alone the corresponding posteriori probabilities  $P_m(\underline{u})$  of the ( $N$ ) coded bits for a number of local iterations, and having to halt when either a known maximum number of local iterations is reached or if a codeword is found. After the first super iteration and during each subsequent super iteration, every component decoder gets its a priori information from the extrinsic information generated during the previous super iteration by all other ( $M-1$ ) decoders. The decoding process continues for all subsequent super iterations until all ( $M$ ) component decoders satisfy the valid codewords, or the super iterations is reached to the maximum number. Finally, the output of highest MCW value from the LDPC component decoder is stated as the best estimate of the transmitted sequence [6][51].

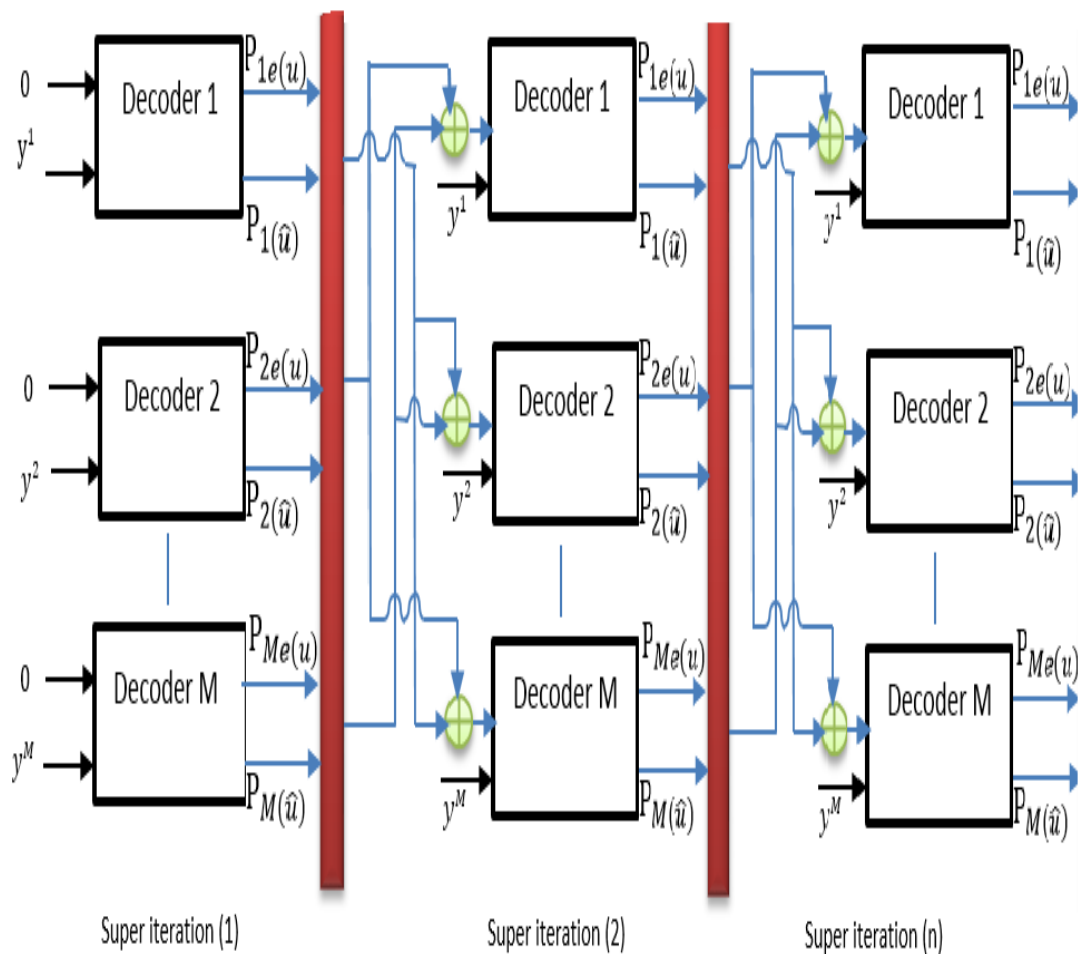


Figure 3.4 Block diagram of the proposed MPCGC decoder.

At MPCGC serial decoding, on the systematic bits the decoder is starting with the lower MCW because the a priori information not available. This produces higher extrinsic information that is advantageous to other LDPC components by speeding up until convergence, and then the higher MCW will start with the extrinsic output from the lower MCW component decoder.

MPCGC parallel decoding could be helpful in delaying sensitive applications so as to reduce the time of decoding, and the trade-off of this speeding up of the MPCGC parallel decoding will be partly degradation in performance, depending on the MCW values of the LDPC component when it is compared with the MPCGC serial decoding.

### 3.6 The Sum Product Algorithm (SPA)

In general, the decoders can be one shot receive inputs, compute the hard results and quit, or iterative where the message is being processed and modified via the internal decoder algorithm for many local cycles. In this case, the decoder should converge on a result and then quit the iterative algorithm when the hard decision is correct (i.e. it passes through the parity check matrix), or it quits after the maximum number of iterations has been completed and no satisfactory result has been calculated.

The LDPC decoder uses a soft-decoding iterative algorithm called Sum-Product Algorithm or SPA to calculate the result. In the LDPC decoder, the messages or data are being transferred between the variable and check nodes, and vice versa for iterative decoding. Soft decoding implies that the messages are not just single bit received values but actual probabilities of a received value being 1 or 0 [31]. This method is used to compute the a posteriori probability. During each super iteration, the component decoder receives intrinsic information from the channel along with a priori information from the other component decoder on the systematic information bits (except for the first super iteration).

The (SPA) is a message-passing algorithm that is executed on a bipartite graph. Messages are passed along the edges of the graph between the codeword nodes on the left part of the graph (variable nodes) and the parity check nodes on the right side (check nodes). The main reason for using SPA with likelihoods ratio probabilities instead of the logarithmic domain is to accommodate the a priori (extrinsic) information variable from the other component decoder [47].

The decoding begins with the variable nodes sending to their neighboring check nodes their received messages back and forth, and the decoding continues with a round of messages sent back and forth (and so on) from check nodes to variable nodes. Generally, the messages represent an estimate of the bit associated with the variable node terminal to the edge carrying the message [48]. The (SPA) algorithm can be calculated by following some equations and steps.

Let us consider the parity check matrix  $H$  of LDPC code of dimensions  $(m \times n)$ . The transmitted data vector is represented by  $\underline{x}$  and is of length  $n$  and the received noisy sequence is represented by  $\underline{y}$ . Then to find the most possible sequence  $\underline{x}$  according to  $Hx=0$  with the

likelihood of  $x=+1,-1$  according to the equation  $\prod_l f_l^x$ , let the Gaussian probability density function be centred at  $+1$ .

$$P(y_l|x_l = +1) = \frac{1}{\sqrt{2\pi}\sigma} e^{-\frac{(y_l-1)^2}{2\sigma^2}} \quad (3.14)$$

Also the probability of message vector  $x=+1$  at site  $l$  is

$$P(x_l = +1|y_l) = \frac{P(x_l=+1).P(y_l|x_l=+1)}{[P(x_l=+1).P(y_l|x_l = +1)] + [P(x_l=-1).P(y_l|x_l = -1)]} \quad (3.15)$$

The bits probabilities of the source information are equally

$$[P(x_l = +1) = P(x_l = -1) = \frac{1}{2}]$$

So the equation (3-15) can be as follow;

$$f_l^1 = P(x_l = +1|y_l) = \frac{1}{1 + \exp(\frac{-2y_l}{\sigma^2})} \quad (3.16)$$

Where,  $y_l$  is the channel's output

Also the message probability that equal  $[-1]$  at site  $l$  is

$$f_l^0 = 1 - f_l^1 \quad (3-17)$$

To compute the a priori information coming from other decoder component by updating equation (3-16) to

$$f_l^1 = \frac{1}{1 + \left[ \frac{P(x_l=-1)}{P(x_l=+1)} \right] \exp(\frac{-2y_l}{\sigma^2})} \quad (3.18)$$

Where,

$\frac{P(x_l=-1)}{P(x_l=+1)}$  denotes the a priori information obtainable from the other component decoders on the systematic information bits.

To produce the posteriori probabilities by (SPA) algorithm for all bits when the bipartite graph of  $H$  matrix included no cycles, the quantity  $q_{ml}^x$  means the probability that bit  $l$  of  $\underline{x}$  is  $x$  given the received information obtained by checks other than check  $m$  [64][65].

**Initialization:** the variables  $q_{ml}^0$  and  $q_{ml}^1$  are already initialized to the values  $f_l^0$  and  $f_l^1$ , respectively.

**Horizontal step,** we introduce  $\delta q_{ml} = q_{ml}^0 - q_{ml}^1$  then compute for each  $m, l$

$$\delta r_{ml} = \prod_{l \in N(m) \setminus l} \delta q_{ml} \quad (3-19)$$

Then set  $r_{ml}^0 = 1/2(1 + \delta r_{ml})$  and  $r_{ml}^1 = 1/2(1 - \delta r_{ml})$ .

**Vertical step,** for each  $l$  and  $m$  also for  $x=0, 1$  we modify

$$q_{ml}^x = \phi_{ml} f_l^x \prod_{m \in M(l) \setminus m} r_{ml}^x \quad (3-20)$$

Where,  $\phi_{ml}$  equal to  $q_{ml}^0 + q_{ml}^1 = 1$  as well as we can modify the pseudo-posterior probabilities  $q_l^0$  and  $q_l^1$  as follow

$$q_{ml}^x = \phi f_l^x \prod_{m \in M(l)} r_{ml}^x \quad (3-21)$$

The amounts are used to make a temporary bit-by-bit decoding  $x$ , if  $(Hx=0)$  then the decoding algorithm halts. On the other hand, the algorithm repeats from the horizontal step and when the maximum number of local iterations occurs without a valid decoding a failure is stated [1][40][41].

### 3.7 Iterative decoding of MPCGC

Maximum Likelihood decoders are not efficient on the bit error probability; therefore, the alternative solution is to choose Maximum A Posteriori (MAP), which is optimal in this case. Decoding of MPCGC is like the scenario of turbo decoding without using interleaver through the decoder component, as each LDPC decoder component computes the posteriori probability by using sum product algorithm (SPA) with modification to accommodate the priori (extrinsic) information available from other decoder components. Whereas, super iteration is the method of exchanging information between four component decoders, while local iteration is one complete cycle of (SPA) for single LDPC component.

The super iteration computes a specific number of local iterations of each component decoder before passing to other LDPC component. In addition, the process of exchanging any data between decoder components continuously until decoders converge on a valid codeword or a higher number of super iterations are achieved. The best estimation of the transmitted data

has been selected from the output of the higher MCW component of LDPC decoder [7][58]. All component decoders use the SPA in calculating their a posteriori probability.

At each super iteration, every component decoder uses their parity check matrix to run the SPA algorithm. MPCGC is flexible and allows the choice to stop the iterations without completed unnecessary super iterations when convergence has occurred.

Every super iteration and every component LDPC decoder makes a hard decision based on the updated a posteriori information, and verifies that it is a valid codeword. Whenever all component LDPC decoders declare a valid codeword, the MPCGC decoder will be terminated as shown in Figure 3.5. Moreover, in turbo decoding strategy, the turbo decoder has the option to go through a specific number of iterations even after a few iterations when convergence is declared [66].

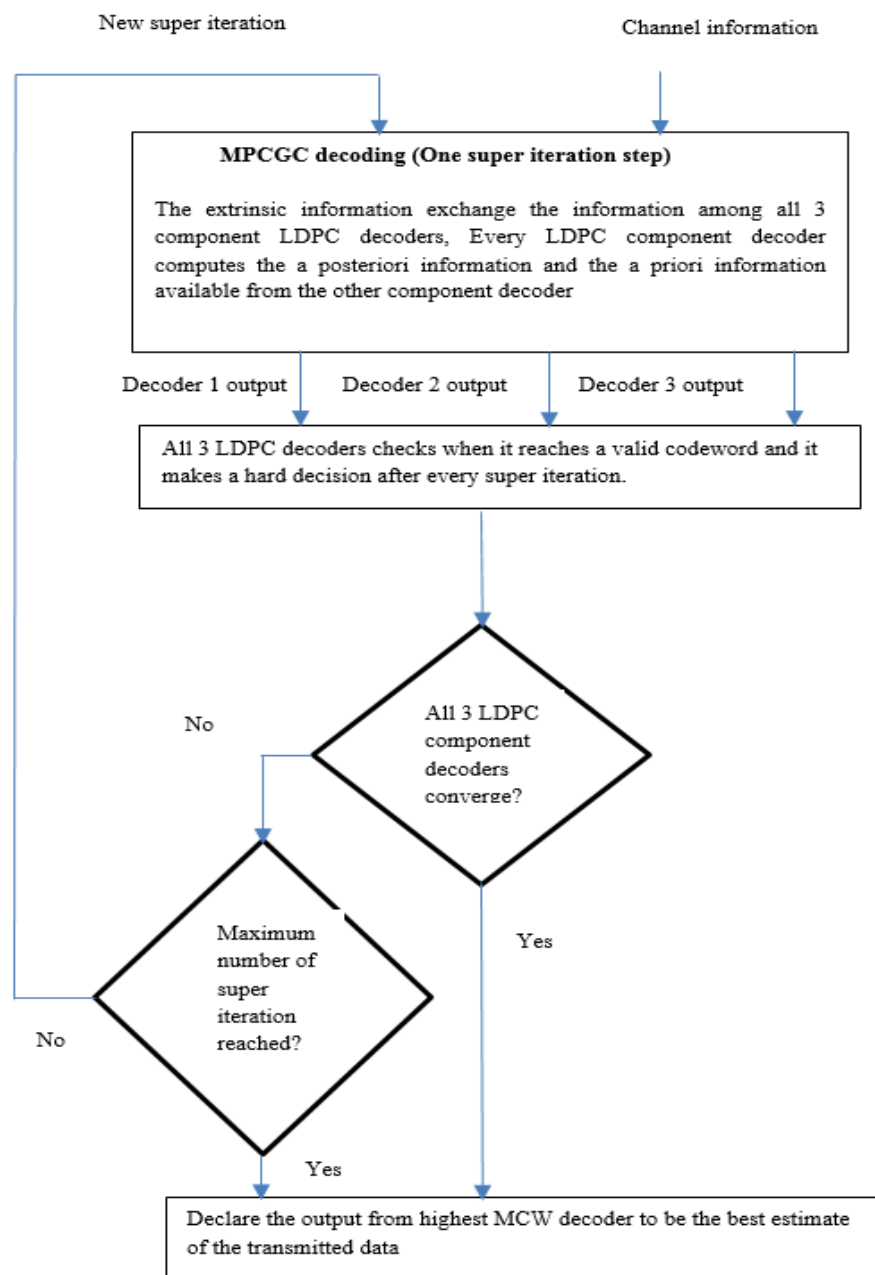


Figure 3.5 MPCGC decoding flow chart.

To calculate the BER of the proposed MPCGC system, the Monte Carlo method has been done as shown in the flow chart in Figure 3.6. To understand the calculations of the a priori (extrinsic) information among the component decoders, let's select the easiest way of the parallel concatenation by using two LDPC components that work together in parallel. Firstly, the received sequence bits from the channel were de-multiplex the total codeword into two component vectors  $y_1$  and  $y_2$  then deliver them to the first and second component LDPC decoder simultaneously. Secondly, each component decoder computes own posteriori

information then the extrinsic information will be calculated and exchanged to transfer to other component decoder to calculate the a priori information for the next super iteration of the MPCGC system as shown in Figure 3.7.

For MPCGC of three component decoders the performance is better than two or single components decoders but the trade off in the higher complexity due to the exchanging of the extrinsic information between the different decoder components. After the demultiplexer re-divided, the received sequence into three codewords  $y_1, y_2$  and  $y_3$  later transmitting them to the other components decoders simultaneously. Furthermore, the decoders in the first super iteration compute the calculations of exchanging the extrinsic information from the other two LDPC component decoders. Then updating of the equations (3-14), (3-15) and (3-18) to the equations (3-22) and (3-23) by adding the modulus factors  $k_1$  and  $k_2$  of the extrinsic information as a priori information. However, each component decoder computes own extrinsic information but the decoder exchanges the extrinsic information with the other two component decoders. Equations (3-22) and (3-23) represents how we calculate the extrinsic information among three component decoders [67].

$$f_l(1) = \frac{1}{1 + \left[ k_1 \left( \frac{p(x_l = -1|y_l)}{p(x_l = +1|y_l)} \right) k_2 \left( \frac{p(x_l = -1|y_l)}{p(x_l = +1|y_l)} \right) \exp \left( \frac{-2y_l}{\sigma^2} \right) \right]} \quad (3.22)$$

$$f_l(0) = \frac{1}{1 + \left[ k_1 \left( \frac{p(x_l = -1|y_l)}{p(x_l = +1|y_l)} \right) k_2 \left( \frac{p(x_l = -1|y_l)}{p(x_l = +1|y_l)} \right) \exp \left( \frac{2y_l}{\sigma^2} \right) \right]} \quad (3.23)$$

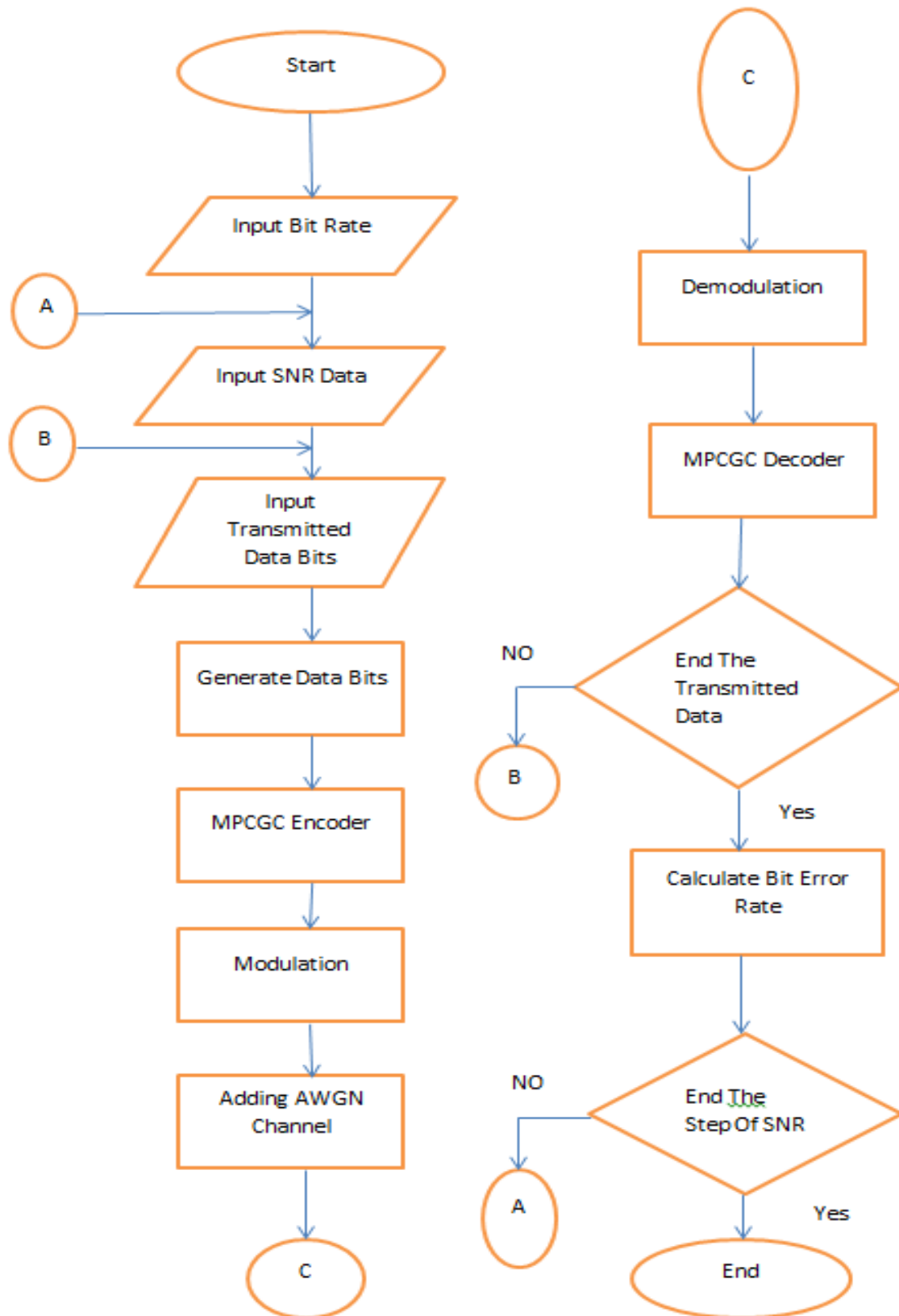


Figure 3.6 BER calculation according to the Monte Carlo method.

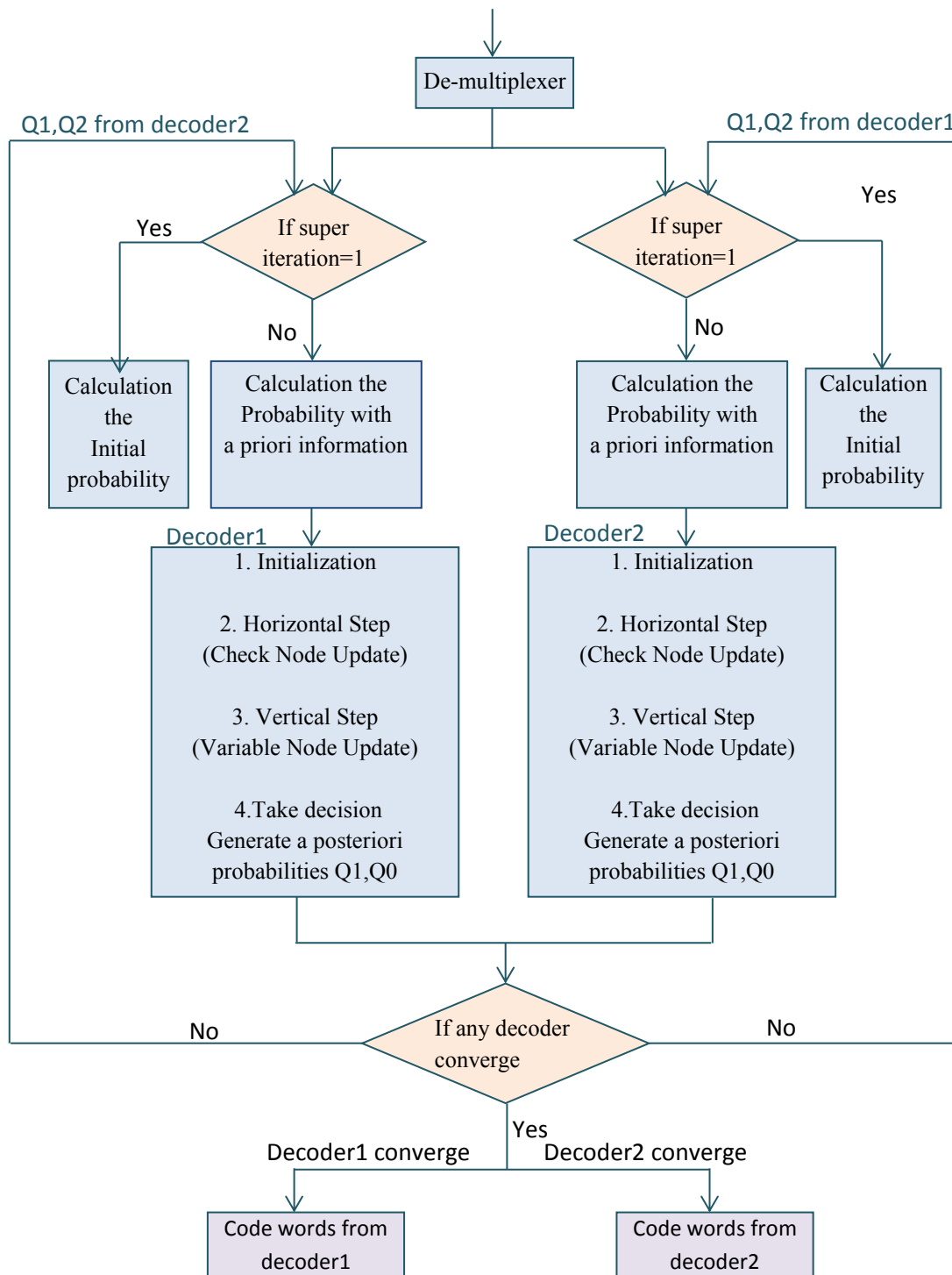


Figure 3.7 Decoding algorithm of two component decoders for MPCGC.

### 3.8 MCW Combination and code design

Selection of a proper combination of matrices is an important step because it has a direct impact on the BER performance, as the MPCGC contains a number of component decoders, and the parity check matrices should be different.

First of all, the MCW (Mean Column Weight) is to be discussed, which is the number of ‘1’s (the average number of column weight) in whole matrix, as each column has different column weights. In this regard, the minimum value should be 1 and the maximum value is defined as ‘m’. Moreover,  $\lambda_i$  is a fraction by which the proportion of columns is depicted whose weight is equal to i at the parity matrix. Thereafter, the MCW can be computed as under:

$$MCW \triangleq \sum_{i=1}^m i\lambda_i \quad (3.24)$$

According to an earlier research study, it was revealed that the LDPC codes having low MCW provides better BER performance compared to the higher MCWs at low to moderate ( $E_b/N_0$ ) region, while at high ( $E_b/N_0$ ) region, it gives poorer performance. The primary objective of the MCW design is selecting the low MCW at low to moderate ( $E_b/N_0$ ) region, while design high MCW at high ( $E_b/N_0$ ) region [63].

We can calculate the SNR (signal-to-noise ratio) on the basis of the mean value  $\mu$  and the variance value  $\sigma^2$  which are given below,

$$SNR = \frac{\mu^2}{\sigma^2} \quad (3.25)$$

At this point, mean value  $\mu$  can be calculated for log-likelihood on the basis of Gaussian distribution.

$$\mu = \frac{\sigma^2}{2} \quad (3.26)$$

For each individual LDPC codes having different MCWs, the probability analysis has been simplified by the Gaussian approximation through estimation technique rather than the actual probability density of extrinsic information is to be simulated. In this regard, the better quality of extrinsic information is represented by the higher SNR value [68].

To represent the quality of the extrinsic information of the MPCGC model. Three component parallel decoders are a simple way (less complex than four) to design and well study the exit

chart effect on the appropriate MCWs values (MCW1=1.94, MCW2=2.81 and MCW3=1.81) in each LDPC component decoder.

The SNR can be denoted by the SNR<sub>i</sub> for the a priori information, which represents the input bits for each LDPC component decoder, and the SNR for the extrinsic information (output bits) is basically the SNR<sub>o</sub>. It is comprehensible that better performance in low SNR<sub>i</sub> is demonstrated by the code with low MCW and a rapid increase in the SNR<sub>o</sub> is seen with relatively high MCW, as the SNR<sub>i</sub> is increased in moderate area. By upholding the desirable asymptotic performance, the decoding performance is increased by the combination of three parallel decoder schemes. In addition, to attain a good performance, the value of three MCWs is essential.

Figure 3.8, Figure 3.9 and Figure 3.10 represent the effect of the MCW in the extrinsic information at different Eb/N<sub>0</sub> regions 0 dB, 0.5 dB and 1.3 dB respectively. The Input-Output standard case is depicted by the diagonal dotted lines, while the (SNR<sub>o</sub>) versus (SNR<sub>i</sub>) of LDPC component decoders represented by their MCWs is demonstrated by the solid lines. At LDPC decoder, the output of the extrinsic information represents the SNR<sub>o</sub> and is directly calculated and measured. With the equation,  $\mu = 2 \times \text{SNR}_i$  and  $\sigma^2 = 4 \times \text{SNR}_i$ , the a-priori inputs to the LDPC decoders (SNR<sub>i</sub>) are assumed to have Gaussian pdfs [63]. While associating SNR<sub>o</sub> of various MCWs decoders with the Input=Output, the standard case suggests that at low Eb/N<sub>0</sub> region, the coding can decrease the SNR<sub>o</sub> instead of increasing it, if not designed correctly. It is easy to understand that besides quickly generating higher SNR<sub>o</sub>, codes with maximum MCWs would begin to take control with the increase in the SNR<sub>i</sub>. Nevertheless, in case of low SNR<sub>i</sub>, they all together bad at lower MCWs [69].

In a multiple parallel concatenation scheme, the system used three LDPC codes for reducing the BER at low to moderate Eb/N<sub>0</sub> region while keeping the desirable asymptotic performance.

A comparatively lower MCW is entailed in the first code as shown in Figure 3.8, which has the potential to offer maximum SNR<sub>1o</sub> in the early few iterations especially when low SNR<sub>1i</sub>. From the first component decoder, the MPCGCs decoder would be driven by the relatively high SNR<sub>1o</sub> for quick convergence, as it cause (as a priori information SNR<sub>i</sub>) to the other LDPC component.

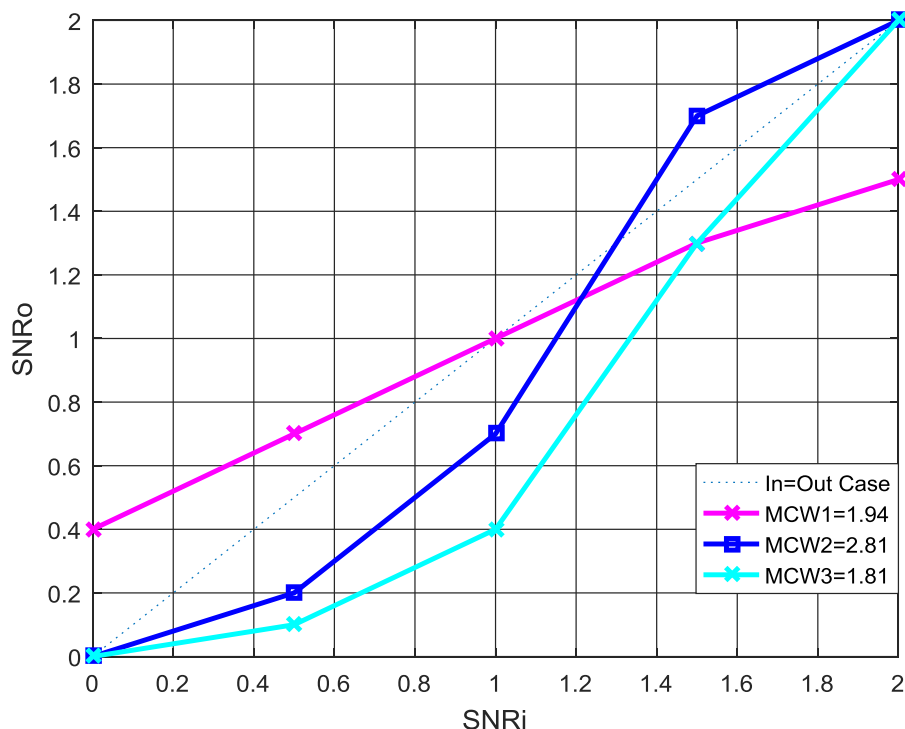


Figure 3.8 Design effect of MCW on the extrinsic information quality at  $E_b/N_0=0$  dB.

Since the higher  $MCW=2.81$  of the second component decoder as shown in Figure 3.9 is rapidly directed to the cross point, where it goes ahead by developing maximum  $SNR_{2o}$  and the phenomenon converges as a result. Furthermore, the higher  $SNR_o$  as it cause (as a priori information  $SNR_i$ ) to the third component decoder. The final code has lower  $MCW=1.81$  in the third component decoder as shown in Figure 3.10 producing higher  $SNR_o$  leads to converge faster. To give the optimum performance possible under the code length constraints and given  $E_b/N_0$ , the MPCGC decoder parameters (code length,  $MCW_1$ ,  $MCW_2$ ,  $MCW_3$ ) are optimized, so that the codes that demonstrate a great performance around a specific  $E_b/N_0$  could be designed. Upon selecting  $MCW_1$ ,  $MCW_2$  and  $MCW_3$ , a completely designed (higher than the Input-Output case) output extrinsic information provided by any these component codes was maintained as desired. The optimum codes combination was chosen so that this condition could be fulfilled at the specified  $E_b/N_0$ . Since lower minimum distance is usually maintained by the low  $MCW$  codes, they do not exhibit consistent output at higher  $E_b/N_0$ . Hence, to achieve maximum  $SNR_o$  at low  $SNR_i$ , they were only used. Accordingly, the component codes containing the entire  $SNR_o$  region were applied in our design method. However, we attempted to use those as well, which were having a cross point

at lower SNRi. When the cross point is attained, the decoding responsibilities would be expedited from the lower to the maximum MCW decoder as a result of this method.

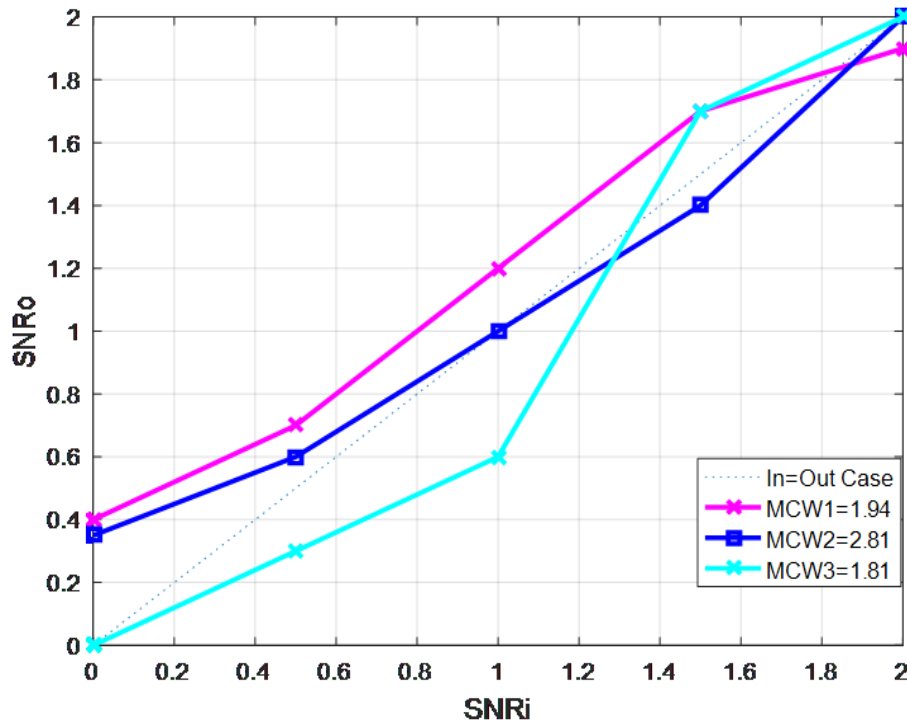


Figure 3.9 Design effect of MCW on the extrinsic information quality at  $E_b/N_0=0.5$  dB.

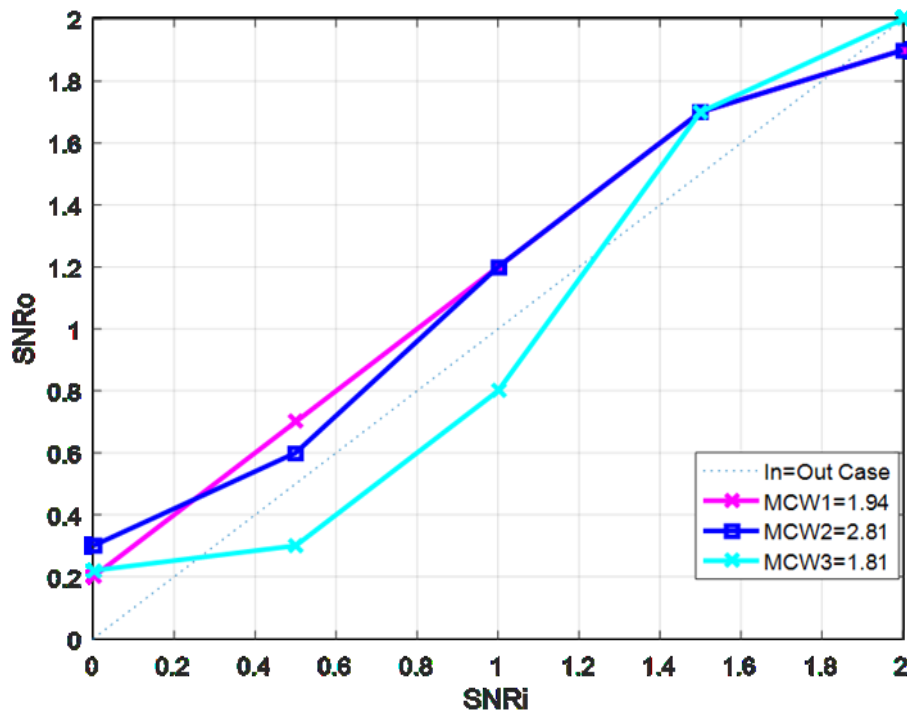


Figure 3.10 Design effect of MCW on the extrinsic information quality at  $E_b/N_0=1.3$  dB.

### 3.9 Simulation and analysis

#### 3.9.1 BER performance analysis

Firstly, the characteristics of MPCGCs are evaluated separately using multiple LDPC component codes. Where, the number of the component decoders has effect on the performance and the complexity of the system. In the case of the four component decoders, the received information part with overall code rate  $R=1/5$  are divided into four equal parts for LDPC component decoders as shown in Figure (3.11) with each code rate  $R=1/2$  and the dimension of the parity check matrix is  $H(200, 400)$ . Furthermore, each LDPC component decoder processes the codewords to receive the main information.

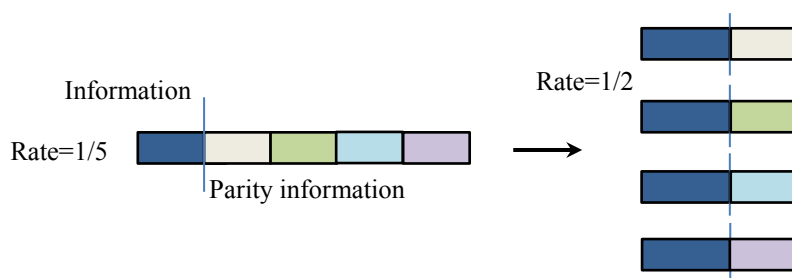


Figure 3.11 Design of four components decoder.

At the transmitter side, the codeword after encoder part is consist from systematic data. Furthermore, the codeword has included the information bits with the parity bits of the four LDPC components. At the receiver side, the performance evaluation was being conducted for perfect channel state information CSI at the receiver; the performance analysis supposed that the channel parameters are well known at the receiver.

Each component decoder is allowed a maximum of 38 local iterations because the maximum number of the local iterations in each LDPC component will not exceed than this value whereas the overall MPCGCs have 30 super iterations. The BER performance of the MPCGC-BPSK over AWGN channel is evaluated and is illustrated in Figure 3.12. The parameters of the four LDPC parallel components of MPCGC have the same parity check dimensions,  $H(800, 1000)$  with different MCWs: code rate  $R=1/5$ ,  $MCW_1=2.04$ ,  $MCW_2=2.73$ ,  $MCW_3=2.79$  and  $MCW_4= 1.89$  with overall code length  $N=1000$ . Furthermore, the parameter of the four LDPC serial components of MPCGC have the same parity check dimensions,  $H(800, 1000)$  with different MCWs: code rate  $R=1/5$ ,  $MCW_1=2$ ,  $MCW_2=2.55$ ,  $MCW_3=2.79$  and  $MCW_4= 2.35$  with overall code length  $N=1000$ . Again, the parameters of the equivalent single irregular LDPC code that is used for comparison are

$R=1/5$ ,  $MCW= 2.7$ ,  $N=1000$ . As shown in Figure 3.12, the parallel MPCGC has a gain of 0.2 dB (at BER  $2e-4$ ) when compared to the equivalent single irregular LDPC with the same parameters. Moreover, the parallel MPCGC provide 0.4 dB gain compared to the serial MPCGC, also, single LDPC has a gain 0.25 dB compared with serial MPCGC decoder. However, the serial MPCGC performs worse than parallel MPCGC decoder and single component LDPC decoder.

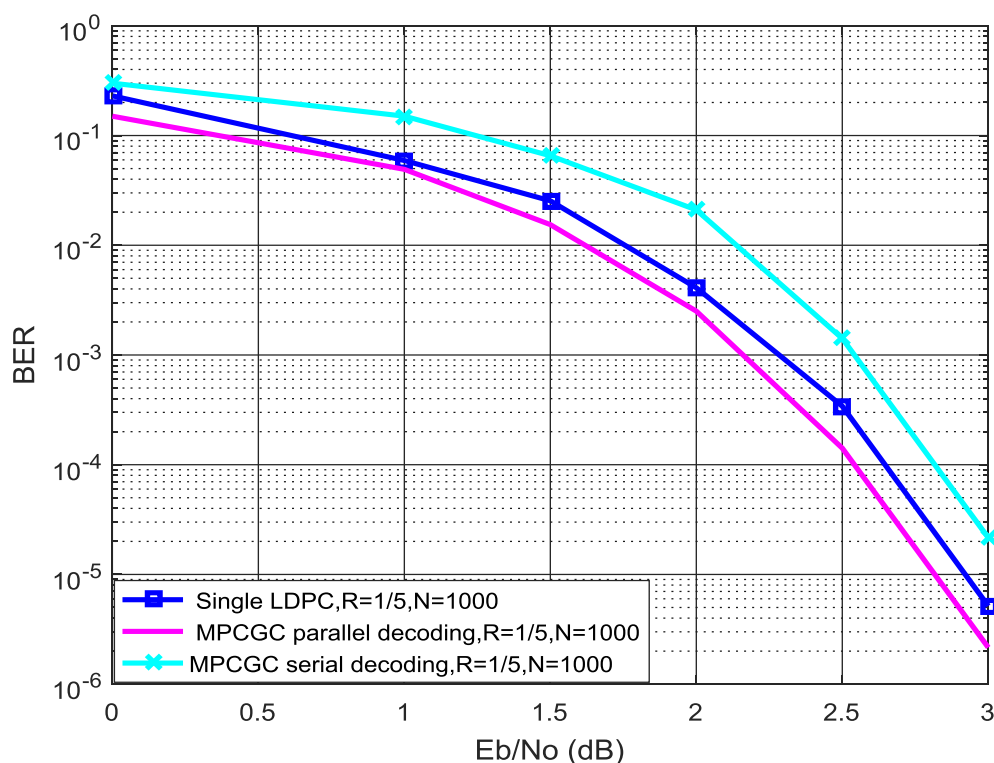


Figure 3.12 BER comparisons for different LDPC coding model over AWGN channel.

To study the effect of different MCW on the performance of the LDPC codes as shown in Figure 3.13, the parallel MPCGC at high  $E_b/N_0$  region has a gain of 0.3 dB (at BER  $2e-4$ ) when compared to the equivalent single irregular LDPC with less MCW at the same parameters. Moreover, the performance of the single LDPC codes with high MCW outperform the performance of the single LDPC codes with less MCW at only low  $E_b/N_0$  region. The complexity of the MPCGC for four components decoder is higher than the complexity of three component decoder as will be explained in the next section; therefore we will focus more on the performance of MPCGC of three component decoders.

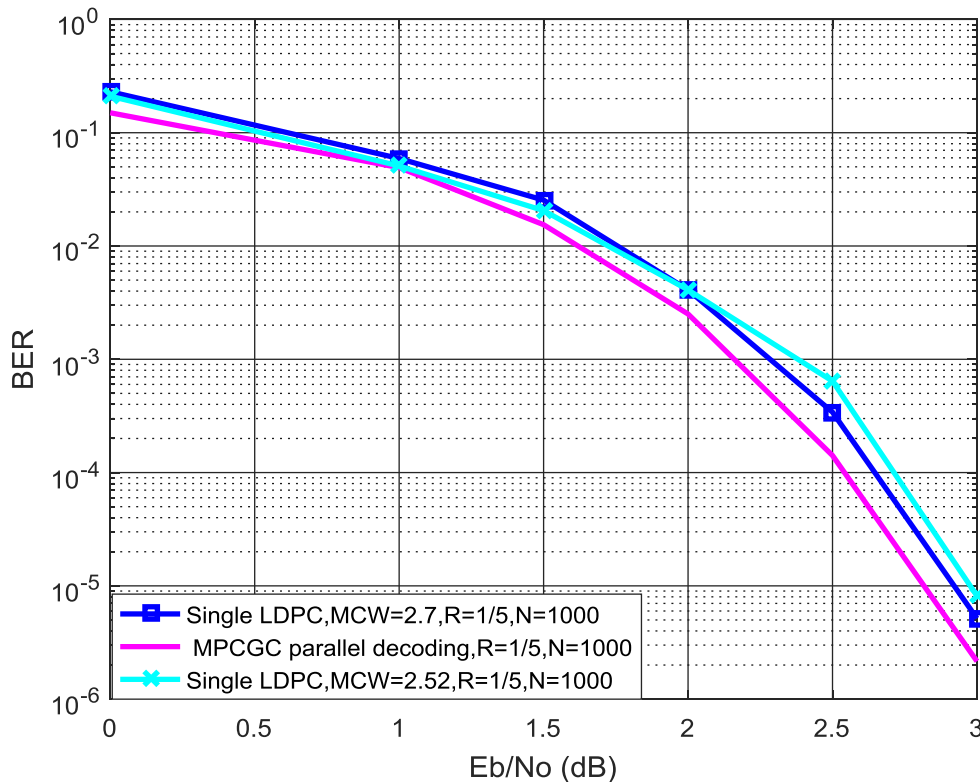


Figure 3.13 Effect of MCW on the different LDPC coding model over AWGN channel.

In the case of the three component decoders, the received information part with overall code rate  $R=1/4$  are divided into three equally parts for LDPC component decoders as shown in Figure 3.14 with each code rate  $R=1/2$  and the dimension of the parity check matrix is  $H(192, 384)$ . Furthermore, each LDPC component decoder processes the codewords to receive the main information.

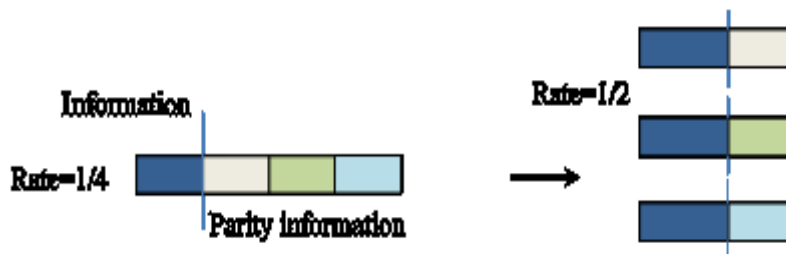


Figure 3.14 Design of three component decoder.

**Secondly**, the characteristics of MPCGCs parallel decoding are evaluated separately, by using three LDPC component codes where each component is allowed a maximum of 38

local iterations whereas the overall MPCGCs have 30 super iterations. The parameters of the three parallel LDPC components of MPCGC have the same parity check dimensions,  $H$  (192,384) with different MCWs: the overall code rate  $R=1/4$ ,  $MCW_1=1.94$ ,  $MCW_2=2.81$ ,  $MCW_3=1.81$  and  $N=768$ . Again, the parameters of the single irregular LDPC code that is used for comparison are  $R=1/4$ ,  $N=768$  and  $MCW=3.0794$  with 50 local iterations. The BER performance of the MPCGC-BPSK over AWGN channel is evaluated and illustrated in Figure 3.15, the MPCGC has a gain of 0.8 dB (at BER  $2e-4$ ) when compared to the conventional single irregular LDPC at the same parameters. Furthermore, the MPCGC performance outperforms by 1.3 dB (at BER  $1e-3$ ) compared with the serial MPCGC decoder with parameters:  $R=1/4$ ,  $MCW_1=2$ ,  $MCW_2=2.56$ ,  $MCW_3=2.67$ .

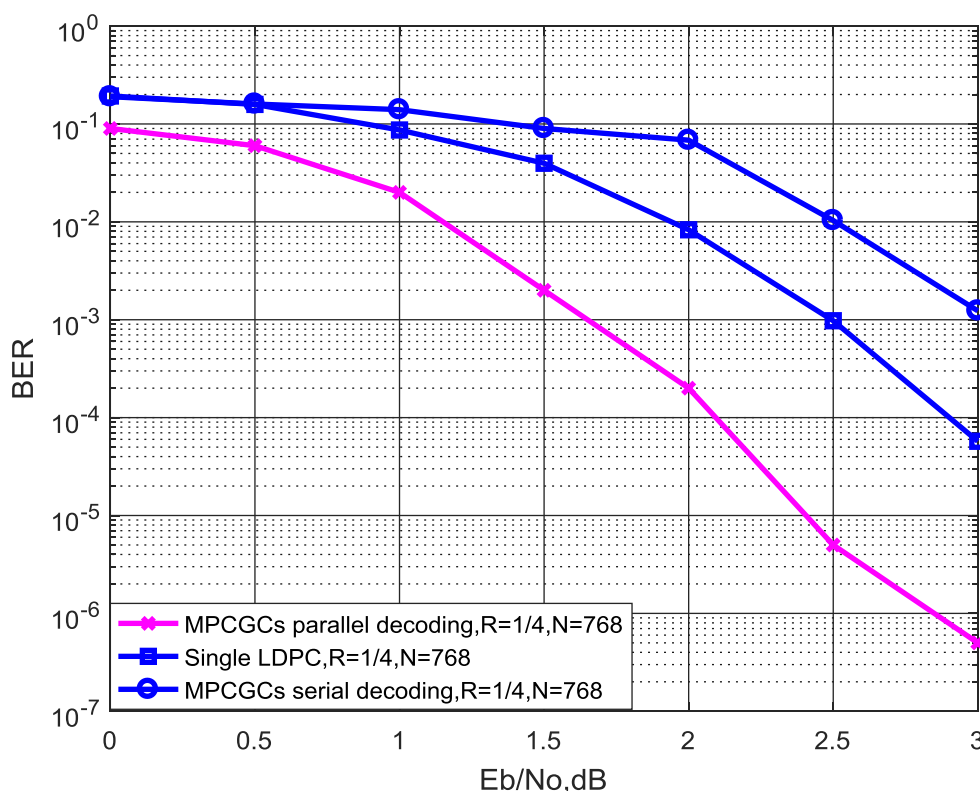


Figure 3.15 BER comparison for different LDPC coding model over AWGN channel.

Moreover, the MPCGC shows 0.2 dB gain improvements at ((at BER  $2e-4$ )) when compared with the result reported by Kim et. al using the same parameters [70] as shown in Figure 3.16.

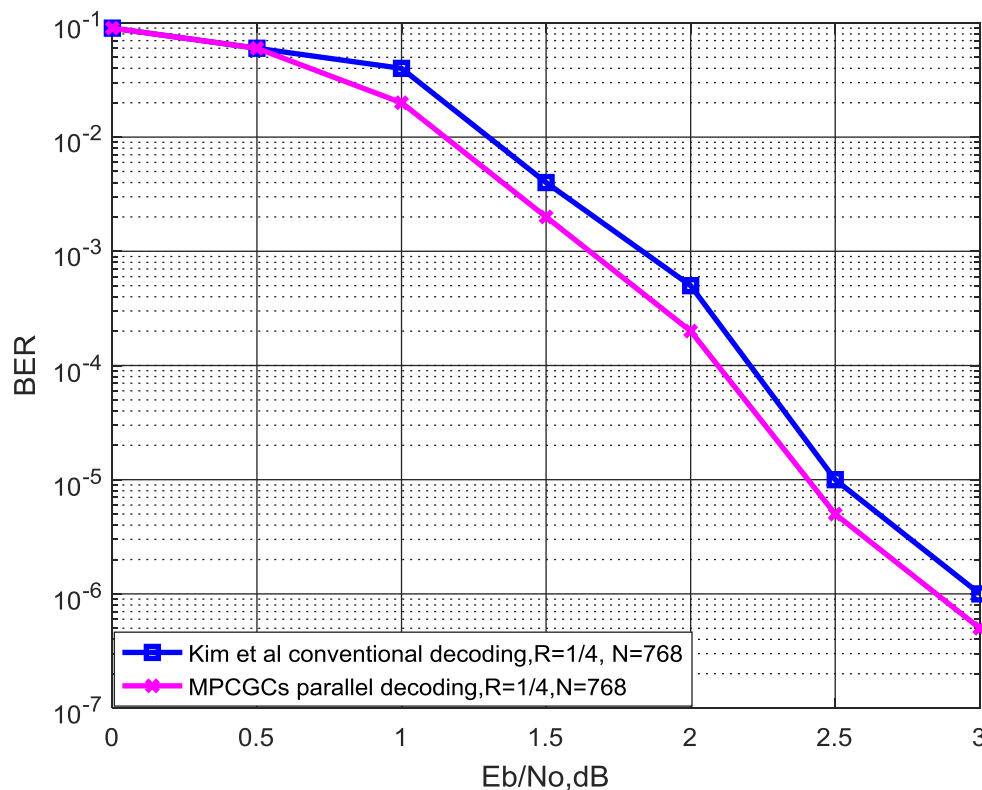


Figure (3.16) BER comparison for different parallel concatenation LDPC coding model over AWGN channel.

For multi-level modulation and bandwidth efficiency in wireless communication system, we utilized and analyzed the MPCGC of the three parallel LDPC codes with multilevel modulation scheme such 64 QAM.

The BER performance of the MPCGC-64 QAM over AWGN channel is evaluated and is illustrated in Figure 3.17, the MPCGC-64 QAM has a gain of 0.7 dB (at BER  $1e-4$ ) when compared to the conventional single irregular LDPC at the same parameters.

**Thirdly**, the maximum capacity achieved for MPCGC system for both modulation BPSK and 64 QAM over AWGN channel has been calculated according to the BER calculation. The MPCGC parameters are used for capacity calculation as follows, the overall code rate  $R=1/4$ ,  $MCW_1=1.94$ ,  $MCW_2=2.81$ ,  $MCW_3=1.81$  and  $N=768$  the parameters of the single irregular LDPC code that is used for comparison are  $R=1/4$ ,  $N=768$  and  $MCW=3.0794$ .

Figure 3.18 shows that MPCGC-BPSK provides has better capacity achieved at compared to the conventional single LDPC.

In addition, Figure 3.19 shows that the capacity achieved of MPCGC-64 QAM is higher compared to the conventional single LDPC.

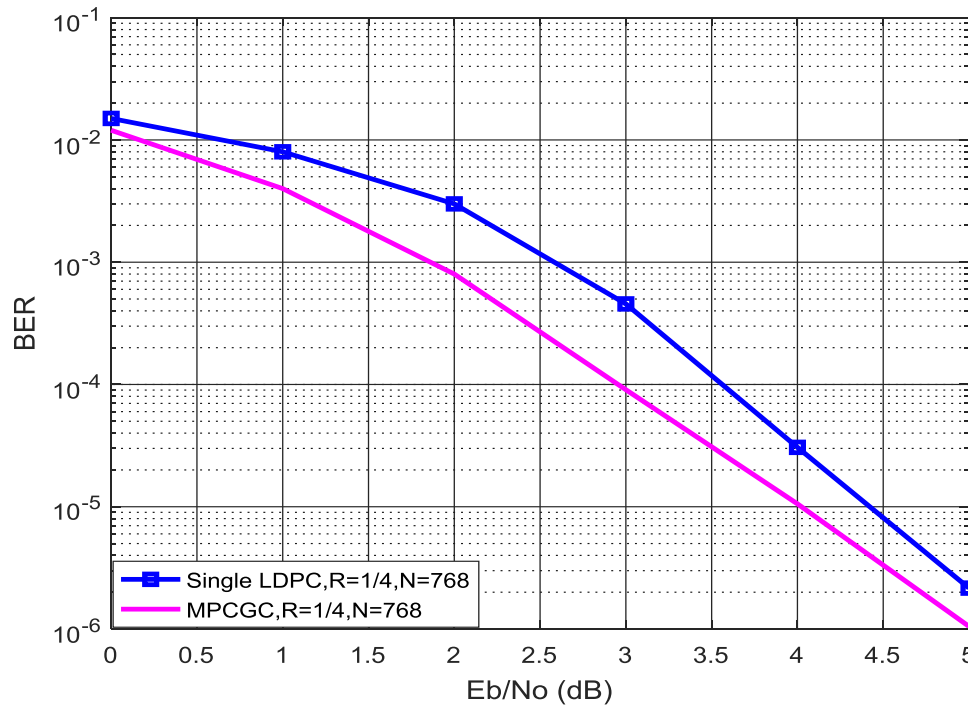


Figure 3.17 BER comparison for different LDPC coding model over AWGN channel.

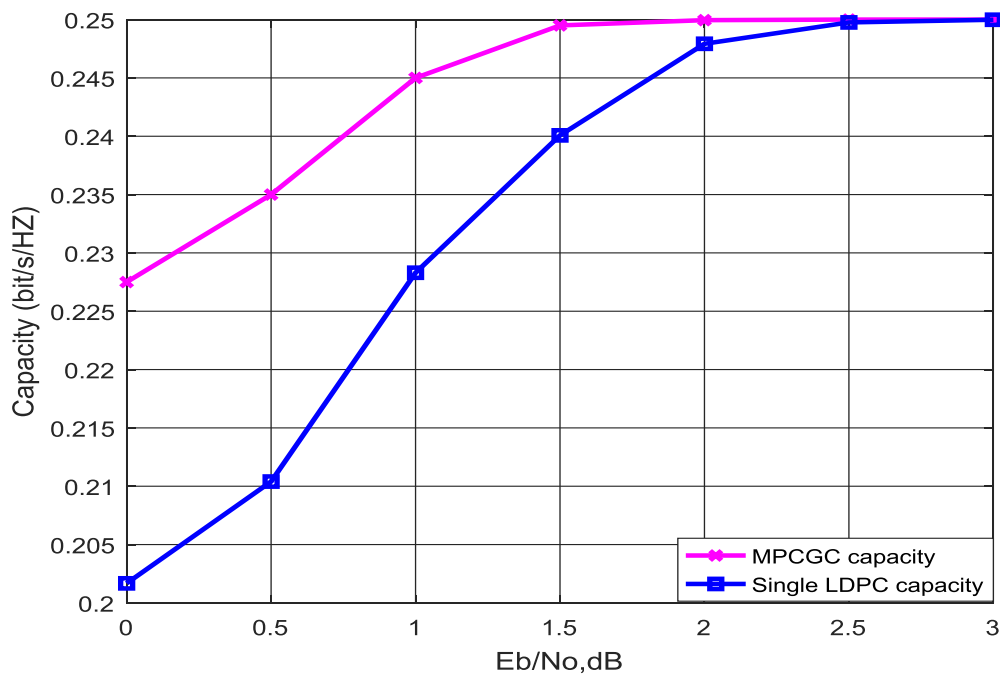


Figure 3.18 Capacity achieved for different coding model over AWGN channel.

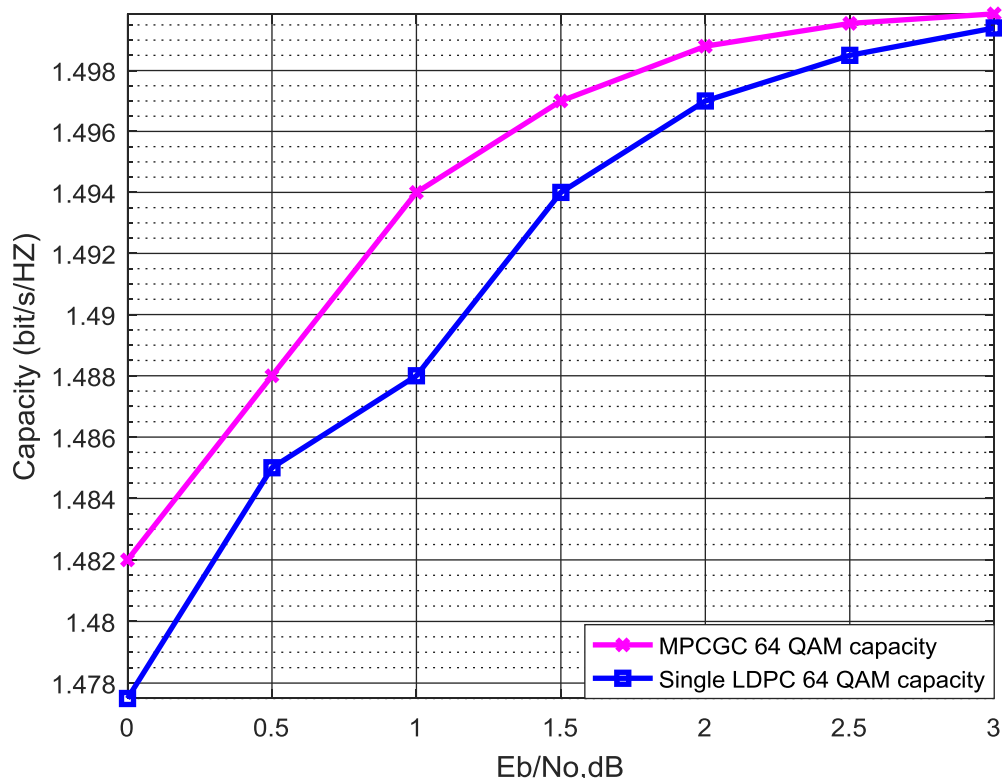


Figure 3.19 Capacity achieved for different coding model over AWGN channel.

### 3.9.2 MPCGC complexity analysis

LDPC complexity for a particular code is proportional to the type of decoder and the density of the parity check matrix. The sum product algorithm has an important advantage in reduced complexity in turbo codes. To estimate the complexity of MPCGC, we calculated the average number of local iterations per each LDPC code needed with different  $E_b/N_0$  values [48]. Firstly, in our case, a MPCGC of three parallel component decoders executes a maximum of 30 super iterations; each component decoder in each super iteration performs a maximum of 38 local iterations at the received data then passes the extrinsic information to the next decoder and so on. The MPCGC decoder generally for each super iteration performs a maximum of  $(3 \times 38)$  local iterations, which are done by 3 LDPC decoders. For the sake of a fair comparison between MPCGC and LDPC codes, the decoding complexity per iteration can be estimated in terms of the maximum number of edges in the Tanner graph of the code which can be calculated as  $(N \times MCW)$  for a single LDPC code [71]. Therefore for a MPCGC in each super iteration, the maximum number of edges can be calculated according to,

$$\text{Total edges} = \text{Number of iterations} \sum_{i=1}^M N_i M C W_i \quad (3.27)$$

On this basis, a preliminary complexity analysis and comparison have been carried out in terms of Eb/No and the results in terms of the maximum number of iterations and edges are given in Table (3.1) and illustrated in Figures 3.20 and 3.21. The results show that the advantages of MPCGC can be exploited without significant additional complexity.

Table 3.1 Complexity comparisons results.

Eb/No	BER		PER		Iterations		Total Edges	
	LDPC	MPCGC	LDPC	MPCGC	LDPC	MPCGC	LDPC	MPCGC
0	1.9e-1	9e-2	9.8e-1	7 e-1	3.42e3	3.1e3	8.01e6	7.82e6
0.5	1e-1	7e-2	9 e-1	5e-1	3.35e3	2.49e3	7.87e6	4.92e6
1	7.6e-2	2e-2	5 e-1	1e-1	1.20e2	1.27e3	2.80e6	3.18e6
1.5	1e-2	1.3e-3	2.4e-1	1.1 e-2	400	500	9.42e5	1.25e6
2	1e-3	2e-4	7 e-2	1.2 e-3	305	400	7.42e5	9.37e5

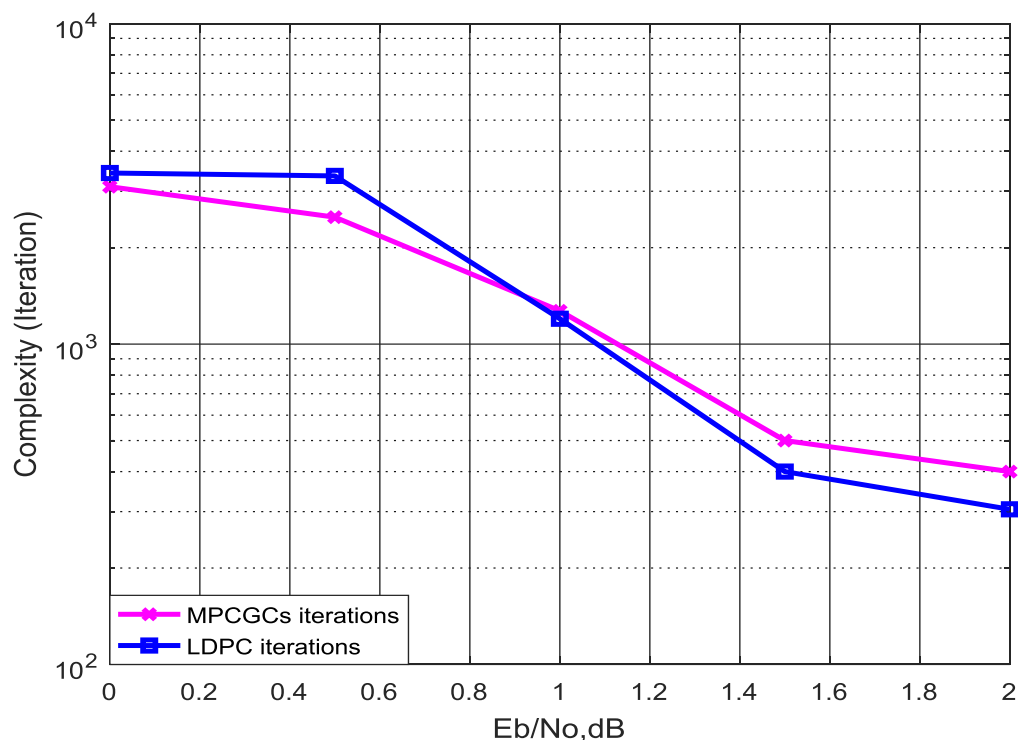


Figure 3.20 Complexity and performance comparison between LDPC and MPCGC.

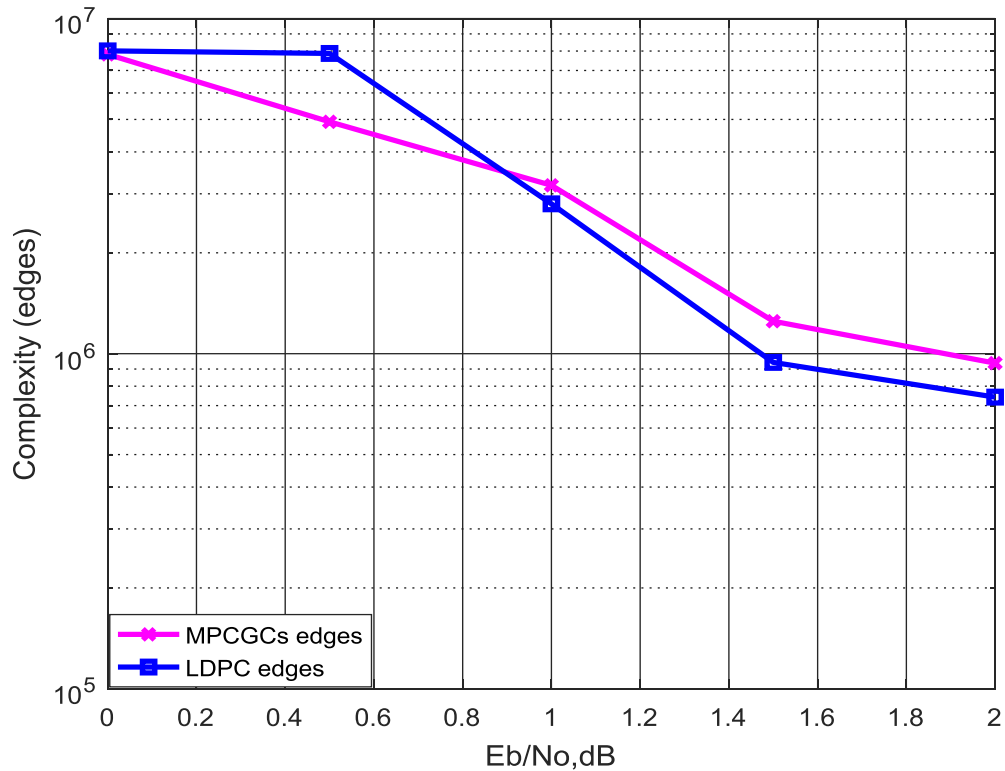


Figure 3.21 Complexity and performance comparison between LDPC and MPCGC.

Secondly, the results show that the complexity of the proposed 4 components MPCGCs exploited higher decoding complexity when compared with the conventional MPCGC system in terms of iterations and edges as shown in Figures 3.22 and 3.23. Moreover, the advantages of the conventional MPCGCs can be exploited without significant additional complexity.

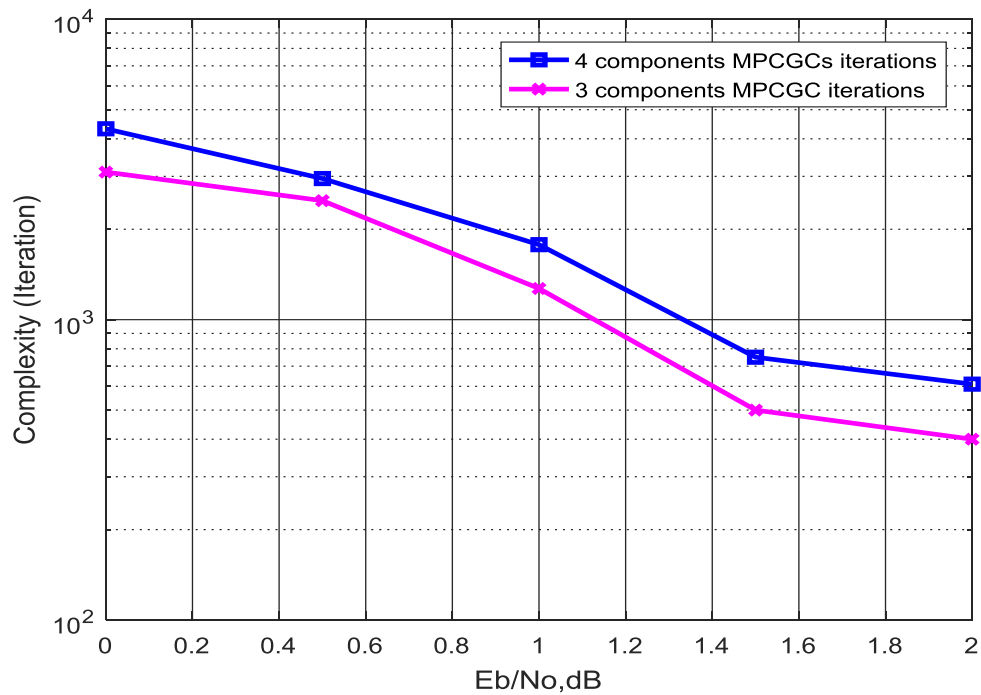


Figure 3.22 Complexity and performance comparison between different components of MPCGC.

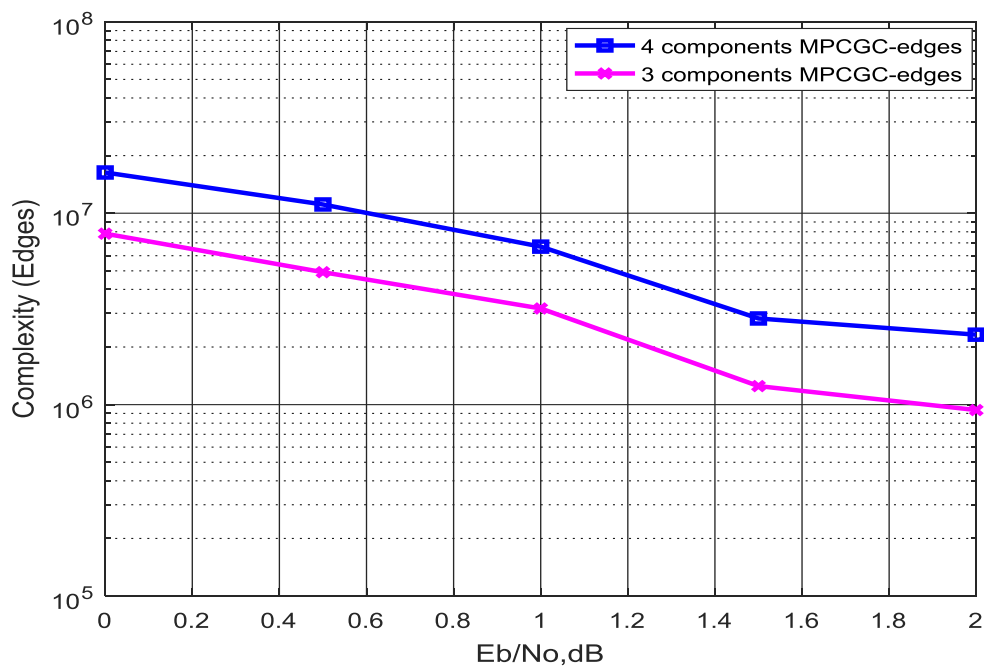


Figure 3.23 Complexity and performance comparison between different components of MPCGC.

### **3.10 Summary**

This chapter focused on the performance of the MPCGC scheme evaluated over a BPSK-AWGN channel. It is shown that the MPCGC structure yields superior coding performance in both three and four components LDPC decoders configurations when compared to the original single-long LDPC component with the same parameters. In addition, MPCGC has higher capacity achieved compared to the single conventional LDPC. It is also shown that the good design for MCW values of MPCGC provides better performance than random variables.

The preliminary complexity analysis in terms of number of edges and iterations has shown that the MPCGC structure does not incur significant additional cost in low  $E_b/N_0$  region. But at high  $E_b/N_0$  region the complexity in terms of iterations and total edges has increased due to the increasing in the MCW value of the second LDPC component. This increasing in MCW leads to increasing in the density (numbers of 1) of the parity check bits and then a lot of iterations and edges will be needed until converge to the valid codeword.

MPCGC flexibility and performance have the ability to be attractive in applications requiring flexibility while maintaining/ improving system performance with reduced implementation overheads.

## Chapter 4

# Efficient Puncturing Method For Multiple Parallel Concatenated Gallager Codes

### 4.1 Introduction

In this chapter, we propose a novel and efficient puncturing method for Multiple Parallel Concatenated Gallager Codes (MPCGC). MPCGC uses low-density parity check code (LDPC) as component codes for generating variables of code rates and reducing the decoding complexity for different applications. The proposed punctured MPCGCs system is analyzed over AWGN and flat Rayleigh fading channels. Simulation results show improved performance when compared to a single long LDPC code with the same parameters before and after puncturing. The proposed MPCGCs structure have the potential to be deployed in applications where flexibility in forward error control coding is required with reduced encoding and decoding complexity.

The so-called turbo code structure underlying MPCGCs helps to conquer the encoding and decoding complexity of a long code into less complex steps, while maintaining the information flow between the component decoders and reducing any information loss between the decoding steps [7]. In this chapter, we further explore MPCGCs by evaluating these codes for both AWGN and flat Rayleigh fading channels and investigating the puncturing of these codes and any performance improvements. The puncturing of parity check bits is applied to forward error correction (FEC) codes in order to design the best rate compatible (RC) codes to obtain a higher code rate from a low rate mother code [55]- [56].

In [74] a method from fundamental properties of punctured LDPC codes is presented and considered. This method depends on the puncturing threshold to obtain lower bounds on the achievable rates over memoryless binary input output symmetric (MBIOS) channels. Moreover, there are two advantages for achievable rate compatible LDPC codes. First, at high code rates the performance degradation had been reduced. Second, it is used with finite length codes without needing to optimize the puncturing properties. In [75] an efficient process to predict iterative belief propagation (BP) is studied using randomly punctured LDPC code ensembles over a binary input AWGN channel. In addition, the results obtained

show that the predictions were accurate compared with values that were calculated using density evolution for different puncturing.

In [76], a good LDPC puncturing distribution for rate compatible punctured code (RCPC) was investigated and analyzed with Gaussian Approximation. The results show the convergence performance of punctured LDPC codes and the capability to predict the asymptotic performance. In [77][78], the achievable rates and decoding complexity of punctured LDPC codes over parallel channels is considered and discussed. The results focused on the derivation of upper bounds of the ensemble LDPC codes using maximum likelihood (ML) decoding over parallel MBIOS channel.

In the rest of the chapter, in section 4.2, presents the concept of the puncturing and the proposed system model. In section 4.3, we present the encoding process of the punctured MPCGC. The decoding process of the punctured MPCGC is given in section 4.4. Followed in section 4.5, by evaluating the BER and PER (packet error rate) for MPCGC and show improved performance when compared with single LDPC codes with the same parameters under both regular, irregular and random puncturing. We show that higher coding gain is achieved with irregular puncturing of MPCGC. Furthermore, complexity analysis of the proposed punctured MPCGC is presented and evaluated in terms of the maximum number of iterations and edges and compared to the conventional MPCGC model. Finally, the chapter summary is presented in the section 4.6.

## 4.2 Punctured MPCGC codes

To apply puncturing in MPCGC[79][80], let us consider the code rate  $R=k/n$ , where  $k$ ,  $n$  are the length of the information bits and codeword, respectively. The diagram of the proposed system is shown in Figure 4.1.

For any codeword length and code rate the proposed puncturing methods can be made for the codeword. A subset of the codeword bits are removed before the codeword is transmitted to the receiver. A set of  $x$  bits punctured from the codeword has the effect of minimizing the length of the codeword from  $n$  to  $n - x$ . After puncturing a codeword with a puncturing fraction  $\Theta = x / n$ , the resulting code rate is

$$R_{new}(\Theta) = \frac{R_{old}}{1-\Theta} \quad \Theta \in (0,1) \quad (4.1)$$

Where  $R_{\text{new}}$  and  $R_{\text{old}}$  represent the new and mother code rate respectively, and  $R_{\text{new}}(0) = R$  is the original (unpunctured) code rate. In this chapter, we study and analyze three different methods to puncture the resulting MPCGC codeword as shown in the example in Figure 4.2. To study these methods, we use an MPCGC with a code rate  $R=1/4$  with information bits  $k=192$  and total code length  $N=768$  with 3 component codes each of code length  $n=384$  with a code rate  $R=1/2$ .

The aim of using puncturing with MPCGCs is to maximize the code rate from  $1/4$  to  $1/2$ . In the first method, after the MPCGC encoder stage the ensemble bits are randomly punctured by removing random parity bits from each component LDPC codeword. There are two ways for removing random bits. Firstly, removing random 128 bits from each component LDPC codeword to ensure getting the overall 192 parity bits that is lead to reduce the new codeword to half but, this procedure provides worse BER performance compared with the other methods.

Secondly, the random puncturing is performed by removing randomly fixed sequence of 384 bits from the codeword to keep only 192 parity check bits to let the overall code rate equal  $1/2$ . Moreover, to remove 384 bits from the codeword we need randomly removing 92,142 and 150 bits respectively from the three parity bits.

The first 92 bits have been removed from the first parity check ( $\overline{P1}$ ), as well as removing randomly fixed sequence 142 bits from the second parity check ( $\overline{P2}$ ) and removing randomly fixed sequence 150 bits from the third parity check ( $\overline{P3}$ ) respectively.

In the second method, the ensemble bits are punctured regularly, which means removing a fixed part from bits at the same location from each component LDPC codeword. The regular puncturing is performed by removing fixed 128 bits from the end of the first parity check ( $\overline{P1}$ ), also removing fixed 128 bits from the end of the second parity check ( $\overline{P2}$ ) and removing fixed 128 bits from the end of the third parity check ( $\overline{P3}$ ) respectively to keep 192 bits from the codeword.

In the third method, the ensemble bits are punctured irregularly, which means removing a fixed part from bits at different location from each component LDPC codeword to get an optimal puncturing pattern that reduces the complexity of the system decoder.

The irregular puncturing is performed by removing fixed 128 bits from the end of the first parity check ( $\overline{P1}$ ), also removing fixed 128 bits from the beginning and the end of the second parity check ( $\overline{P2}$ ) and removing fixed 128 bits from the beginning of the third parity check ( $\overline{P3}$ ) respectively. There is a trade off in terms of degradation in bit error rate (BER) and Packet error rate (PER) performance due to reducing the codeword length.

At the receiver, the positions of the punctured bits according to the type of the puncturing should be known, so the de-puncturing process estimates as zeros the positions of the received punctured bits and keep as is the systematic information bits and the other parities. After the first iteration, at the decoder the punctured bits set to 0 then the value of likelihood ratios (LLR's) of the punctured bits are calculated as 0.5 then proceeds with the decoding operations of the other received bits. At the channel part, both AWGN and flat fading channel has added to the encoded information as follows:

The flat fading channel has complex impulse response  $h(t)$  and can be represented as:

$$h(t) = h_1(t) + jh_2(t) \quad (4.2)$$

Where,  $h_1(t)$  and  $h_2(t)$  represents the zero mean Gaussian distribution which are Rayleigh distributed as follows:

$$|h(t)| = \sqrt{|h_1(t)|^2 + |h_2(t)|^2} \quad (4.3)$$

The pdf of Rayleigh distribution of equation ((4.3) can be as follows [81][82]:

$$f(y) = \frac{2y}{\sigma^2} e^{-\frac{2y}{\sigma^2}} \quad (4.4)$$

$$\text{Where, } \sigma^2 = E(|h(t)|^2) \quad (4.5)$$

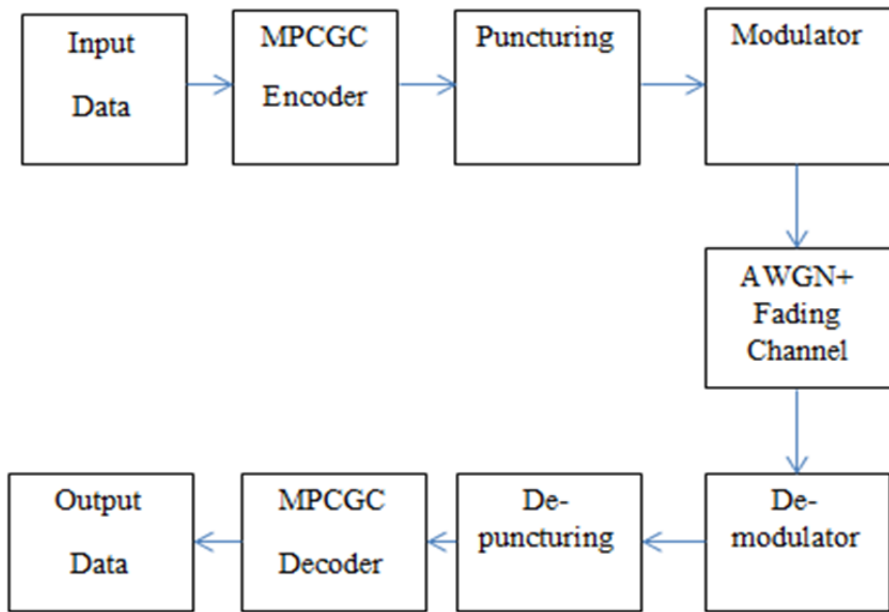


Figure 4.1 Block diagram of the proposed efficient punctured MPCGC system.

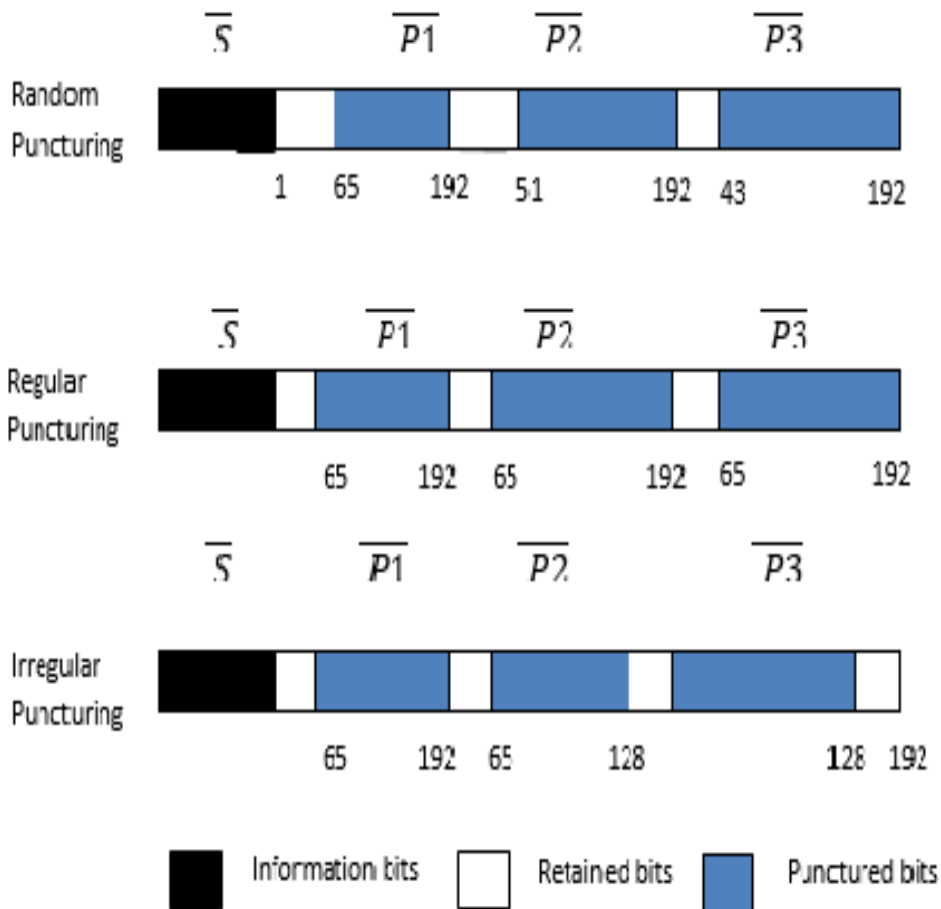


Figure 4.2 Methods of MPCGC puncturing after MPCGC encoder.

### 4.3 MPCGC parallel encoder

MPCGCs are constructed by combining two or more relatively simple LDPC encoders component codes. This irregular LDPC combination improves the system performance when compared with a single long LDPC code. We will consider three LDPC components instead of four for less complex calculations.

Let  $M$  represent the number of three LDPC parallel encoders that are used to encode the information bits  $K$  leading to generate a codeword ( $N$ ). Each component code can be described by a  $(k, n)$  generator matrix.

The parallel concatenation method is used to build an overall length  $N$  and a codeword rate,  $R=1/(M + 1)$  code.

The MCW is an easy and flexible measure to describe the structure of an MPCGC. The parity check matrices of the component LDPC codes are constructed based on selecting the appropriate value for the MCW. It represents the symbol (left) node degree distribution of the Tanner graph.

Many improvements can be achieved by blocking short cycles in the parity check bits of  $H$  matrix, while optimizing the bipartite graph depending on better MCWs that are found in the structure phase[63].

After MPCGC encoder as shown in Figure 4.3, the redundant bits will be cancelled or combined by a multiplexer. Thus, the final codeword of MPCGC is  $(\bar{S}, \bar{P1}, \bar{P2}, \bar{P3})$ , where  $\bar{S}$  is the information bits, while  $\bar{P1}, \bar{P2}$  and  $\bar{P3}$  are the parity bits generated by the first, second and third encoders respectively.

The overall complexity of the encoder part can be reduced by breaking the encoding of a long code length into shorter (in this case 3) codes.

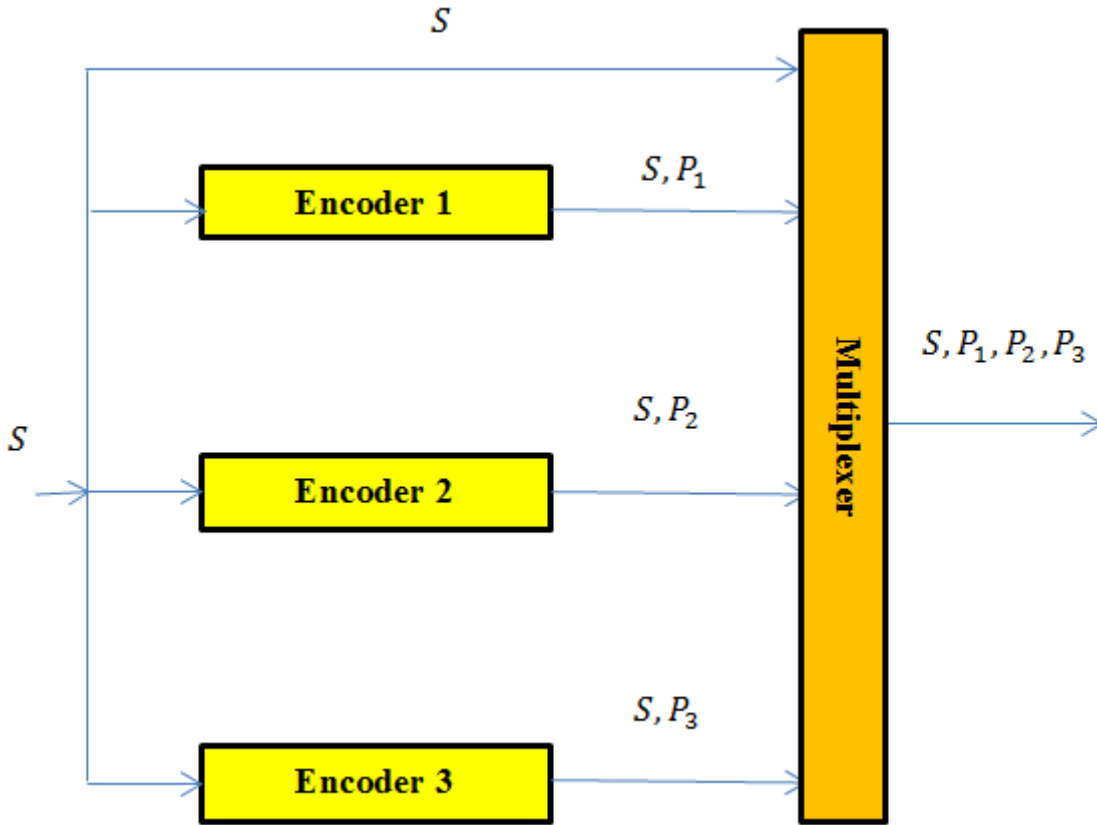


Figure 4.3 Block diagram of MPCGC encoder.

#### 4.4 Punctured MPCGC parallel decoder

The LDPC component decoder uses the iterative sum product algorithm due to its lower computational complexity. Let the Gaussian probability density function be centered at +1.

$$p(y_i | x_i = +1) = \frac{1}{\sqrt{2\pi}\sigma} e^{-\frac{(y_i - 1)^2}{2\sigma^2}} \quad (4.6)$$

and the probability of message vector  $\underline{x} = +1$  at site  $i$  be

$$f_i^1 = P(x_i = +1 | y_i) = \frac{1}{1 + \exp\left(\frac{-2y_i}{\sigma^2}\right)} \quad (4.7)$$

The MPCGC decoder is assumed to know the position of punctured bits to compute the log likelihood ratios (LLR's) as 0.5. The decoding process of MPCGCs follows the turbo decoding scenario but without using an interleaver among the component decoders. The process of exchanging information between the component decoders can be defined as a super iteration, whereas a local iteration can be defined as a complete one cycle from the sum

product algorithm decoding. The MPCGC has the flexibility to stop both the local and super iterations at convergence. During the first super iteration, all M component decoders launch processing information simultaneously using the sum product algorithm (SPA). Each using the received sequence ( $d^0$ ) and ( $d^M$ ) without applying any a priori (extrinsic) input since the information bits are equally +1 or -1. For a number of local iterations each LDPC component code tries to decode its own codeword and calculates alone the corresponding posteriori probabilities  $\underline{p}^M(\hat{c})$  of the (N) coded bits. This decoding will halt when either a known maximum number of local iterations is reached or if a unique codeword is found. When the first super iteration is completed, each LDPC component decoder will get its own a priori information from the extrinsic information of all other (M-1) decoders. For all other subsequent super iterations the decoding process continues until all (M) component decoders obtained the valid codewords, or reaching the higher number of super iterations. [57].

## **4.5 Simulation results and discussion**

### **4.5.1 BER performance analysis**

Firstly, the characteristics of MPCGCs parallel decoding are evaluated separately before puncturing, by using three LDPC component codes where each component is allowed a maximum of 38 local iterations whereas the overall MPCGCs have 30 super iterations. The parameters of the three LDPC components of MPCGC have the same parity check dimensions, H (192,384) with different MCWs: the overall code rate  $R=1/4$ ,  $MCW_1=1.94$ ,  $MCW_2=2.81$ ,  $MCW_3=1.81$  and  $N=768$ . Again, the parameters of the equivalent single irregular LDPC code that is used for comparison are:  $R=1/4$ ,  $MCW=3.07$ ,  $N=768$  with 50 local iterations. The BER performance of the MPCGC-BPSK over AWGN channel is evaluated and is illustrated in Figure 4.4, the MPCGC has a gain of 0.5 dB (at BER  $2e-4$ ) when compared to the equivalent single irregular LDPC with the same parameters. Furthermore, the MPCGCs performance outperforms by 1.3 dB the single short LDPC code with parameters:  $R=1/2$ , H (192,384), and  $MCW=2.8$ . The MPCGC shows 0.25 dB gain improvements when compared with the result reported by Kim et. al using the same parameters [70].

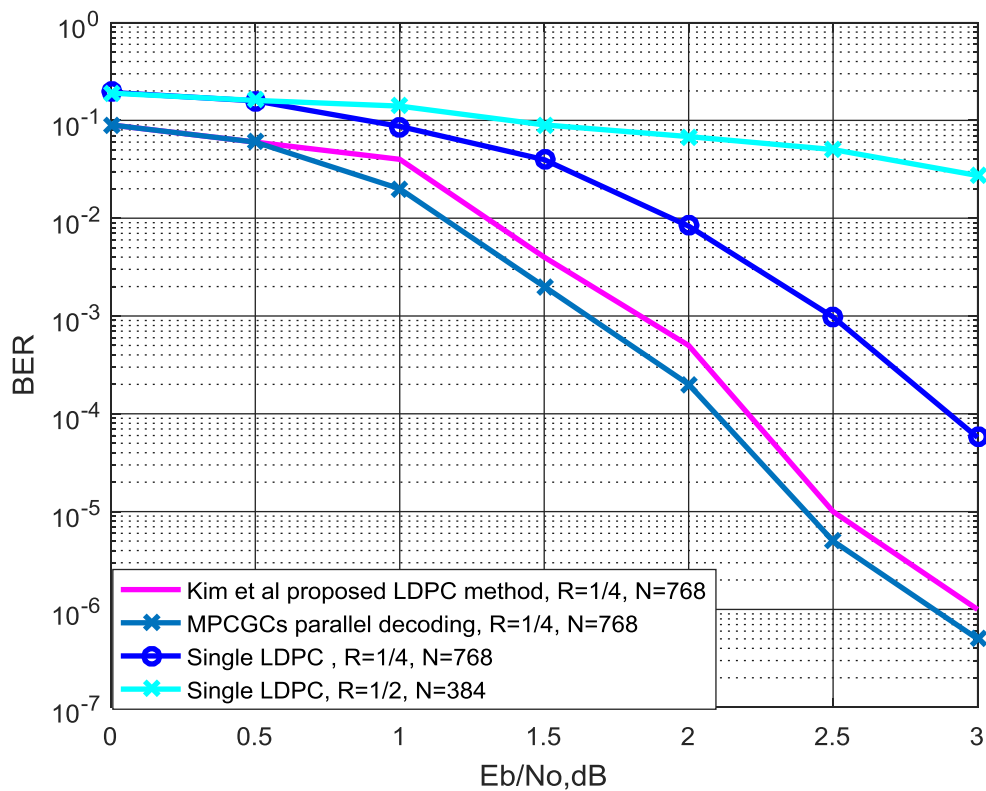


Figure 4.4 BER comparison for different LDPC coding model over AWGN channel.

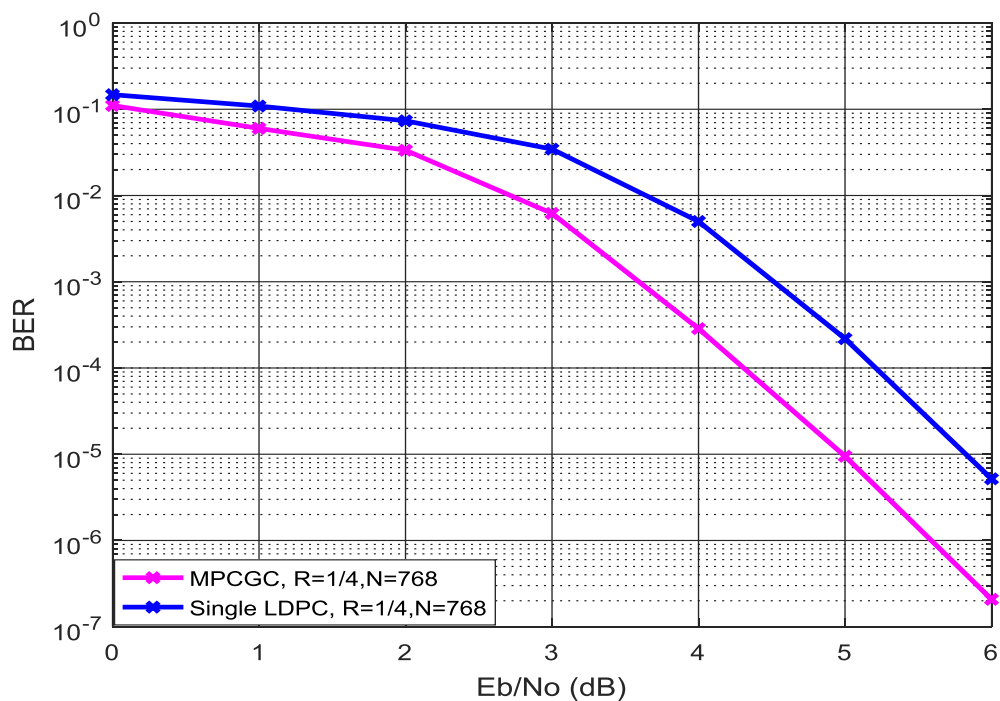


Figure 4.5 BER comparison of MPCGC with LDPC over flat fading Rayleigh channel.

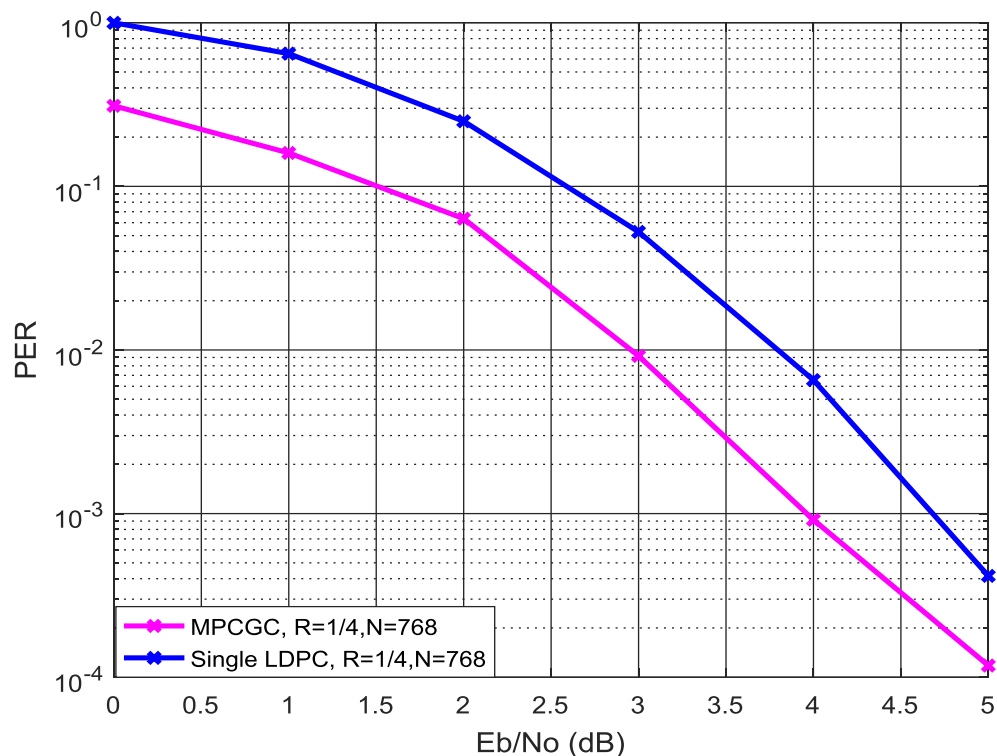


Figure 4.6 PER comparison of MPCGC with LDPC over flat fading Rayleigh channel.

The BER and PER performance of MPCGCs are evaluated over a flat fading channel. The MPCGCs provides a gain of 0.4 dB when compared with the single LDPC codes with the same parameters  $R=1/4$ ,  $N=768$  as shown in Figures 4.5 and 4.6.

The puncturing performance of the proposed designed MPCGCs was evaluated. After encoding, the codeword  $N=768$  is punctured by a puncturing fraction  $\Theta=0.5$  to be  $N=384$  for improving the BER performance as well as reduce the decoding complexity and to increase the transmission code rate from  $1/4$  to  $1/2$ . Figures 4.7 and 4.8 show the different BER and PER comparison of punctured MPCGCs with BPSK over AWGN channel.

In the random puncturing method, when removing randomly 128 bits from each component LDPC codeword, the simulations show worse BER performance compared to when removing unequal numbers of bits from each parity LDPC codeword.

The irregular puncturing provides better performance at low and high  $E_b/N_0$  region when compared to the original without puncturing single LDPC with  $1/2$  code rate,  $MCW=2.75$  and  $N=384$ . In addition, the only performance degradation is in the medium  $E_b/N_0$  region.

Furthermore, the irregular and regular puncturing both outperform random puncturing by 1 and 0.7 dB at BER  $1e-4$  respectively. Moreover, the irregular and regular punctured MPCGCs show 0.5 and 0.4 dB gain improvement respectively compared with the same parameters of single regular punctured LDPC codes. In addition, when compared with low MCW component of single original LDPC without puncturing with  $R=1/2$ ,  $N=384$  and  $MCW=1.79$ , the performance of MPCGC with irregular puncturing outperforms by 1.75 dB at  $BER=1e-3$ .

Figures 4.9 and 4.10 show the different BER and PER comparison of the proposed punctured MPCGCs over a flat Rayleigh fading channel; the irregular and regular punctured MPCGCs show 0.7 and 0.4 dB gain improvements at BER  $1e-3$  when compared with the single punctured LDPC codes with the same parameters.

In addition, the performance with irregular puncturing is very close to the performance of the original code without puncturing for a single LDPC with  $1/2$  code rate,  $MCW=2.75$  and  $N=384$  at low and medium  $E_b/N_0$  region and provides better performance at the high  $E_b/N_0$  region after 4 dB; the irregular and regular MPCGC puncturing outperforms the random puncturing by 2 and 1.5 dB at BER  $2e-3$  respectively. When compared with low MCW component of single original LDPC without puncturing with  $R=1/2$ ,  $N=384$  and  $MCW=1.79$ , the performance of MPCGC irregular puncturing outperforms the single original LDPC by 3 dB when  $BER=8e-3$ .

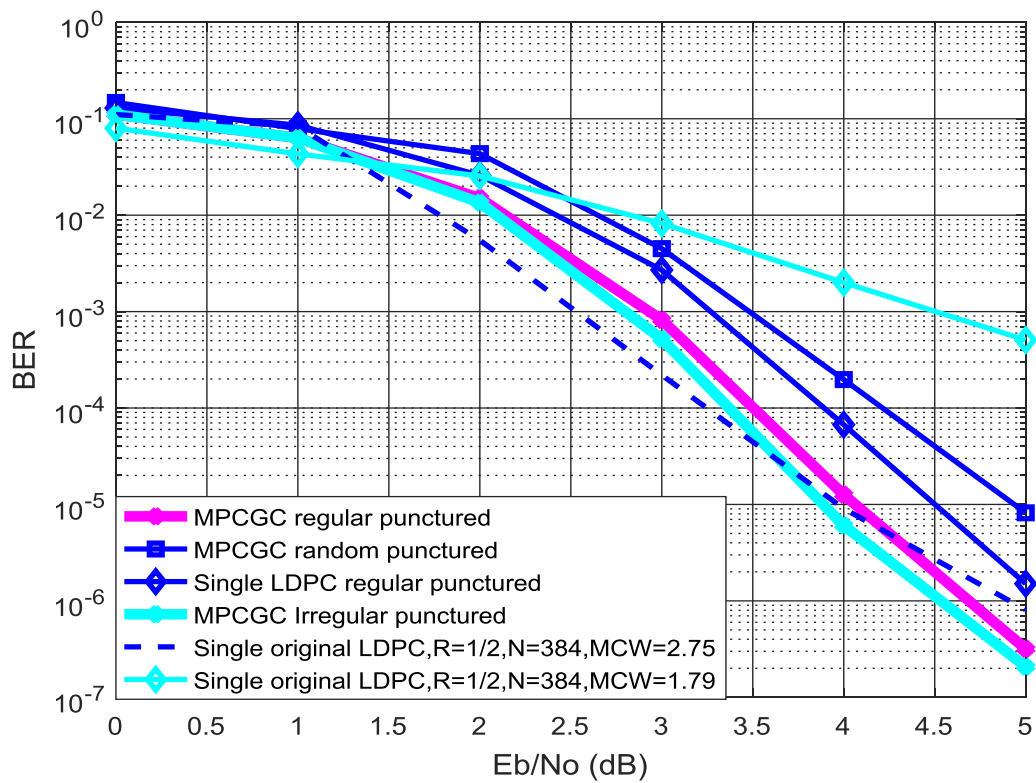


Figure 4.7 BER performance of different punctured MPCGC over AWGN channel

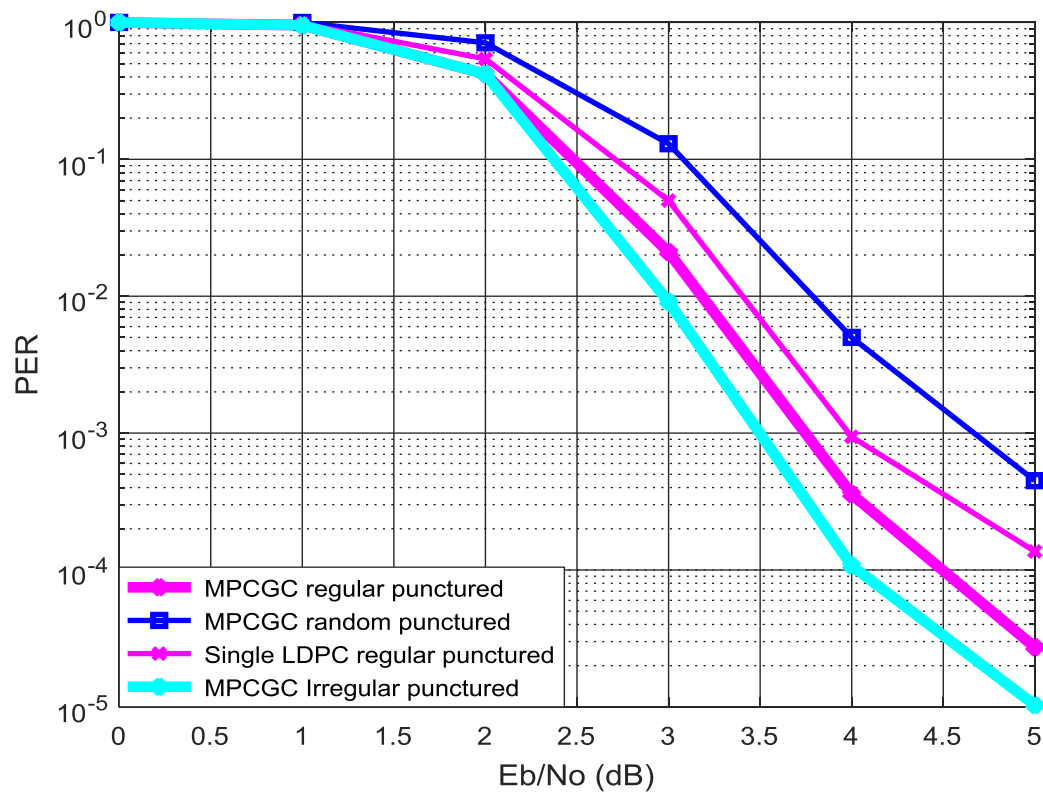


Figure 4.8 PER performance of different punctured MPCGC over AWGN channel.

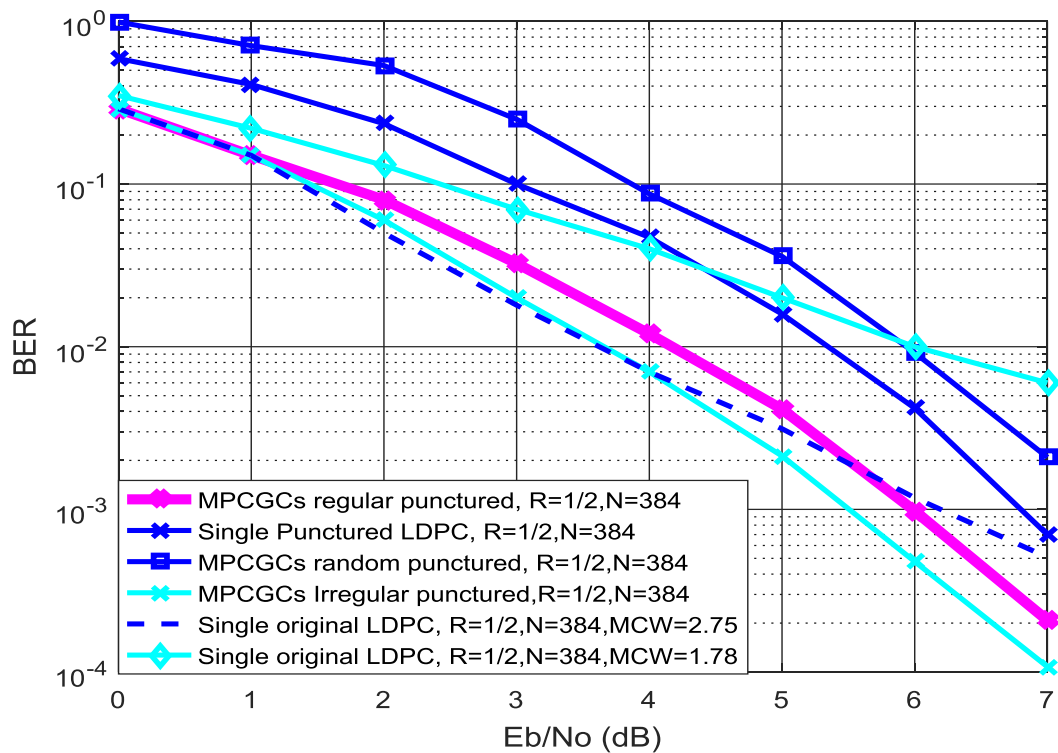


Figure 4.9 BER comparison of punctured MPCGC with LDPC over flat Rayleigh fading channel.

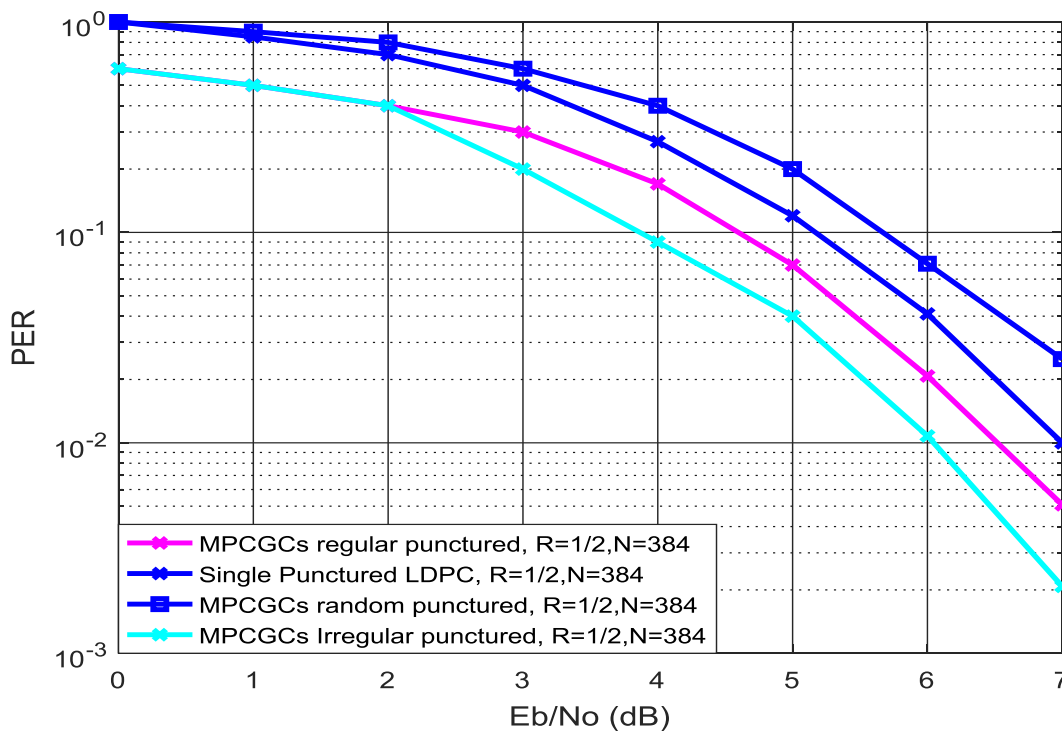


Figure 4.10 PER comparison of punctured MPCGC with LDPC over flat Rayleigh fading channel

#### 4.5.2 MPCGC complexity analysis

LDPC complexity for a particular code is proportional to the type of decoder and the density of the parity check matrix [14]. The sum product algorithm has an important advantage, which is that it is less complex than other decoding algorithms used in turbo codes. To estimate the complexity of MPCGCs, we calculated the average number of local iterations per each LDPC code needed with different  $E_b/N_0$  values [7].

In our case, an MPCGC executes a maximum of 30 super iterations; each component decoder in each super iteration performs a maximum of 38 local iterations on the received data then passes the extrinsic information to the next decoder and so on.

The MPCGC decoder generally for each super iteration performs a maximum of  $(3 \times 38)$  local iterations which are done by 3 LDPC decoders. The decoding complexity per iteration can be estimated in terms of the maximum number of edges in the Tanner graph of the code which can be calculated as  $(N \times MCW)$  for a single LDPC code [71]. Therefore, for a MPCGC in each super iteration, the maximum number of edges can be calculated as shown below,

$$\text{Total edges} = \text{Number of iterations} \sum_{i=1}^M N_i MCW_i \quad (4.8)$$

On this basis, the complexity analysis and comparison have been carried out in terms of  $E_b/N_0$  and the results in terms of the maximum number of iterations and edges are illustrated in Figures 4.11 and 4.12.

The results show that the complexity of the proposed punctured MPCGCs can be reduced compared with the conventional MPCGC system. Furthermore, at the decoder the LLR values are calculated as 0.5 since the values of punctured bits set to 0 which it cause reducing the decoding complexity due to reduction in the number of the overall required iterations as well the decoder will converge quickly. Moreover, the advantages of the proposed punctured MPCGCs can be exploited without significant additional complexity.

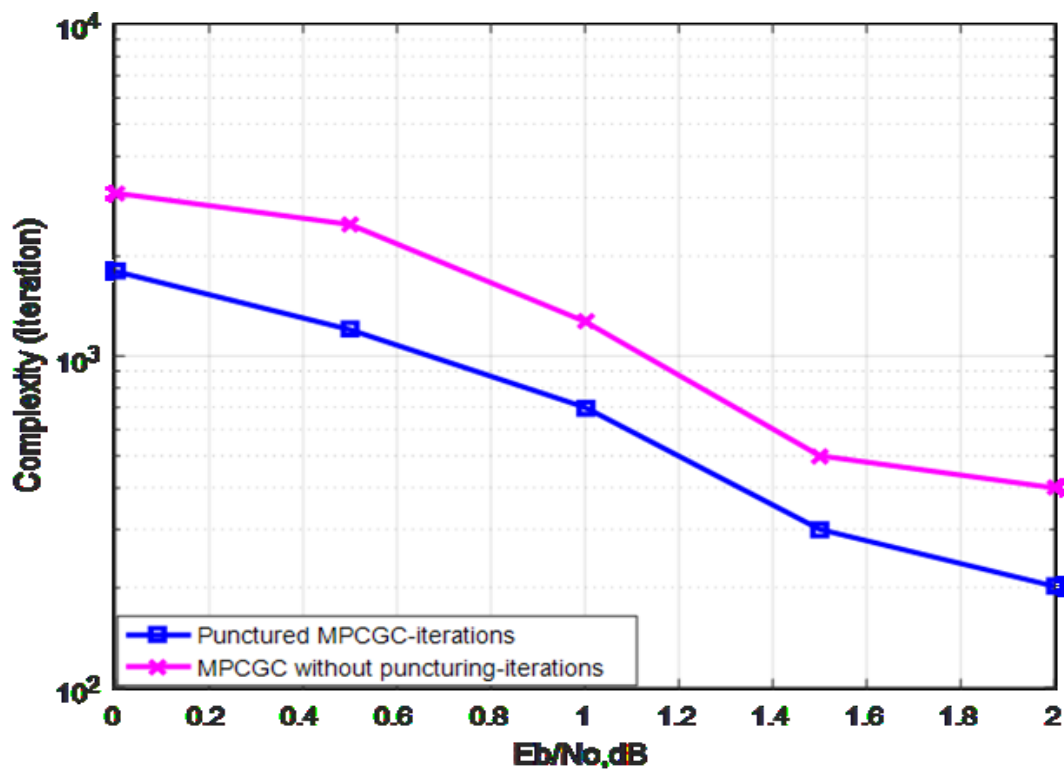


Figure 4.11 Complexity and performance comparison between punctured MPCGCs and conventional MPCGC

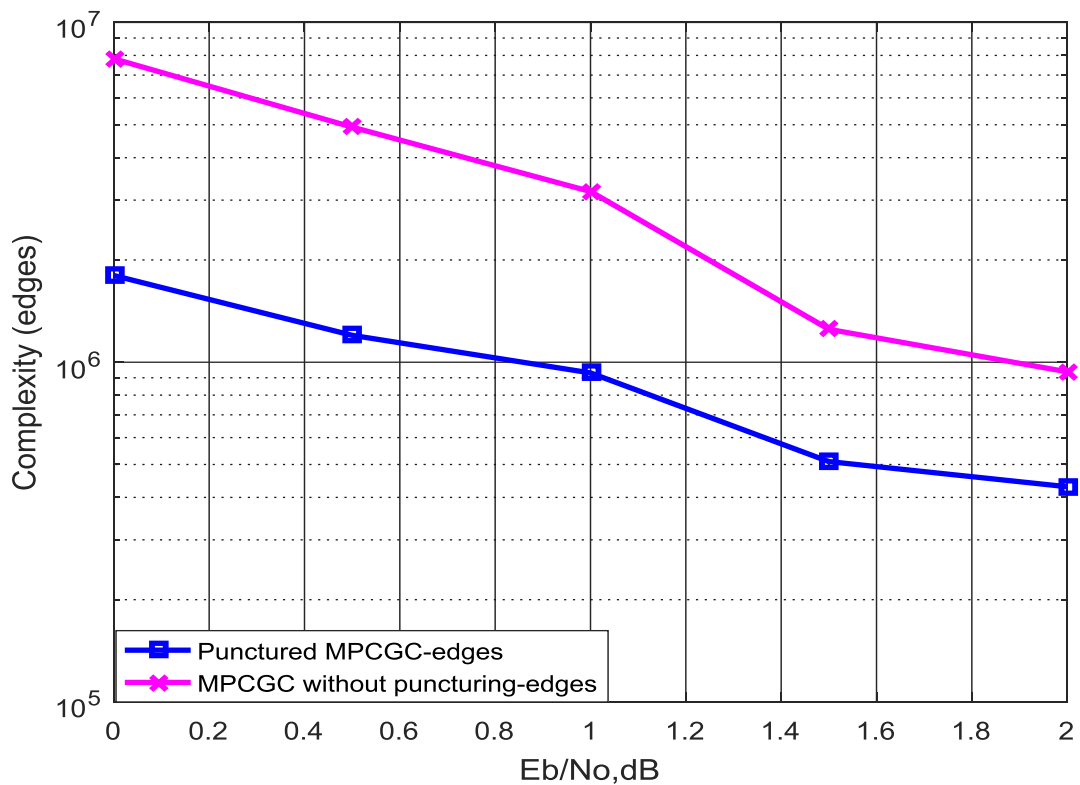


Figure 4.12 Complexity and performance comparison between punctured MPCGCs and conventional MPCGC

## 4.6 Summary

This chapter focused on an attractive proposed novel punctured MPCGCs scheme evaluated over AWGN and flat Rayleigh fading channels for the first time to the best of our knowledge. It is shown that the MPCGCs structure yields superior coding performance both with and without puncturing when compared to the original single-long LDPC component with the same parameters.

It is also shown that irregular puncturing achieves better performance than regular and random puncturing in MPCGCs. The complexity analysis in terms of number of edges and iterations has shown that the efficient proposed MPCGC structure has less complexity compared with the conventional MPCGCs structure. The benefit from reducing complexity by reducing the memory requirement for decoding than that of the single LDPC.

## Chapter 5

# Performance Analysis of Multiple Parallel Concatenated Gallager Codes for WiMAX Applications

### 5.1 Introduction

WiMAX system performance can be significantly improved to achieve excellent error correction performance by utilizing powerful Forward Error Correction Codes. In this chapter, we investigate the use of Multiple Parallel Concatenated Gallager Codes (MPCGC) in IEEE 802.16/WiMAX. Computer simulation results confirm that the proposed MPCGCs-WiMAX system shows better performance with an improvement in gain when compared to a single long LDPC-WiMAX system. Moreover, by using the proposed coding scheme, lower computational complexity can be achieved than the long LDPC code due to multiple smaller lower codes.

WiMAX (Worldwide Interoperability for Microwave Access) is a telecommunication technology that was first introduced in 2001 [83]. The IEEE 802.16 standard is a fixed broadband Wireless Access. This standard works with the physical layer and the medium access control layer. Moreover, it offers the alternative way to wired broadband standards such as DSL. There are different physical layer specifications due to different applications and frequency bands that are supported by the WiMAX standard [80][84].

The frequency band operation of the first version of the IEEE802.16 is 10 - 66 GHz and needs line-of-sight (LOS) towers. After that, the standard extended the frequency operation to 2-11 GHz through different physical (PHY) specifications. This enable the Non Line Of Sight (NLOS) connections that require techniques which efficiently attenuate the impairment of fading and multipath and to solve the weakness of Wi-Fi networks [85][86].

In this chapter we focus on the improvement of performance of the WiMAX system based on the IEEE 802.16 standard modulation technique, in particular, using the MPCGC system based on LDPC coding over an AWGN (Additive White Gaussian Noise) channel [83].

The remaining organization of this chapter as follows; in section 5.2 the WiMAX scenario has been explained in detail. In section 5.3 the proposed system model of the MPCGC-WiMAX physical layer is presented. The main assumptions needed to work with the system model of MPCGC-WMAX has been done in section 5.4. Followed by presenting the

simulation results and discussion of the research in section5.5, this include the BER performance and the effect of the girth removable on the parity bits. Finally, the chapter summary is presented in section 5.6.

## 5.2 WiMAX Scenario

As terrestrial mobile communication systems are just one of many applications competing for suitable bandwidth, there has been a rapid growth in the demand for high-speed mobile wireless communications and the use of the radio spectrum. In non-line-of-sight environments the systems operating reliably with propagation distance of 0.5 - 30 km, and at velocities up to 100 km/hr or higher. Due to excessive channel path loss and excessive Doppler spread at high velocity being resulted the current wave standard is used for vehicular communications and it is that operate at carrier frequency of 5.9GHz [87-89]. The value of the radio spectrum is made extremely high as the spectrum available for mobile applications is limited. On the basis of the 802.16 MAN standard constitute the WiMAX standard, whose development was conducted by the WiMAX forum [90]. Due to the IEEE 802.16/WiMAX standard being the simplest method for applying MPCGC techniques and for showing the enhancements on the WiMAX system, it was the physical layer used in this thesis. The same subcarrier frequency spacing is maintained by the WiMAX standard, which utilizes orthogonal frequency division multiplexing (OFDM), with different factors, such as system bandwidth, Fast Fourier transform (FFT) size and number of sub channels, at the same time [91][92].

For wireless communication systems, OFDM technology will be a main method to achieve the high data capacity and spectral efficiency requirements. The architecture has to be known for the visualization of physical layer design and transmission control. The line of sight (LOS) and non-line of sight (NLOS) communication links are present in WiMAX architecture, which can be seen in Figure 5.1 [83]. The modulation BPSK schemes can also supported by the 802.16/WiMAX standard. Alongside higher throughput via orthogonal multi-carrier system in comparison to the traditional single carrier system. In addition, by using the cyclic prefix, the eliminating inter-symbol interference (ISI) will be possible. The utilization of OFDM as the underlying technology can be reduce complexity by using FFT processing [93][94][95]. In 2011, a flexible decoder architecture presented to support LDPC codes to work with IEEE 802.16e standard. The dual-mode Flex-SISO decoder was proposed using multiple parallel Flex-SISO cores as a basic building block in LDPC and Turbo

decoder to increase the decoding throughput [96]. In 2012, a partial parallel LDPC decoder based on TDMP with normalized MSA algorithm was proposed. The decoder supports any code rate and code length defined in WiMAX network. Furthermore a parallel shifter based shuffle network was designed to enable the decoder to support all the 19 code length [97]. In 2015, an optimized LDPC codes in WiMAX physical layer network coded two way relay channel using noncoherent FSK modulation. The BER performance was improved through EXIT based optimization of Tanner graph variable node degree distributions. Moreover, by maintaining the extended irregular repeat-accumulate (EIRA), the computational complexity of the standard codes were preserved in the optimized codes [98].

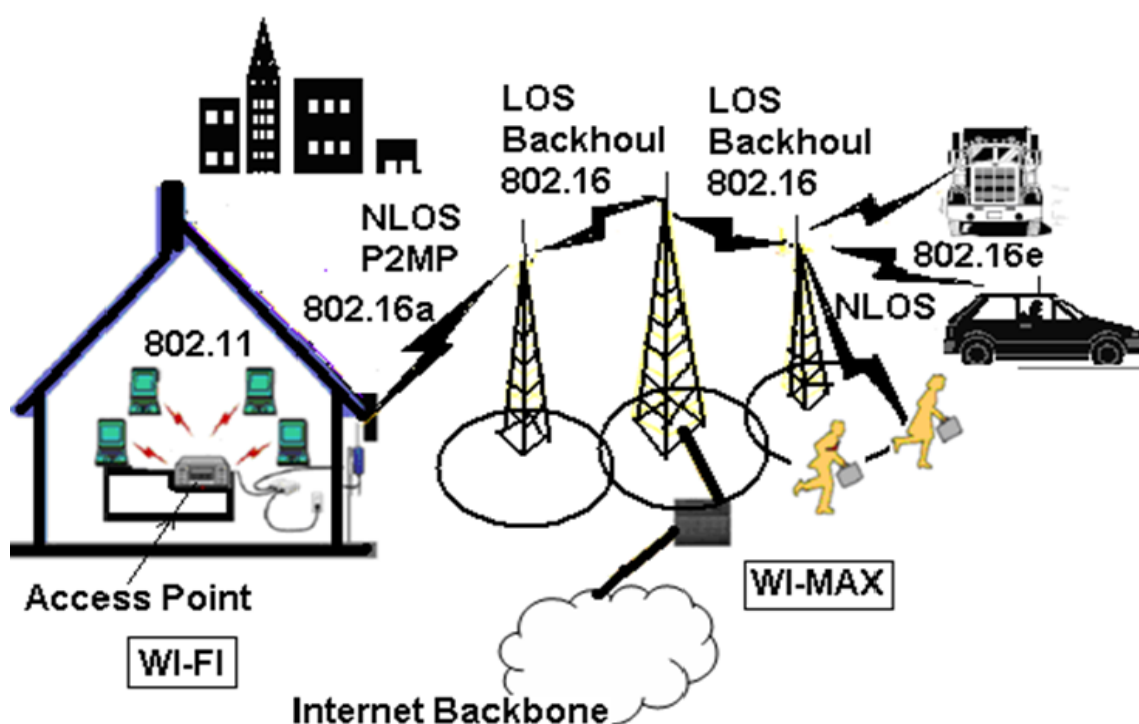


Figure 5.1 WiMAX systems.

### 5.3 WiMAX Physical Layer Model

The WiMAX physical layer model, as shown in the block diagram in Figure 5.2 is based on OFDM [36]. The system model combines MPCGCs with OFDM to implement and improve the WiMAX 802.16 standard [99].

The baseband WiMAX system has four major parts:

1. MPCGCs Encoder/ Decoder for the WiMAX 802.16 standard
2. Interleaving/ Deinterleaving

### 3. Modulation/ Demodulation

### 4. OFDM transmitter/Receiver

In this block diagram, random data is generated. The proposed MPCGC encoder is designed to provide the advantage of breaking the equivalent long single LDPC code into multiple smaller codes with lower complexity and thus improve the overall system performance.

The irregular LDPC codes provide lower encoding/decoding complexity with better performance. The parity check matrices of the single LDPC-WiMAX standard based on the QC-LDPC is built up and designed based circular right shifted. The entire parity check matrix is a set from a systematic linear block with different cyclic shifts, which allows reduction in complexity as well.

There are four code rates supported in the WiMAX standard  $1/2$ ,  $2/3$ ,  $3/4$  and  $5/6$ . Every base of the  $H$  matrix has 24 columns. For every code rate, the base model parity check matrix is defined for the largest acceptable code length ( $N=2304$ ). The expansion factor ( $z$ ) varies from 24 to 96 with increments 4 and is equal to  $N/24$  for code length  $N$  [100]. For instance, the code length 768 has expansion factor  $z=32$ . Figure 5.3 shows the structure of the parity check matrix  $H$  (384,768) of the standard for a single LDPC with code rate  $1/2$ ,  $z=32$ ,  $N=768$  [101].

The second type of matrix that will be evaluated over MPCGC-WiMAX will be the parity check matrices irregular codes based on gallager design with specific well-designed MCW for each LDPC component.

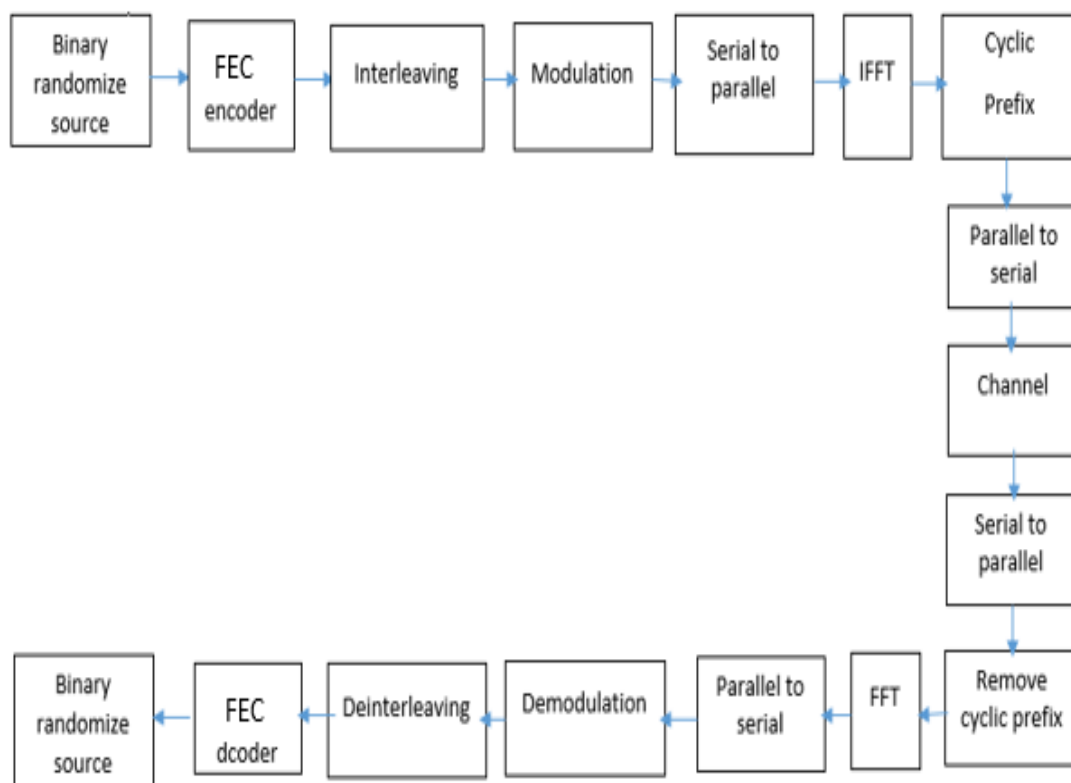


Figure 5.2 Block diagram of WiMAX-OFDM physical layer model.

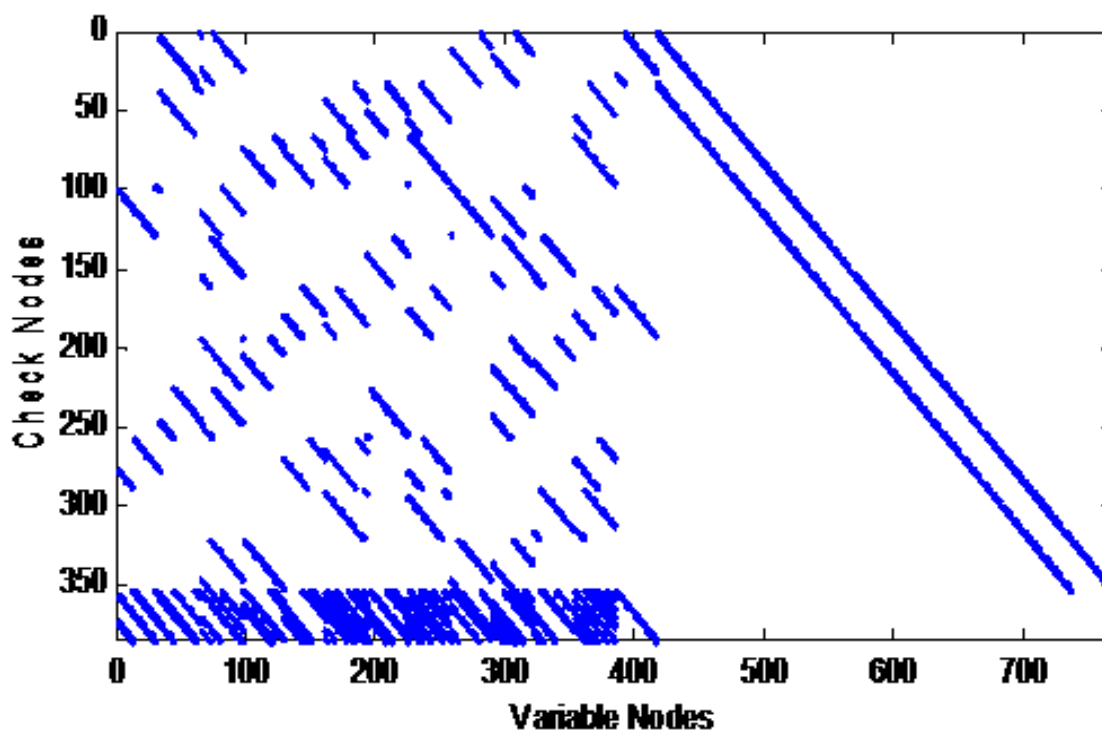


Figure 5.3 Structure of the parity check matrix of WiMAX IEEE 802.16 standard with  $\frac{1}{2}$  code rate and 768 code length.

## 5.4 The WiMAX model assumptions

In this case study, many simulation parameters of IEEE 802.16/WiMAX in the system are used as shown in Table (5.1) below. The Matlab program simulates BPSK modulation with different channels through the Monte Carlo method. The aim is to show the performance improvements of the superior forward error correction MPCGC-WiMAX against the conventional WiMAX system. However, the frequency selective fading channel can be used instead of flat fading channel for future work. All component decoders use the SPA in calculating their a posteriori probability. At each super iteration, each component decoder uses their parity check matrix to run the SPA algorithm.

Table 5.1 WiMAX simulation Parameter.

<b>OFDM, FFT size</b>	<b>256</b>
<b>Number of data subcarriers</b>	<b>192</b>
<b>Code length</b>	<b>768</b>
<b>Modulation scheme</b>	<b>BPSK [-1,+1]</b>
<b>Channel model</b>	<b>AWGN, Flat fading channel</b>
<b>Cyclic prefix</b>	$\frac{1}{4}$
<b>Channel Bandwidth</b>	<b>2.5 MHz</b>

### 5.4.1 MPCGC Encoder/Decoder

Three LDPC component encoders (mixed in parallel) as presented in the previous chapter are used for controlling errors in data transmission over an AWGN and flat Rayleigh fading channel. The MPCGC is used as forward error correction (FEC) to encode and decode the message which is sent in a redundant way.

### 5.4.2 Interleaving

The process of reordering the data sequence in deterministic format is called interleaving. The interleaving is used by making permutation process to the encoded data and the main reason for using the interleaver to protect the transmitted data from errors and make the FEC high robust and reliable.

The inverse of interleaving is the deinterleaving at the receiver side, where the original data has been restored from the received sequence [66]

### 5.4.3 BPSK modulator

The BPSK signal can be defined as the shifting in the phase of the continuous carrier in response to the amplitude of the original data. The phase shift between the digital data is  $180^\circ$ , which is convenient choice because it simplifies the modulator design.

The PSK signal can be written as:

$$\Phi_1(t) = A\sin(w_c t) \quad (5-1)$$

$$\Phi_2(t) = -A\sin(w_c t) \quad (5-2)$$

Where  $\Phi_1(t)$  represents the [0] bit and  $\Phi_2(t)$  represents the 1 bit.

### 5.4.4 Serial to parallel transformation

The purpose of using the serial to parallel transformation stage in the OFDM system is to convert the input serial to parallel data so as to enable transmitting in each OFDM symbol. The data is placed on each symbol according to the modulation scheme used and the number of subcarriers. On the other hand, at receiver the reverse process will be applied to the data, with the subcarriers being transformed back to the original serial data stream.

### 5.4.5 Inverse Fast Fourier Transform (IFFT)

The conventional modulation scheme at the transmitter side is modulated the data. Then all individual modulated carriers are summarized or multiplexed to form an OFDM signal. The block IFFT is used as transducer system in the OFDM signal.

The IFFT is a mathematical concept that will convert the signal from the frequency domain where it is represented as the phase or amplitude of a particular frequency in the time domain. In frequency domain, the individual sub carriers is corresponded to the discrete samples of IFFT. The generality of the sub carriers is modulated with data as any unmodulated signals such outer subcarrier is set to zero amplitude.

The frequency guard band provides zero sub carriers before the Nyquist frequency and efficient take place to generate the signal [102][103].

### 5.4.6 Additive white Gaussian noise (AWGN)

The noise is an unwanted signal that tends to disturb the transmitted signal. The AWGN (with zero mean and fixed power spectral density) is added to the modulated signal at the output of the modulation unit. Furthermore, it is like the properties of white light therefore it is called white because it has flat power spectral density, so in time domain the auto correlation of the noise is set to zero for any non-zero time offset.

The value of the variance  $\sigma^2$  depends on the bit energy  $E_b$  of the transmitted signal and the signal to noise at the input (for more details in Appendix A). The process of adding the AWGN noise to the transmitted signal for a given  $SNR$  (specified in dB) can be calculated by [85].

1. Calculating the power signal

$$E_s = \frac{1}{N} \sum_{i=0}^{N-1} u(i)^2 \quad (5-3)$$

Where  $u$ = transmitted data,  $N$ =length ( $u$ )

1. Converting the  $SNR$  in  $dB$  to linear scale  $SNR_{linear}$  then finding the noise vector from Gaussian distribution of noise variance as follows.

$$E_b/N_0 = 10^{\frac{SNR}{10}} \quad (5-4)$$

And

$$\sigma = \frac{1}{\sqrt{(2 * R * (\frac{E_b}{N_0}))}} \quad (5-5)$$

Where,

$E_b/N_0$ , the energy per bit to noise power spectral density ratio

$R$  is the code rate and  $\sigma$  is the standard deviation, therefore the total noise

$$\text{Noise} = \left( \frac{1}{\sqrt{(2 * R * (\frac{E_b}{N_0}))}} \right) * [\text{randn}(1, N) + j * \text{randn}(1, N)] \quad (5-6)$$

## 5.5 Simulation Results and Discussion

### 5.5.1 Girth removable analysis

The decoding process of LDPC codes is quickly computable when the Tanner graph of the parity check matrix includes no loops. Usually, LDPC contains many loops which directly effect on the speed of the sum product algorithm. To overcome the effect of girth on the LDPC performance by choosing the appropriate codes with longer girth of Tanner graphs. However, the removal of girth 4 is sufficient and better way to increase the convergence. The approach of removing a rectangle form of four 1s in the H matrix by redistributing some elements inside parity check matrix. The state of H matrix without girth four, if and only if 1s are all the elements of the matrix  $[H^T H]$  except the diagonal line [28].

To make comparison between the detection and removal of girth 4 for both single LDPC-WiMAX and MPCGC-WiMAX. The removal a girth 4 from the standard LDPC-WiMAX parity check matrix H (384,768) with  $\frac{1}{2}$  code rate and MCW=3.04 as shown in Figures 5.4 and 5.5. Also Figures 5.6 and 5.7 showed the detection and removal a girth 4 from the MPCGC-WiMAX parity check matrix H (192,384) with  $\frac{1}{2}$  code rate and MCW=2.757.

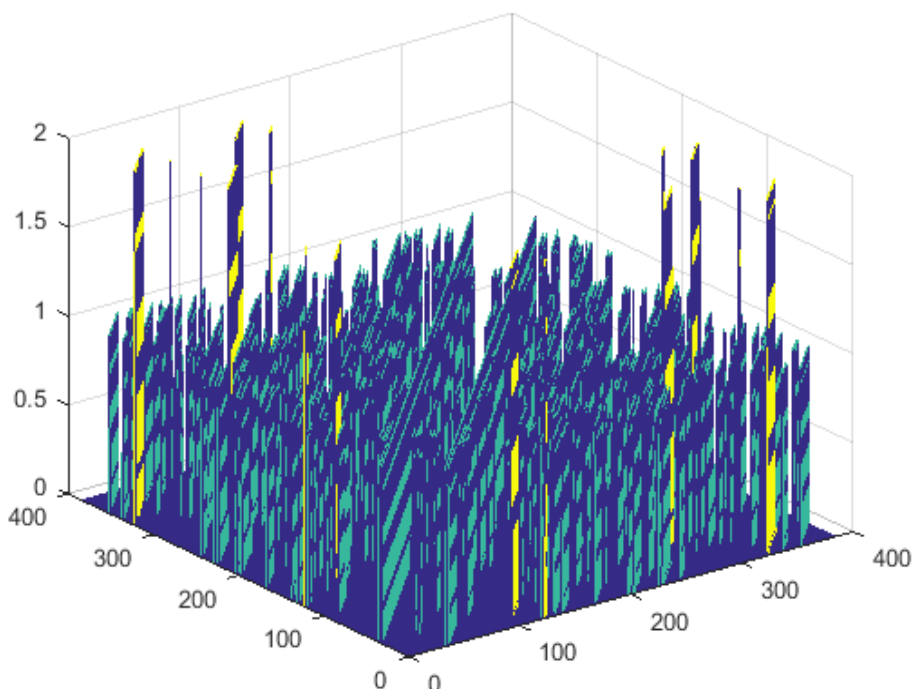


Figure 5.4 Entries of standard LDPC-WiMAX parity check matrix with girth 4.

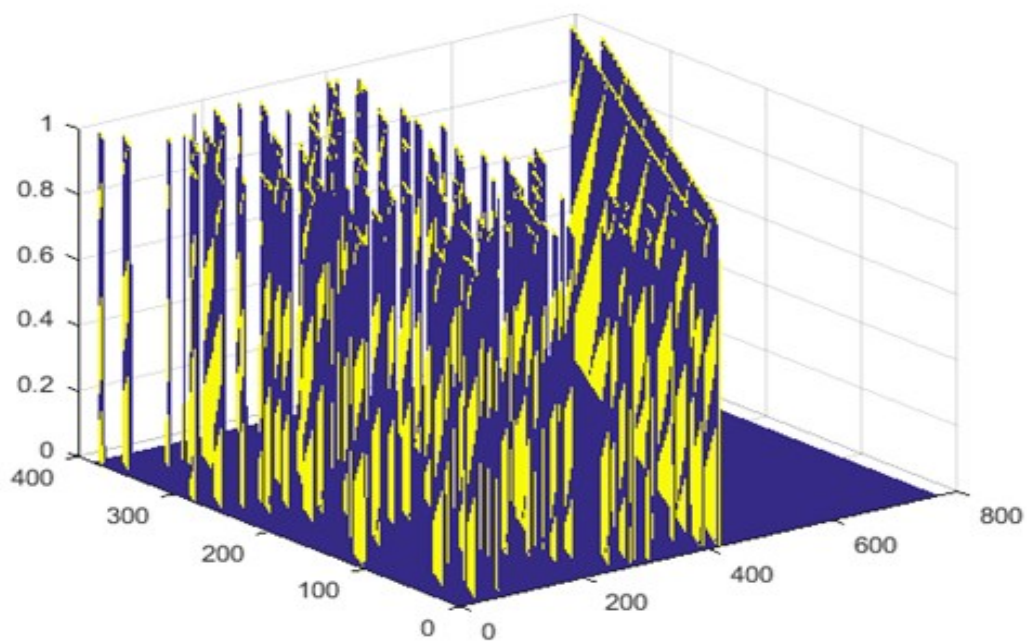


Figure 5.5 Entries of standard LDPC-WiMAX parity check matrix with free girth 4.

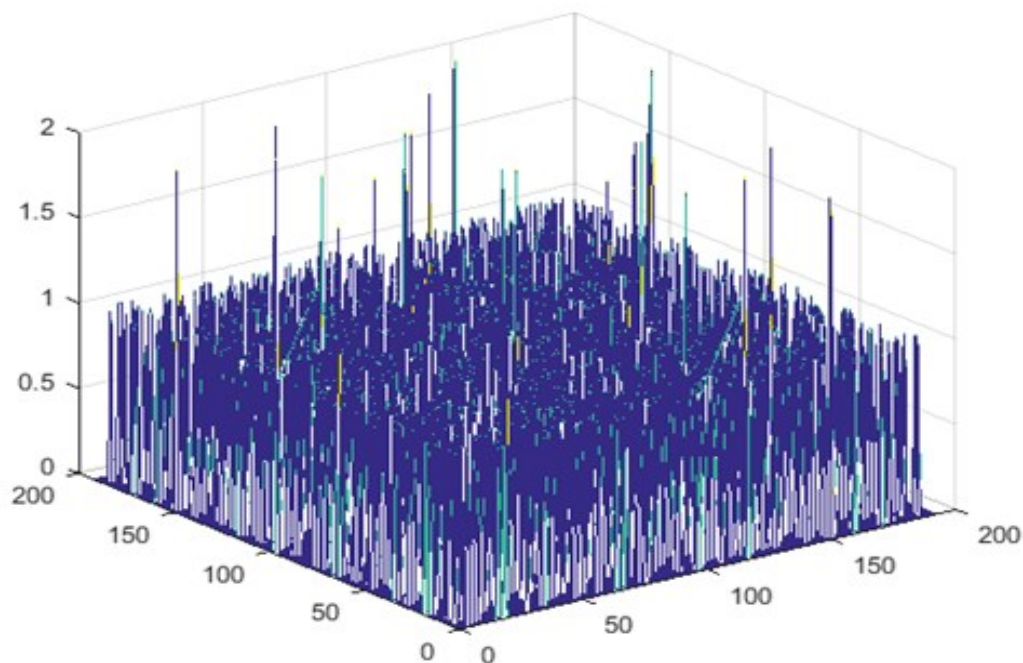
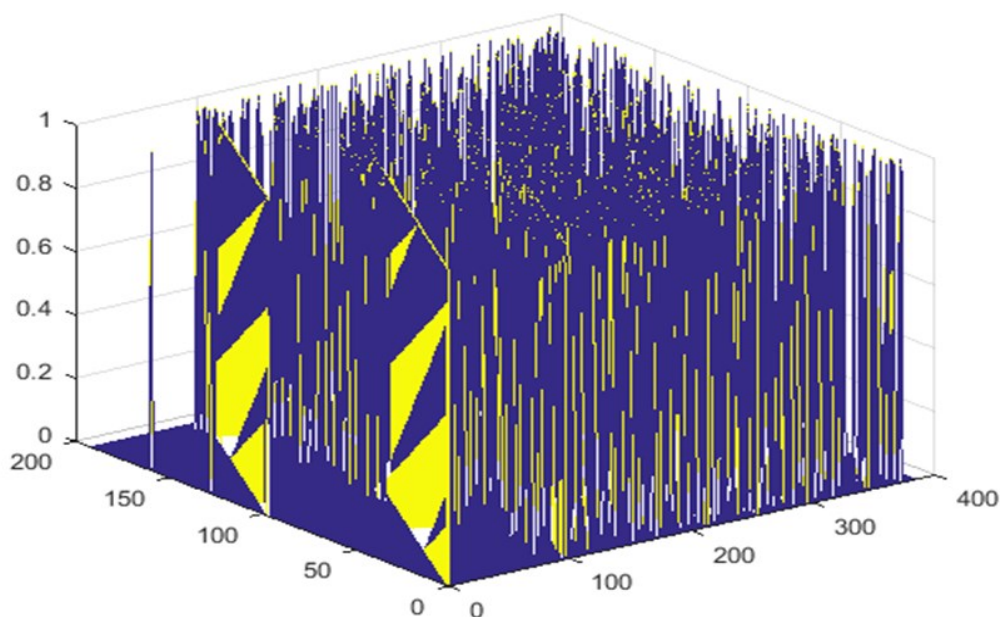


Figure 5.6 Entries of MPCGC-WiMAX parity check matrix with girth 4.



**Figure 5.7** Entries of MPCGC-WiMAX parity check matrix with free girth 4.

### 5.5.2 BER performance analysis

Firstly, the characteristics of MPCGCs parallel decoding are evaluated separately without WiMAX application as shown in Figure 5.8 using three LDPC component codes where each component is allowed a maximum of 38 local iterations whereas the overall MPCGCs have 30 super iterations.

The BER performance of the MPCGCs is evaluated and is illustrated in Fig. (5.8). The parameters of the three parallel Gallager LDPC components of MPCGC have the same parity check dimensions,  $H$  (192,384) with different MCWs: code rate  $R=1/4$ ,  $MCW_1=1.94$ ,  $MCW_2=2.81$ ,  $MCW_3=1.81$  and  $N=768$ . Again, the parameters of the equivalent single irregular LDPC code that is used for comparison are:  $R=1/4$ ,  $MCW=3.07$ ,  $N=768$ , the MPCGC has a gain of 0.5 dB (at BER  $2e-4$ ) when compared to the equivalent single irregular LDPC with the same parameters. Furthermore, the MPCGCs performance outperforms by 1 dB the single short LDPC code with parameters:  $R=1/2$ ,  $H$  (192,384), and  $MCW=2.8$ . The MPCGCs show 0.2 dB gain improvements when compared with the result of reported proposed method by Kim et. al using the same parameters [70]. Secondly, the performance of

a single LDPC-WiMAX baseband transceiver for IEEE 802.16 has been calculated according to the simulation parameters in table (5.1) with a 256 size FFT[104].

The quasi-cyclic LDPC codes represent the base of the WiMAX networks as well as producing low computational complexity in the encoder and decoder part. Moreover, the required iterations in the decoder part are reduced compared to the Gallager codes as will be explained in detail in the next chapter.

The parameters of the LDPC code used for comparison are  $R=1/2$ ,  $N=768$  and the WiMAX parity check matrix standard  $H$  (384,768). The encoding process of single LDPC-WiMAX is calculated by constructing the generator matrix  $G$ , such that  $G.H^T=0$  where  $G$  is obtained by inversion of the parity check matrix concatenated with the identity matrix of the same size. Then the codewords are calculated by multiplying the message frame with the generator matrix  $G$ .

The encoding process of MPCGCs-WiMAX is calculated by concatenated three small random LDPC codes into parallel concatenation with the same parity check matrix dimensions  $H$  (192,384) with different MCWs. The decoding process is calculated by parallel concatenation of three LDPC components by using the sum product. As shown in Figure 5.9, the performance is enhanced showing for example a gain 0.3 dB improvement at BER  $2e-4$  when compared with the same parameter of single LDPC-WiMAX according to the reported result by Teodor et. Al [105]. Also shown in Figure 5.9, that the MPCGCs-WiMAX outperforms single LDPC-OFDM by 0.8 dB at the same parameters[95].

We noticed also at moderate SNR region the packet error rate PER performance of the MPCGCs parallel decoding outperforms single irregular LDPC-OFDM component decoder at the same parameter by achieving gain about 0.4 dB at BER= $1e-3$  as shown in Figure 5.10.

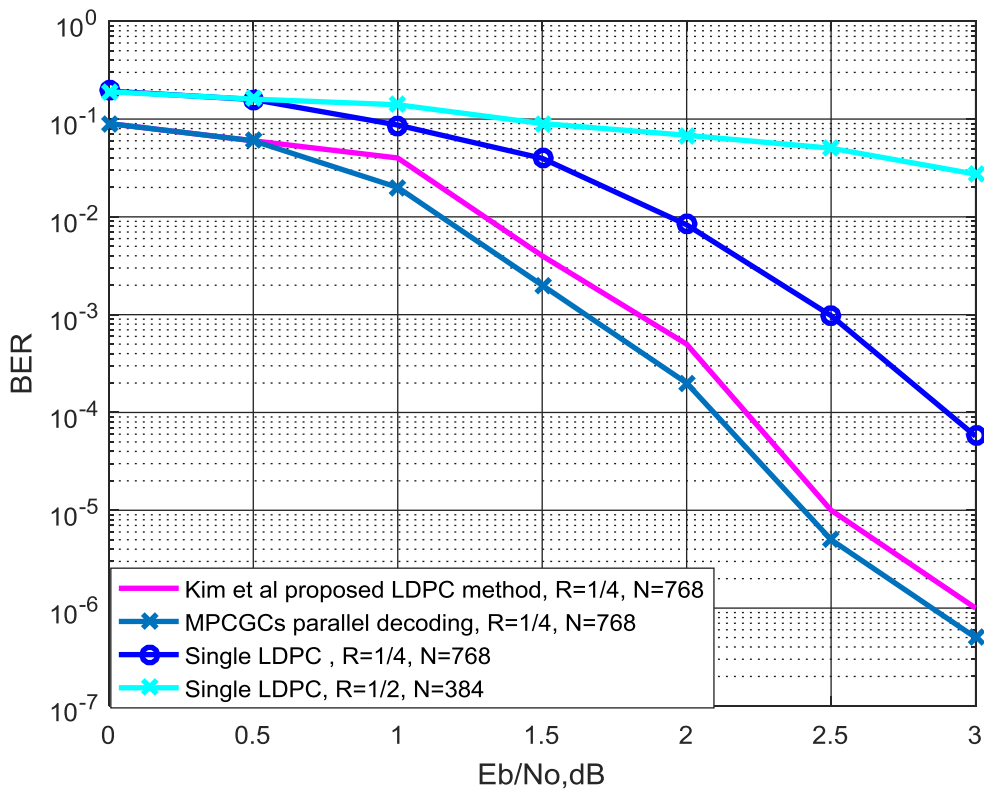


Figure 5.8 BER comparison for different LDPC coding model.

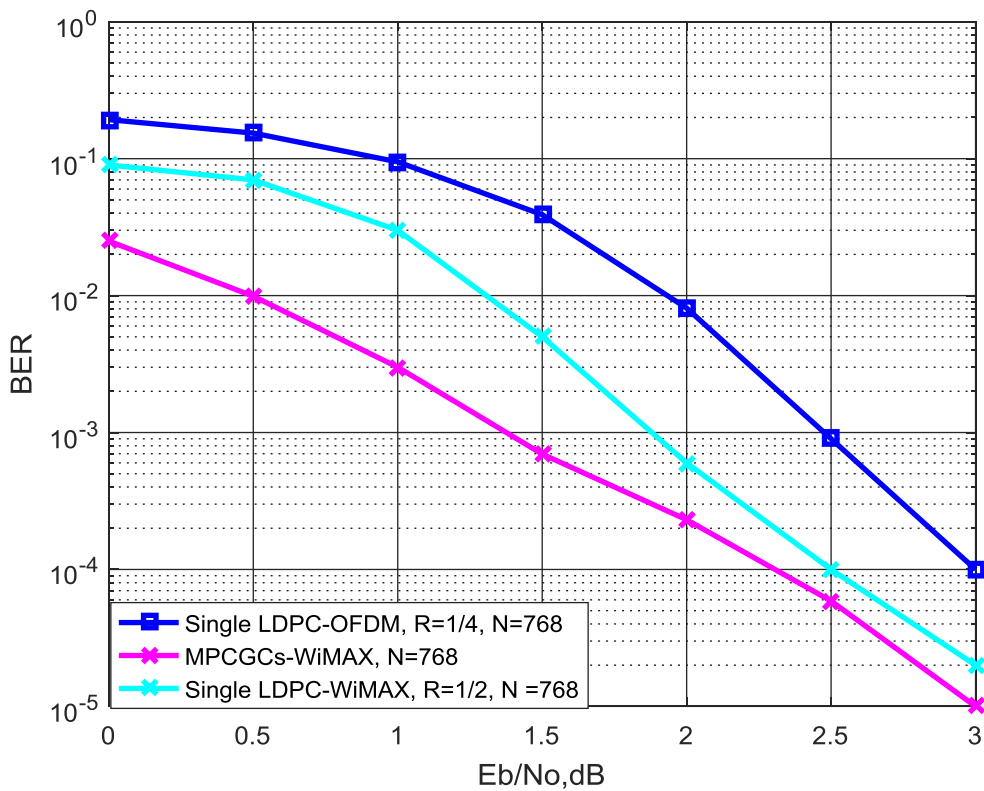


Figure 5.9 BER comparison of WiMAX coding model.

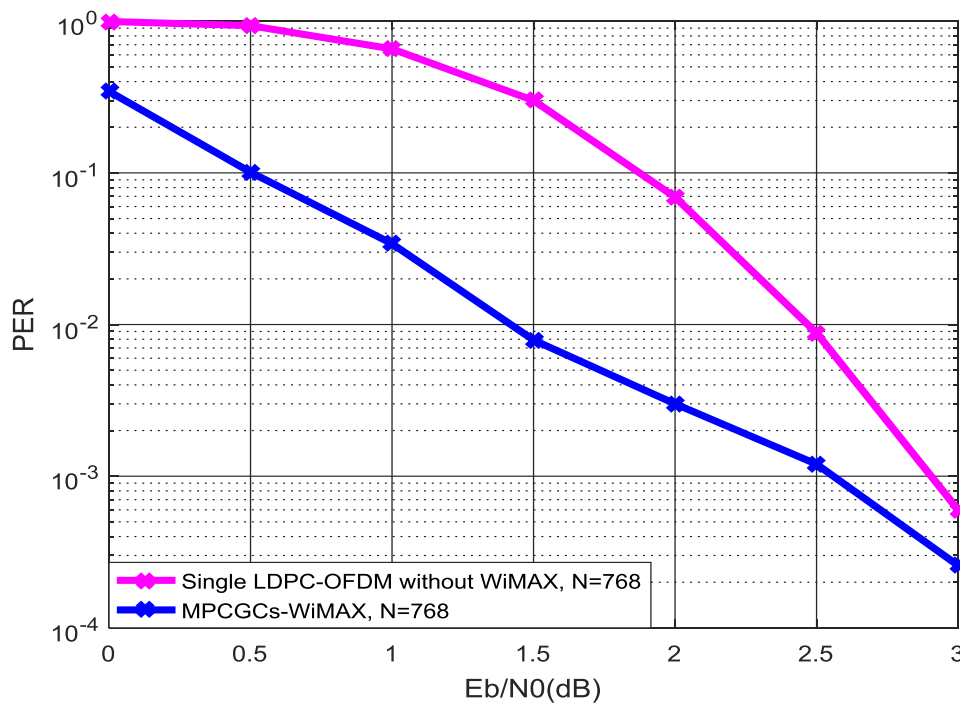


Figure 5.10 PER comparison for MPCGC-WiMAX system and single LDPC-OFDM.

To enhance the BER performance of the standard MPCGC-WiMAX application and reduced the decoding complexity. The puncturing performance of the proposed designed MPCGCs were applied to upgrade the code rate to half. After encoding, the codeword  $N=768$  is punctured by a puncturing fraction  $\Theta=0.5$  to be  $N=384$  for enhancing the BER performance at only high  $E_b/N_0$  region as well as reduce the decoding complexity and to increase the transmission code rate from  $\frac{1}{4}$  to  $\frac{1}{2}$ . In the punctured design, we will use the irregular puncturing to get the best performance for the WiMAX system. The irregular puncturing is performed well compared with the other puncturing techniques as mentioned in the previous chapter. The process of puncturing the codeword is done by removing fixed 128 bits from the end of the first parity check, moreover removing fixed 128 bits from the beginning and the end of the second parity check also removing fixed 128 bits from the beginning of the third parity check respectively. Figure 5.11 show the different BER comparison of WiMAX application over AWGN channel, the punctured MPCGCs-WiMAX outperforms both single LDPC-WiMAX and MPCGCs-WiMAX without puncturing at high  $E_b/N_0$  region only but provides worse BER at low and medium  $E_b/N_0$  region at the same parameters.. Another BER comparison of WiMAX application over flat Rayleigh fading channel as shown in Figure 5.12.

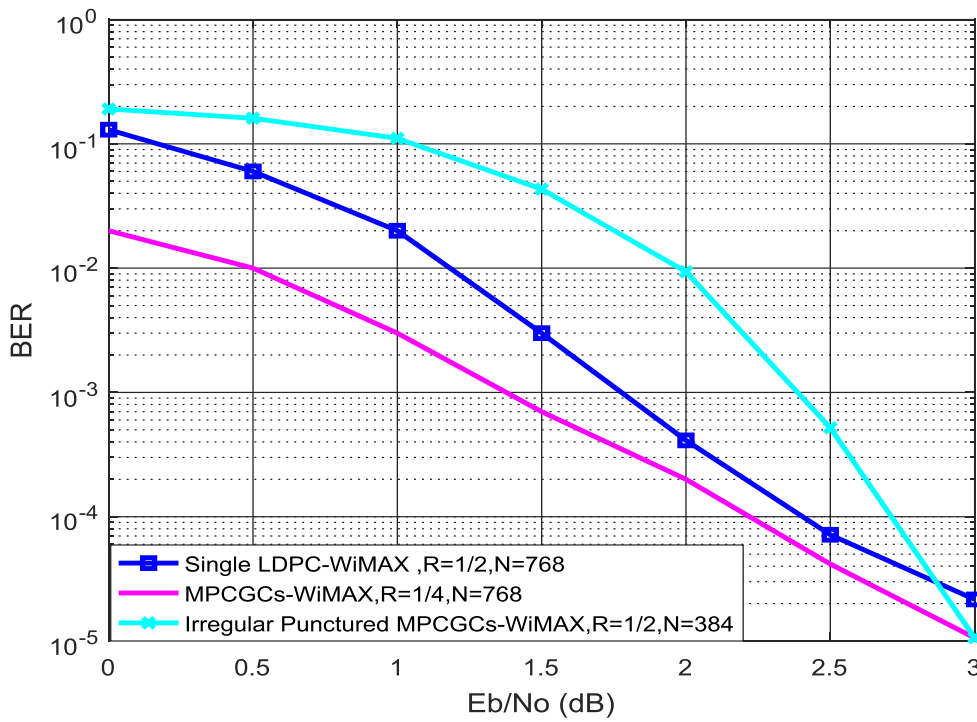


Figure 5.11 BER comparison of WiMAX physical layer model over AWGN channel.

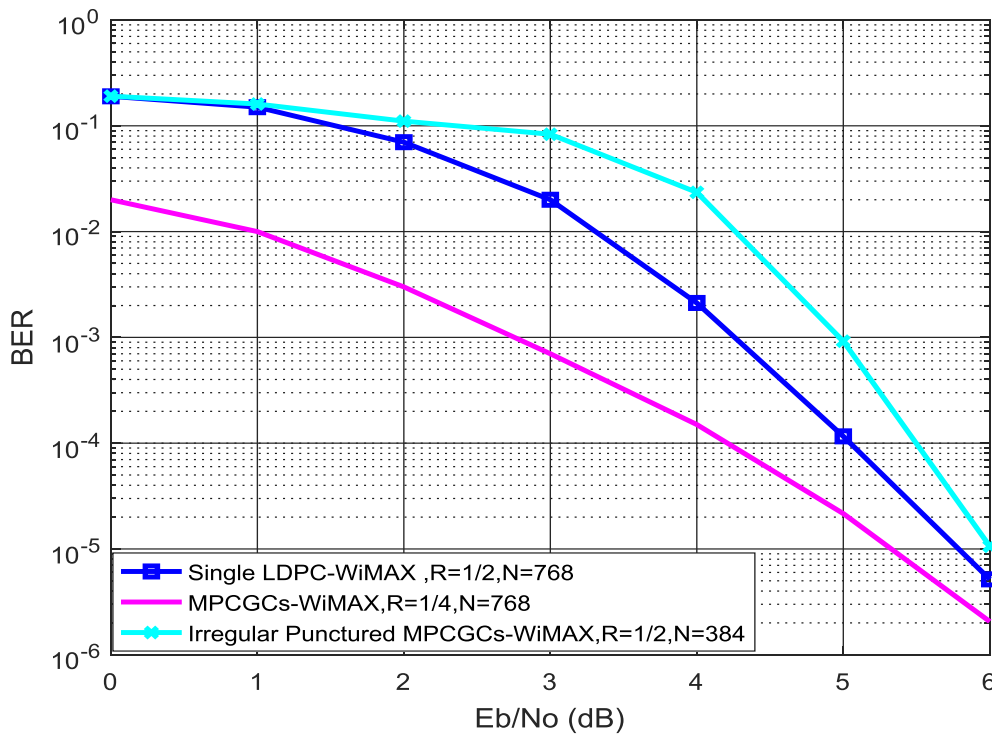


Figure 5.12 BER comparison of WiMAX physical layer model over flat fading channel.

## 5.6 Summary

This chapter focused on investigating the deployment of MPCGCs in the IEEE 802.16 standard physical layer system based on the basic modulation scheme, AWGN transmission and flat Rayleigh fading channel. For the same parameters, the proposed MPCGCs-WiMAX achieves better gain than single-long LDPC based WiMAX. In addition, the MPCGCs scheme shows further advantages when applying irregular puncturing for enhancing and upgrading the code rate from  $\frac{1}{4}$  to  $\frac{1}{2}$  to be compatible with non-puncturing standard WiMAX system. The MPCGC scheme can be a potential scheme for the channel coding in the WiMAX communication system.

## Chapter 6

# Performances analysis of MPCGC with QC-LDPC Codes and MIMO application

### 6.1 Introduction

Quasi-Cyclic (QC) LDPC codes have played important roles in the forward error correction coding (FEC) system to reduce decoding complexity and enhance the system performance. QC-LDPC can be powerful incorporated with the MPCGC system to improve the performance of wireless coded systems.

Structured LDPC codes vary in terms of performance and application complexity. The communication complexity is affected or influenced by check and variables nodes interconnection patterns or code structure. The QC-LDPC codes that are used with MPCGC coding model have the same properties of the QC-LDPC codes used in the WiMAX standard but in different MCW value.

Codes possessing similar and cyclic connections in rows or columns in a sub-matrix are termed as Quasi-cyclic (QC) LDPC codes. QC-LDPC can be encoded in an efficient manner with shift registers owing to their quasi cyclic structure [106][107][108] and uncomplicated address generation mechanism, less memory and localized memory access is required by their decoder architectures. In QC-LDPC codes, shifting of identity sub-matrices leads to the construction of row-column connections.

Shift values of all the sub-matrices of QC-LDPC can be used to characterize it. This is beneficial in a way that a compacted depiction of the matrix and uncomplicated construction is offered by it. QC-LDPC codes can carry out close to the capacity limit as signified in [26] even though row-column connections are limited. A concatenation of circularly shifted sub-matrices with or without zero sub-matrices can help in the formation of a QC-LDPC.

Combinatorial construction and finite geometry techniques can be taken in to account so as to get such structures [27]. A notable work has presented and analysed. Focusing on the simplification of the computational optimization of the minimum distance bounds of QC-LDPC codes in the IEEE802 standards [109]. This simplification in computing the distance bounds are 100 times faster than the previous related researches published a few years ago.

This chapter focusses on investigating a QC- MPCGC structure to enhance the coding performance with reduced overall decoding complexity where component QC-LDPC is

incorporated in parallel. The Layered BP decoding algorithm is adopted with QC-MPCGC instead of the SPA decoder to reduce the overall decoding complexity and enhance the system performance compared with a single conventional LDPC.

The MIMO-MPCGC structure is also investigated in this chapter with its potential to offer high QoS (Quality of Service) with increased data rates and spectral efficiency. Moreover, it helps in reducing the effect of fading channel by achieving high reduction in BER.

The next sections are organized as follows; in section 6.2 the proposed QC-LDPC has been applied to develop and improve the MPCGC performance. In section 6.3, a layered BP QC-MPCGC has been incorporated with MPCGC system to reduce the decoding complexity.

The MPCGC has developed and modified with the MIMO technique to improve and enhance the MIMO-MPCGC performance as shown in section 6.4. Finally, in section 6.5 a complexity analysis has been done and calculated for the QC-MPCGC system.

## 6.2 Proposed QC-MPCGC System Model

The QC-MPCGC physical layer model, as shown in the block diagram in fig. (6.1), is based on the circulant permutation matrices and random Gallager codes with specific column weight. The system model of QC-MPCGC combines three different LDPC codes in parallel to improve the BER performance and reducing the decoding complexity compared with the conventional single LDPC and MPCGC.

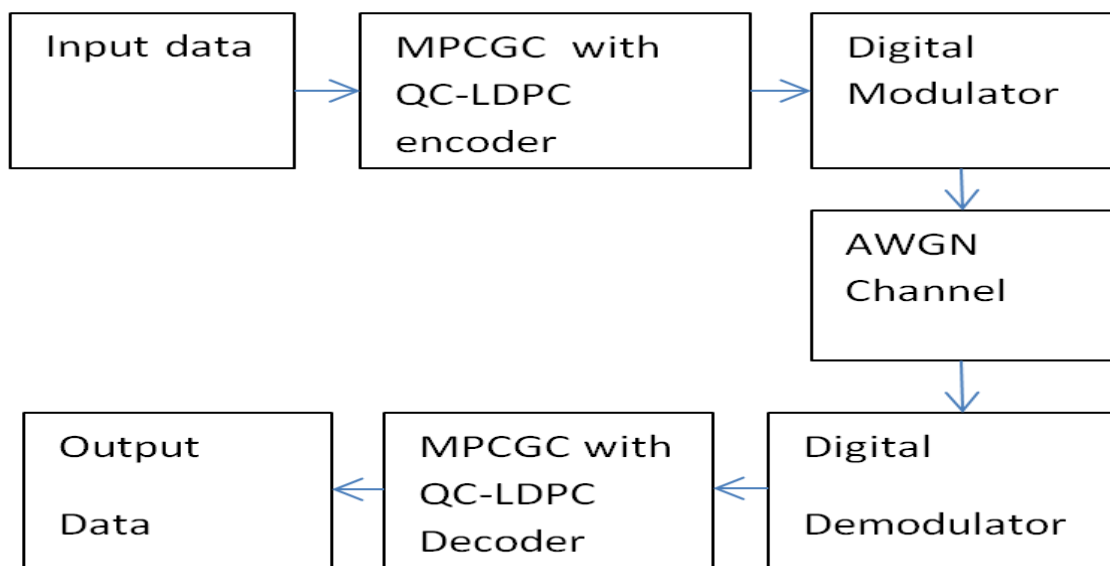


Figure 6.1 QC-MPCGC System Model.

### 6.2.1 QC-LDPC Encoder

The following are the major and foremost steps from the encoding mechanism:

A Quasi-Cyclic is basically a block code in which another code word is obtained by every cyclic shift of a code word by  $p$  positions. Thus, a cyclic code is a QC code with  $p = 1$ . The parity check matrix of the QC-LDPC codes signifies it and it comprises of small square blocks which are zero matrices or circulant permutation matrices [23] [110]. The achieved code is quasi-cyclic (QC) and can be programmed in linear time with the help of shift registers. In addition, an equal code with only identity matrices in the first row block and the first column block of  $H$  can be attained by row and column permutations.

1. The quasi-cyclic code of length  $mp$  is the length of the code word, where  $m$  is the row weight.
2. The column size and row size of the code are multiples of an integer  $p$ .
3. Create  $P^i$  be the  $p \times p$  circulant permutation which moves the identity matrix  $I$  for any integer  $i$ ,  $0 \leq i \leq p$  to the right  $i$  times.
4. We can define the parity check matrix  $H_{mp \times np}$

$$\begin{bmatrix} P_{b11} & P_{b12} & P_{13} & \dots & P_{b1n} \\ P_{b21} & P_{b22} & P_{23} & \dots & P_{b2n} \\ P_{b31} & P_{b32} & P_{b33} & \dots & P_{b3n} \\ \vdots & \vdots & \vdots & \dots & \vdots \\ P_{bm1} & P_{bm2} & P_{bm3} & \dots & P_{bmn} \end{bmatrix} \quad (6.1)$$

Where,  $b_{ij} \in \{0, 1, \dots, p-1, \infty\}$ . Also  $H$  should be full rank

5. Enhancing the size of the circulant permutation matrices  $p$  which is element matrices of  $H$  can help in achieving larger size block LDPC codes.
6. The inversion of the generator matrix  $G$  with identity matrix of the same order yields the generator polynomial.
7. Multiplying the message matrix with the generator matrix puts forward codewords [101][103].

### 6.3 Layered Decoding

Decoding in layers is another significant approach if we shed light on the several approaches directing towards iterative decoding. In such a case, the parity check matrix can act as horizontal layers and every layer can signify a component code. The full code is the resultant of intersections of all these codes (layers). In addition to it, soft-input soft-output (SISO) decoding technique can be implemented to each layer in order. The inputs from the decoder are linked to the channel inputs and extrinsic probability outputs from the SISO decoding on the last layer treated. If essential, this can be applied to previous layers as well as each next layer starts decoding. This process can be continued until the objective is achieved. Iterations in a layer by means of the SISO decoder can be called sub-iterations and the term super iterations can be used for the general process repetitions [111-113].

If a layer is to be decoded, a SISO decoder is implemented to each component code as all the codes are independent in the structure. The obtained outputs are later on delivered to the next layer that is to be decoded. In a scenario of the specific component code, the SISO decoders could be specially derived decoders or for the specific portion of the parity check matrix, these decoders could be grounded on belief propagation [114].

For the SPA, the nodes are sequentially updated by the layered BP (LBP) schedule, also known as shuffled BP and other names, which ensure that the new information available in the graph is properly utilized by the incoming messages used for each update.

Specifically, a network system updates the single node or subsets of all nodes of one type instead of updating all nodes of one type followed by all nodes of the other type. Subsequently, system updates a single or some subset of the nodes of the other type. Until the time that, the check nodes have been updated, the shuffling or alternating is continued [115][116].

This is referred to as the one iteration of the LBP. As compared to the flooding schedule, faster convergence for this schedule is enabled by the latest information on the graph. In the given examples below, as shown in Figure 6.2 below, it consists of multi parts a, b, c and at each part, the first half-step between variable node and check node is red shaded while the second half step is yellow shaded.

Check nodes are sequentially updated in one half-step, and all variable nodes are updated in the second half-step, and this particular step is done in the neighbourhood of the most

recently updated check node. These steps are performed until the time all check nodes have been updated [117].

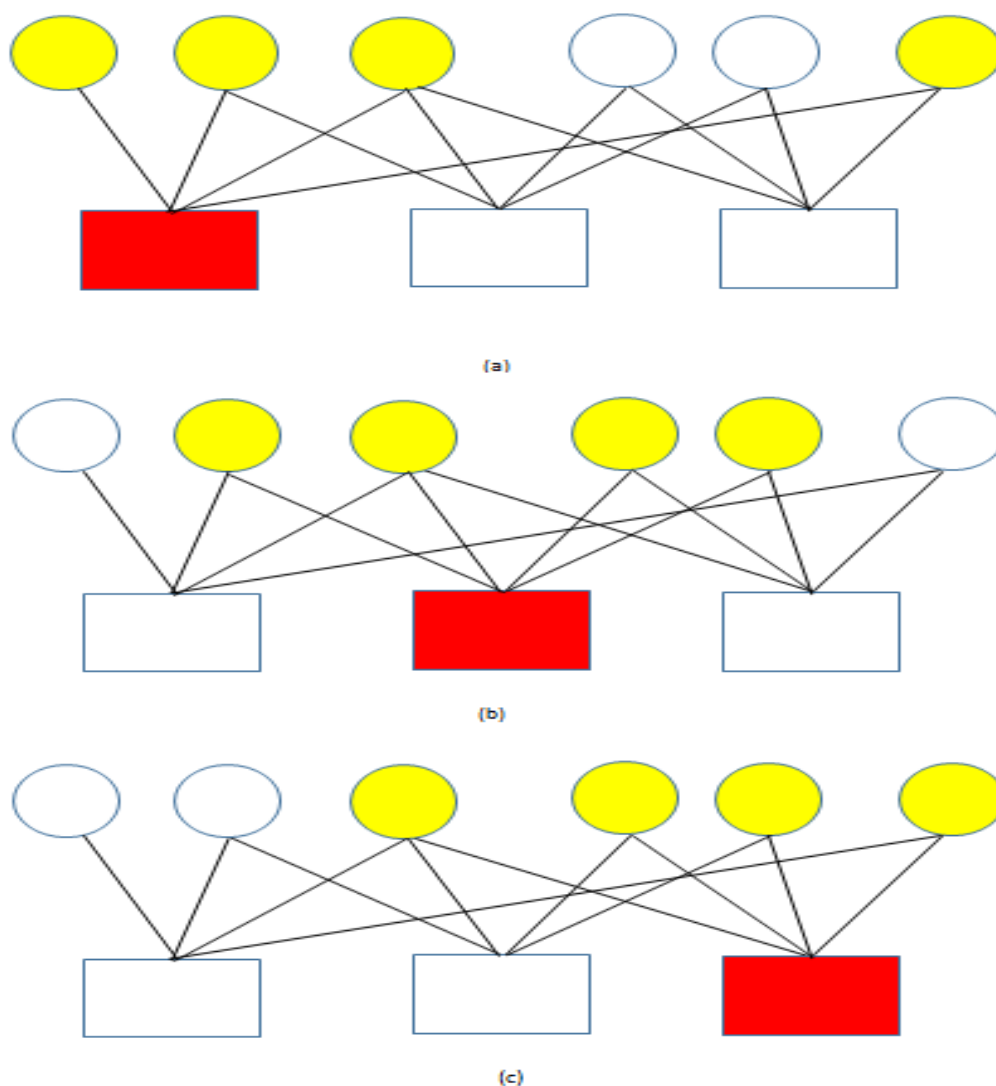


Figure 6.2 Layered schedule between check and variable nodes of the example graph.

#### 6.4 Multiple Input Multiple Output (MIMO)

The popularity of wireless communications, especially mobile communications, has vastly increased. For high spectral-efficiency and high bitrate transmission, such as multi-input multi-output (MIMO) systems [118], transmit diversity schemes have been studied. There is a great enhancing in system performance due to increase in the capacity of the systems as the diversity in both space (antenna) and time domains can be exploited by the MIMO Systems. Nevertheless, only the diversity gain can be exploited by MIMO systems. Therefore, for high

quality communications, there is a requirement of forward error correction coding (FEC) in these systems. There has been application of turbo structure decoding to these systems. Three encoders and three decoders are made use of by the normal LDPC codes. The good error rate performance over MIMO channels can be achieved by the multi-antenna systems with turbo decoding, as it has been demonstrated.

For high quality communications, there is a requirement of forward error correction coding in the MIMO systems. As of late, similar to good error correcting codes, attention has been to acquire low-density parity-check (LDPC) codes [119]. The MIMO systems, where the MIMO-LDPC is the name given to the system, have acquired LDPC codes. As shown in Figure 6.3.

$N_t$  transmits and  $N_r$  receives antennas, where  $N_r \geq N_t$ , has been used for modelling the MIMO system.  $h_{i,j}$  can be used to denote the channel impulse response from the transmit antenna  $i$  to the receive antenna  $j$ . The following denotes the received signal for the system having two transmit and two receive antennas, with the assumption that each transmit antenna transmit the signal  $s = [s_1 s_2 \dots s_n]$  at time  $t$  [120].

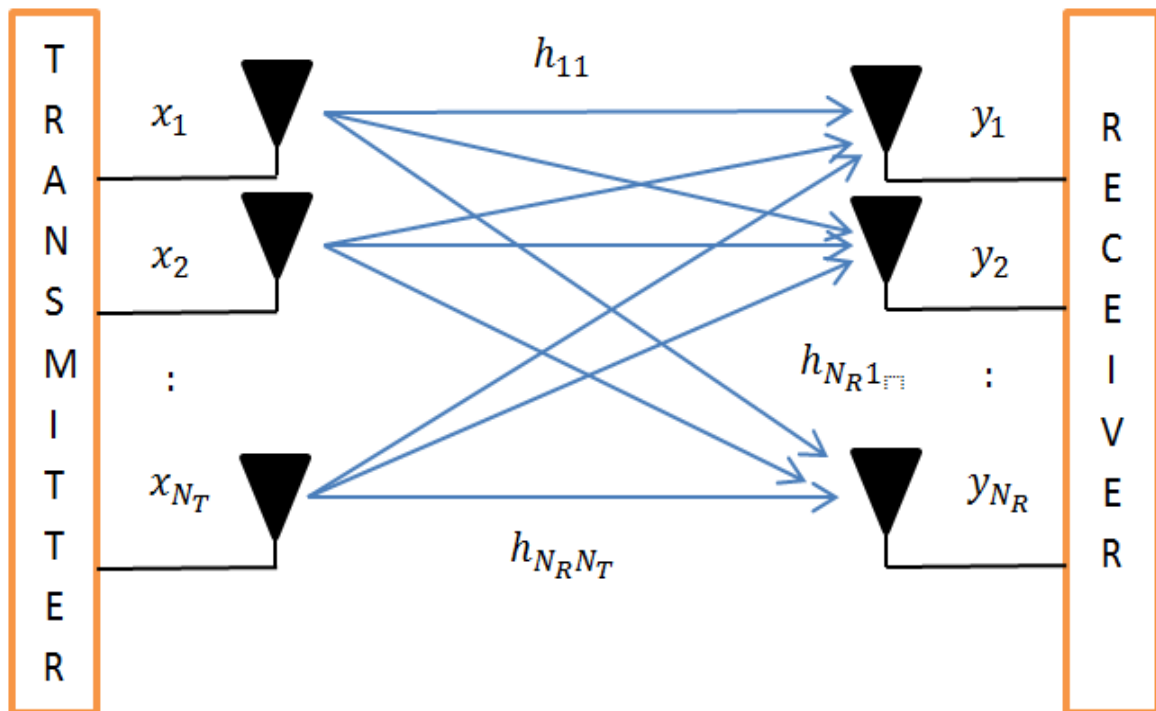


Figure 6.3 MIMO Channel.

## 6.5 Proposed MIMO-MPCGC System Model

For enhancing the MIMO-LDPC's performance, a new MIMO-LDPC system with iterative turbo decoding (MIMO-MPCGC) is proposed in this chapter with three LDPC component encoders and three LDPC component decoders with different LDPC codes.

The MIMO-MPCGC system model is depicted in Figure 6.4. The MPCGC encoder is encoding the modulating bits and mapped as BPSK modulation. The MIMO channel techniques have applied to the BPSK signal by splitting the modulated signal into multi data sequence for transmission by using multi-transmitted antennas. At the receiver, the received signal at each antenna is the superposition of the transmitted data by multi antennas.

The AWGN and fading are added to the received MIMO system. Furthermore, the received corrupted modulated symbols are combined then added to the zero forcing (ZF) equalizer process. After the equalisation the stream is passed to the demodulator and decoder process to get likelihoods of the received symbols. Finally, the recovered data have abstained from the decoding process.

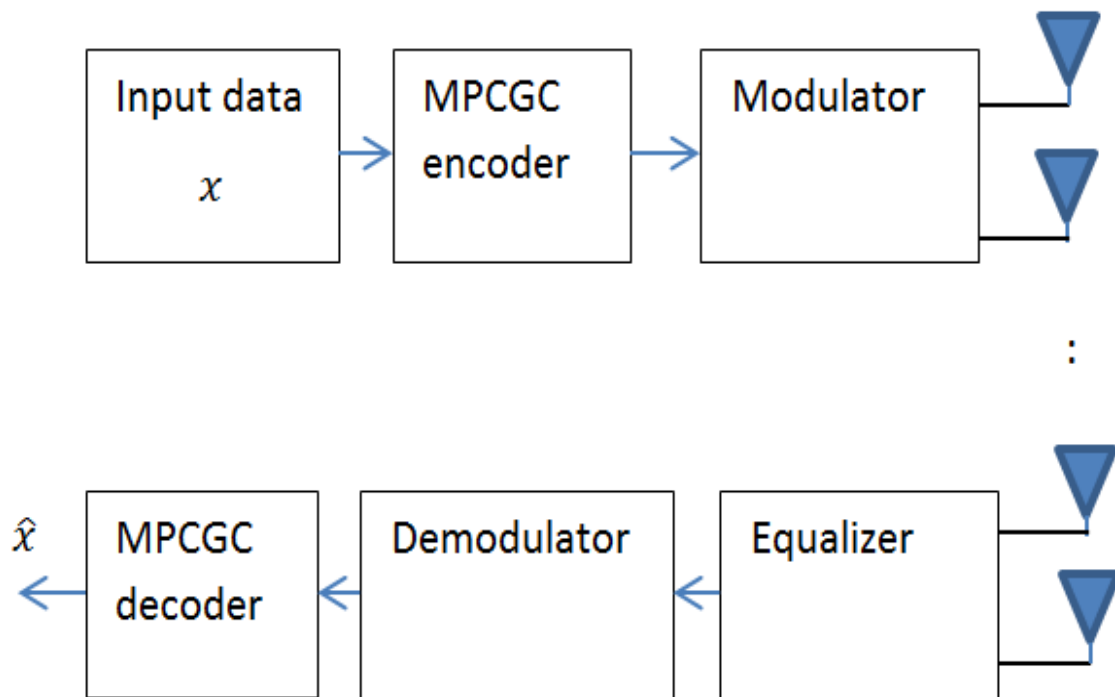


Figure 6.4 MIMO-MPCGC system model.

### 6.5.1 The Channel of the proposed MIMO-MPCGC

Let us assume 2X2 MIMO channels with BPSK modulated signal on fading and AWGN channel. We can represent the received data as

$$y = hX + n \quad (6.2)$$

Where,  $n \in N(0, N_o)$ ,  $n$  represents the zero mean of AWGN and  $N_o$  represents the variance.

For 2X2 MIMO-MPCGC.

$$\begin{bmatrix} y_1 \\ y_2 \end{bmatrix} = \begin{bmatrix} h_{11} & h_{12} \\ h_{21} & h_{22} \end{bmatrix} \begin{bmatrix} x_1 \\ x_2 \end{bmatrix} + \begin{bmatrix} n_1 \\ n_2 \end{bmatrix} \quad (6.3)$$

The receiver has assumed to be known the fading channel coefficients  $h_{11}, h_{12}, h_{21}, h_{22}$  and also known the  $y_1, y_2$

From equation (6.3), we can find the received signal at the first received antenna as

$$y_1 = h_{11} x_1 + h_{12} x_2 + n_1 \quad (6.4)$$

The received signal at the second received antenna as

$$y_2 = h_{21} x_1 + h_{22} x_2 + n_2 \quad (6.5)$$

Where,  $y_1, y_2$  represents the received symbol at the first and second antenna simultaneously

$h$  represents the flat fading coefficient channel as the multipath channel and has one tap, also  $h = 1$  for AWGN channel.

$h_{11}$  represents the channel coefficient from the first transmitted antenna to the first received antenna.

$h_{12}$  represents the channel coefficient from the second transmitted antenna to the first received antenna.

$h_{21}$  represents the channel coefficient from the first transmitted antenna to the second received antenna.

$h_{22}$  represents the channel coefficient from the second transmitted antenna to the second received antenna.

$x_1, x_2$  represents the equal probability of BPSK transmitted modulated signal +1 or -1.

$n_1, n_2$  represents the noise at the first and received antenna.

### 6.5.2 The Channel equalizer of the proposed MIMO-MPCGC

The zero forcing (ZF) equalizer is applied to the MIMO-MPCGC system before the decoding process of the received symbols. Furthermore, the frequency response of the fading channel of the received symbols are inverted and equalized to retrieve the signal and minimize the inter symbol interference (ISI). Later, the received symbols are passed to the SPA decoder of the MPCGCs to detect the original data. Figure 6.5 shows the equalizer model of the MIMO-MPCGC system [121].

The equalized signal of the received symbols at each sample time  $t$  as follow:

$$\hat{X}(t) = y(t) + H_t^{-1}(t) w(t) \quad (6.6)$$

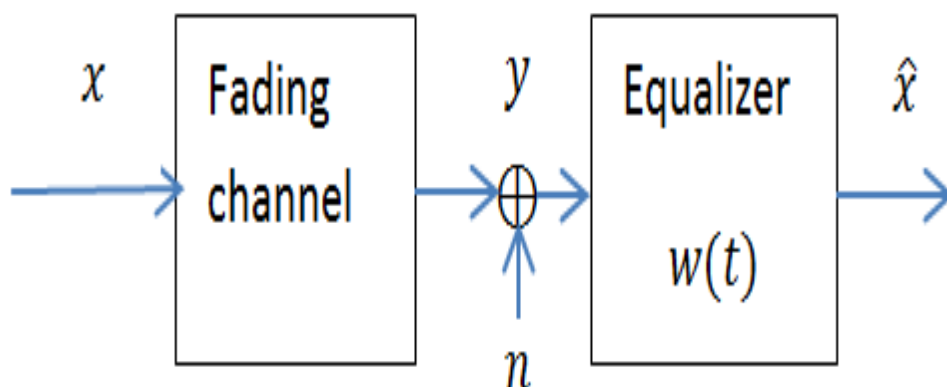


Figure 6.5 Equalizer model.

## 6.6 Simulation results and discussion

### 6.6.1 BER performance analysis

Firstly, the properties of QC-MPCGC are simulated and evaluated by using two different LDPC Gallager component codes with one QC-LDPC component and all gathered in parallel concatenation; also each component is allowed a maximum of 38 local iterations whereas the overall MPCGC have 30 super iterations.

The BER performance of the QC-MPCGCs is evaluated and is illustrated in Figure 6.6 as well compared with the other coding models like MPCGCs, Kim et al result and single conventional LDPC component. The parameters of the three parallel LDPC components of QC-MPCGC have the same parity check dimensions,  $H$  (192,384) with different MCWs: code rate  $R=1/4$ ,  $MCW_1=1.901$ ,  $MCW_2=2.666$ ,  $MCW_3=1.791$  and the overall block length  $N=768$ . Where, the first and third LDPC codes are Gallager codes, while the second LDPC code is circulating construction QC-LDPC with the following parameters; the parity check matrix has the prime number  $p=64$  of the rank of submatrices, the row weight  $k$  of the parity check matrix is 3 and the column weight  $j$  of the parity check matrix is 6. Usually for any number of  $M$  encoders/decoders of the QC-MPCGC there is only one QC-LDPC component considered that controls on the high  $E_b/N_0$  region and is located before the last component. Moreover, for four QC-MPCGC components the location of the QC-MPCGC will be in the third component and so on.

The number of rows  $m$  in the QC-LDPC is  $(kXp) = 3X64=192$ , while the number of columns  $n$  in the QC-LDPC is  $(jXp) = 6X64=384$ . Moreover, the parameters of the equivalent single irregular LDPC code that is used for comparison are:  $R=1/4$ ,  $MCW= 3.07$ ,  $N=768$ ,

The reason for using only one QC-LDPC component with MPCGC is due to the regular circulant permutation of the QC-LDPC codes and the difficulty in designing the specific suitable MCW for each code.

The performance of QC-MPCGC with 3 QC-LDPC codes performs much worse compared to the conventional MPCGC therefore; we used two Gallager components and one QC-LDPC component for best design QC-MPCGC.

The proposed QC-MPCGC has a gain of 0.7 dB (at BER  $2e-4$ ) when compared to the equivalent single irregular LDPC with the same parameters. Furthermore, the QC-MPCGC performance slightly outperforms the conventional MPCGCs at high  $E_b/N_0$  region by 0.1 dB (at BER  $2e-4$ ) with the same parameters.

The QC-MPCGCs provides 0.2 dB gain improvements when compared with the result of the documented conventional method by Kim et. al using the same parameters [70]. Another advantage from incorporating QC-LDPC in the powerful MPCGC is to reduce the decoding complexity in terms of iteration and edges as will be explained in the next section.

The characteristics of QC-MPCGC parallel decoding are evaluated with layered BP decoding instead of SPA, by using three LDPC component codes as the same QC-MPCGC parameters of the above design. As shown in Figure 6.7 the layered BP decoding QC-MPCGC-BPSK over AWGN channel performs slightly worse than both conventional QC-MPCGC with SPA and MPCGC.

In addition, the decoding complexity of the layered BP QC-MPCGC has less complexity in terms of the iterations and edges as will be explained in the next section.

**Secondly**, the performance of 2X2 MIMO application with MPCGC has been simulated and calculated over fading channel with BPSK modulation. Two antennas are involved in both transmitter and receiver.

The BER performance of the MIMO-MPCGC is evaluated and illustrated in Figure 6.8. The parameters of the three parallel LDPC components of MPCGC have the same parity check dimensions,  $H$  (192,384) with different MCWs: code rate  $R=1/4$ ,  $MCW_1=1.901$ ,  $MCW_2=2.81$  and  $MCW_3=1.791$  and the overall block length  $N=768$ . Again, the parameters of the equivalent single irregular LDPC code that is used for MIMO-LDPC comparison are:  $R=1/4$ ,  $MCW=2.8$ ,  $N=768$ .

The 2X2 MIMO-MPCGC provides gain of 0.25 dB (at BER  $1e-4$ ) when compared to the MIMO-LDPC result of the reported method by Deepa and Kumar using the same parameters [118].

Thirdly, the performance of 2X4 MIMO-MPCGC has also evaluated with the same above parameters as shown in Figure 6.9.

The 2X4 MIMO-MPCGCs have two antennas in the transmitter and four antennas in the receiver; the performance of 2X4 MIMO-MPCGC outperforms the conventional MIMO-LDPC by 0.5 dB (at BER  $2e-4$ ) with the same parameters.

**Finally**, Figure 6.10 shows the effect of the multi antenna numbers in both transmitter and receiver of the MIMO system. The BER performance of 2X4 MIMO-MPCGC outperforms the 2X2 MIMO-MPCGC by 3 dB (at BER  $1e-4$ ).

Furthermore, the performance of 2X4 MIMO-LDPC provides 2.8 dB (at BER  $1e-4$ ) when compared to the 2X2 MIMO-LDPC result of the reported method by Deepa and Kumar using the same parameters [118].

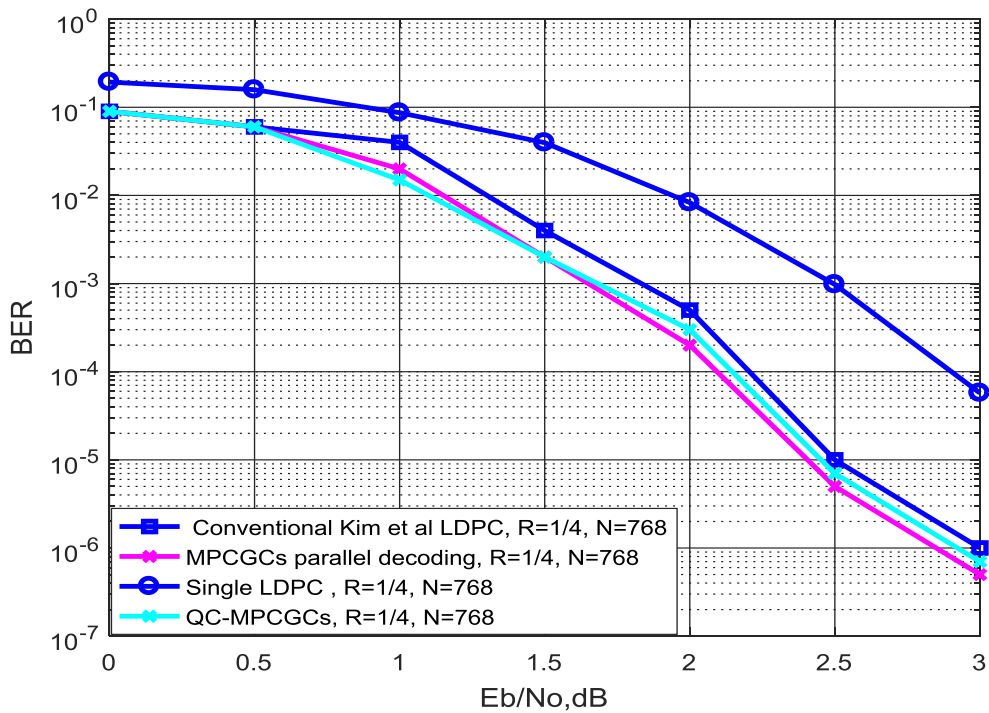


Figure 6.6 BER comparisons of QC-MPCGC and different coding model over AWGN channel.

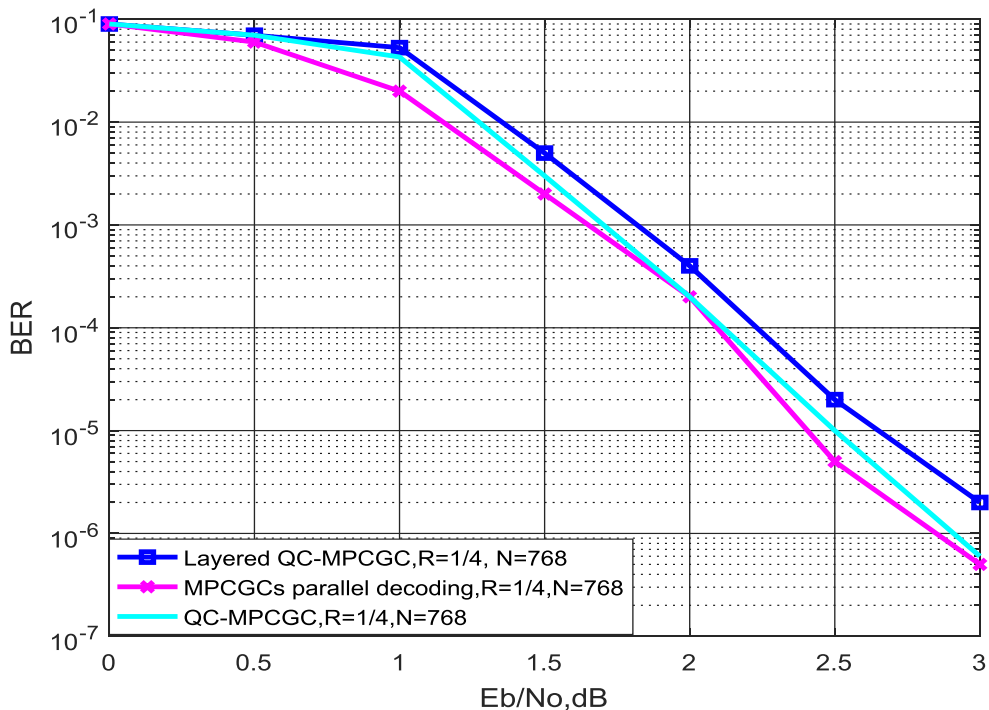


Figure 6.7 BER comparison of Layered QC-MPCGC and different coding model over AWGN channel.

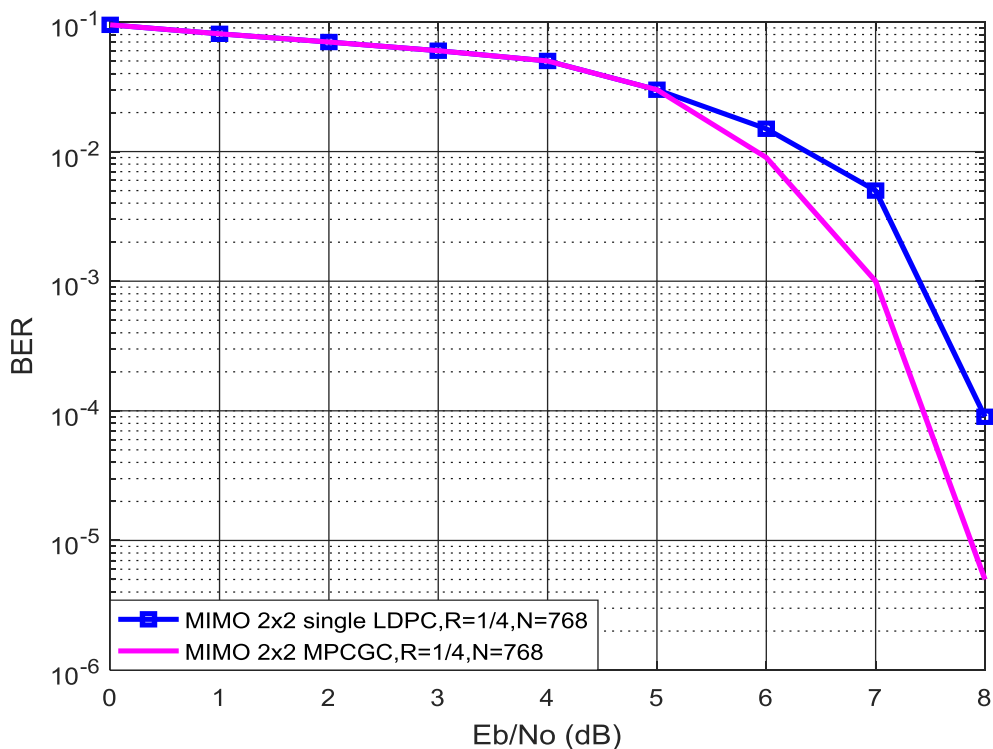


Figure 6.8 BER comparison of 2X2 MIMO-LDPC over fading channel

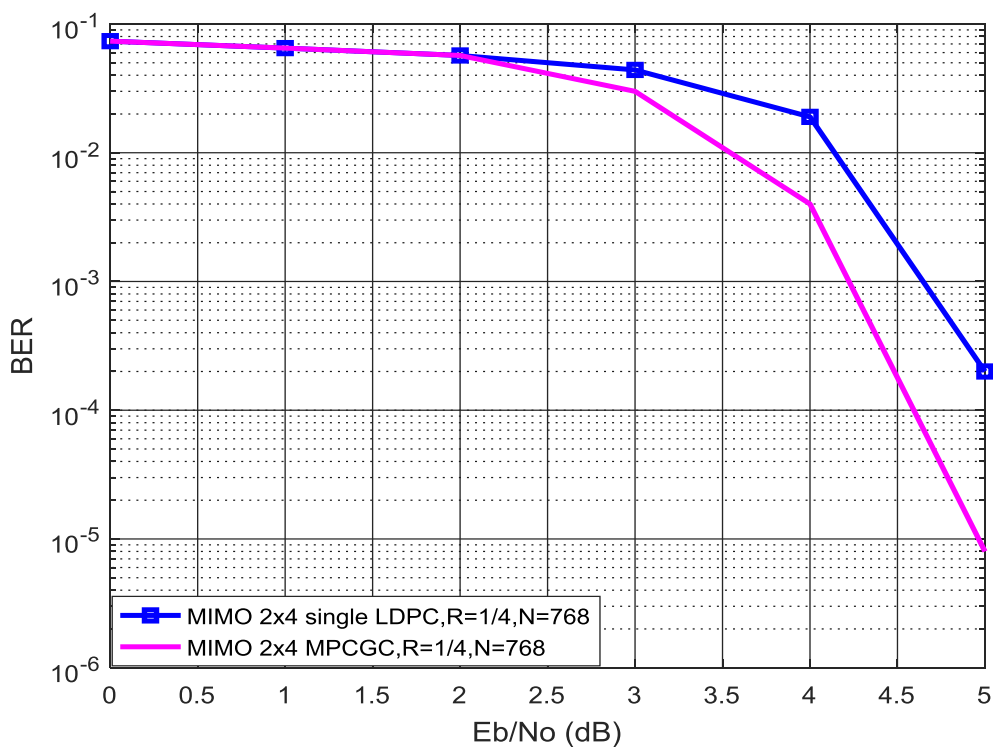


Figure 6.9 BER comparison of 2X4 MIMO-LDPC over fading channel

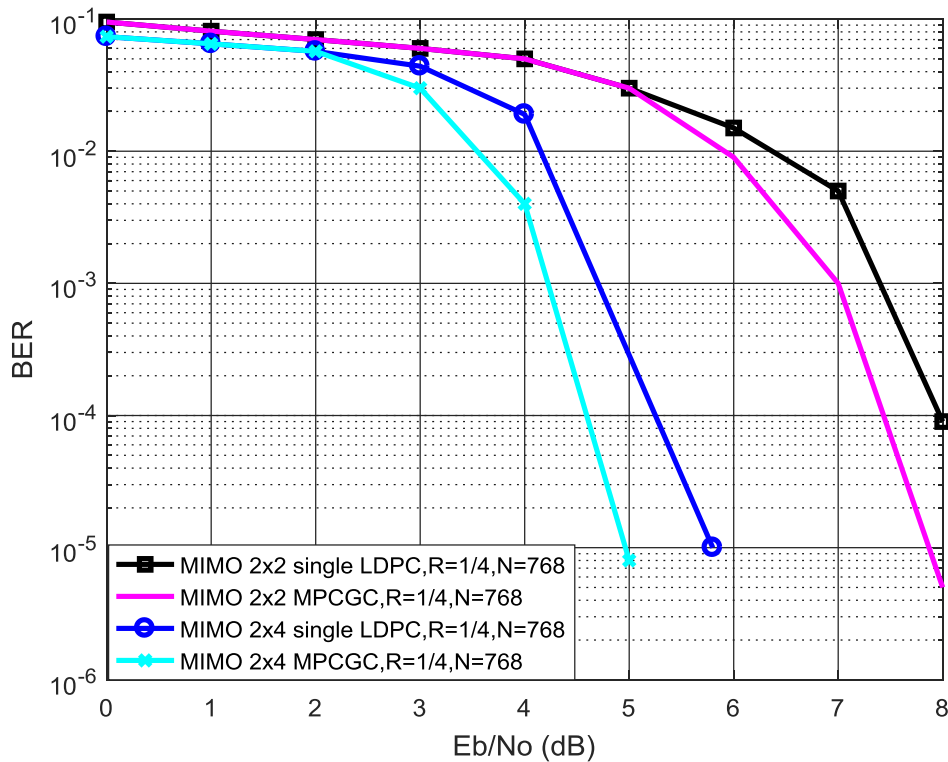


Figure 6.10 BER comparison of MIMO-LDPC over fading channel

### 6.6.2 QC-MPCGC complexity analysis

QC-LDPC code has good performance and suitable for hardware implementation due to its regular circulant permutation matrices. In addition, the encoding complexity of the QC-MPCGC can be reduced due to the process of circular shifting. Moreover, the decoder part can be reduced the computational complexity of the check nodes update [109][122][123].

**Firstly**, the complexity calculation for the QC-MPCGC is done and calculated according to the same process as mentioned in chapter 4. The result in terms of the maximum number of iterations and edges are illustrated in Figures 6.11 and 6.12. The base QC-LDPC matrices of the circulant permutation matrices that are used in the QC-MPCGC model is zero matrix [64x64] with a diagonal one and the other submatrices are circular permutation of this base matrix. Figures 6.13 and 6.14 show the structure of the base matrix (64X64) and the overall parity check matrix (192X384) of the QC-MPCGC respectively. The results show that the complexity of the proposed QC-MPCGC can be reduced significantly when compared with the conventional MPCGC system. Moreover, the advantages of the proposed QC-MPCGC can be exploited without significant additional complexity.

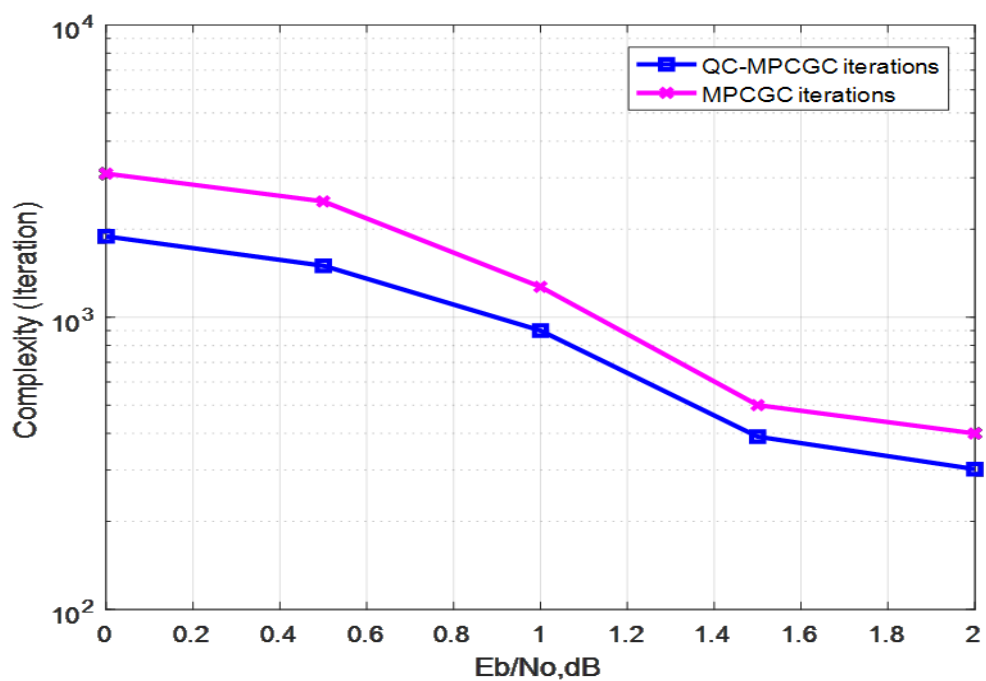


Figure 6.11 Complexity and performance comparison between QC- MPCGC and conventional MPCGC

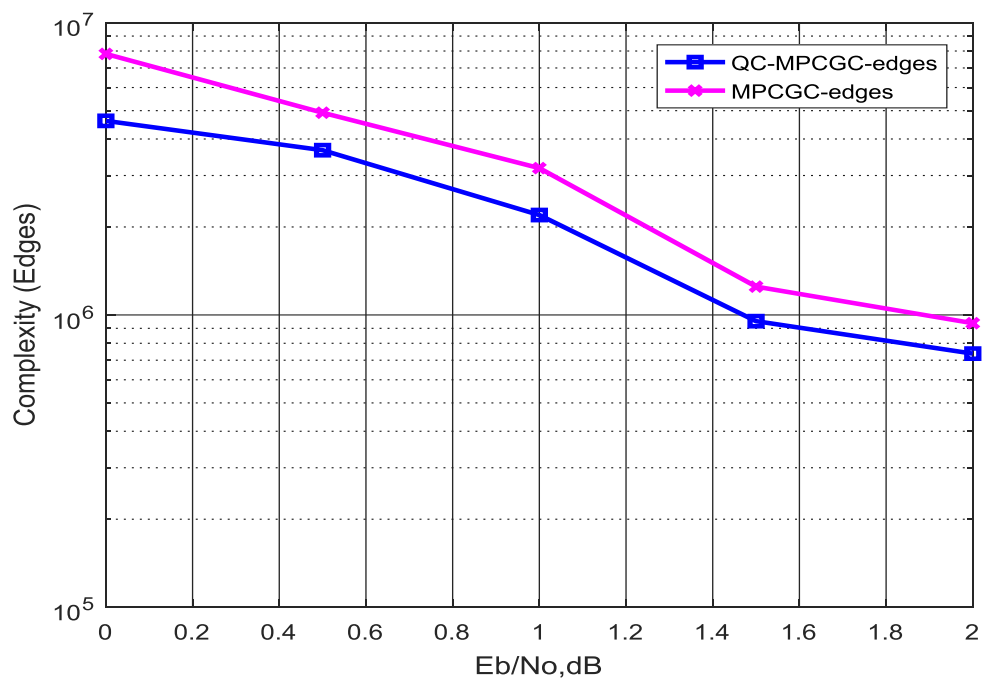


Figure 6.12 Complexity and performance comparison between QC- MPCGC and conventional MPCGC

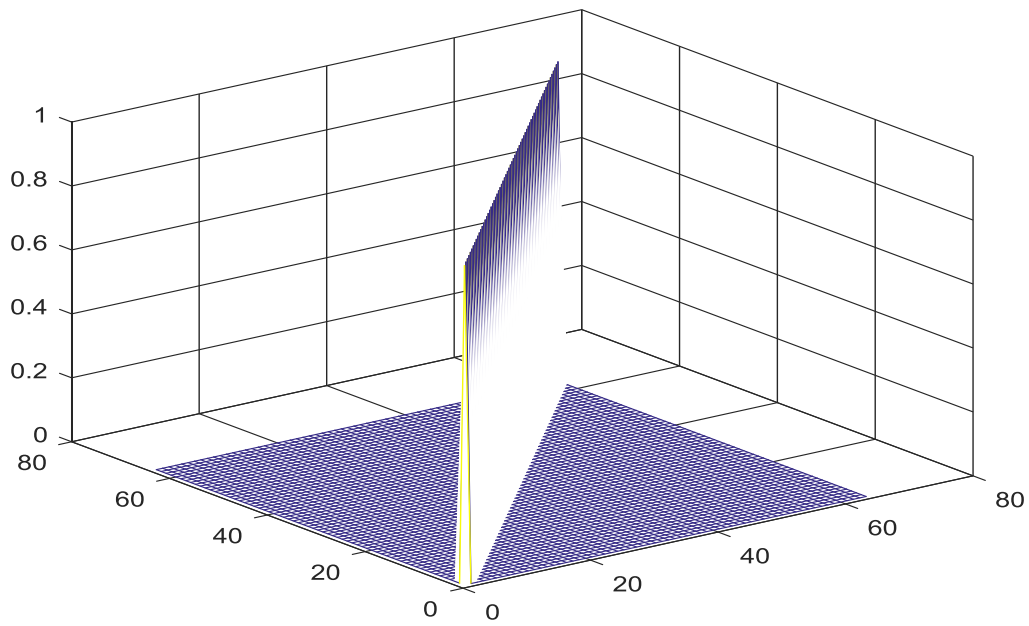


Figure 6.13 Entries of the base matrix (64x64) of the QC-MPCGC

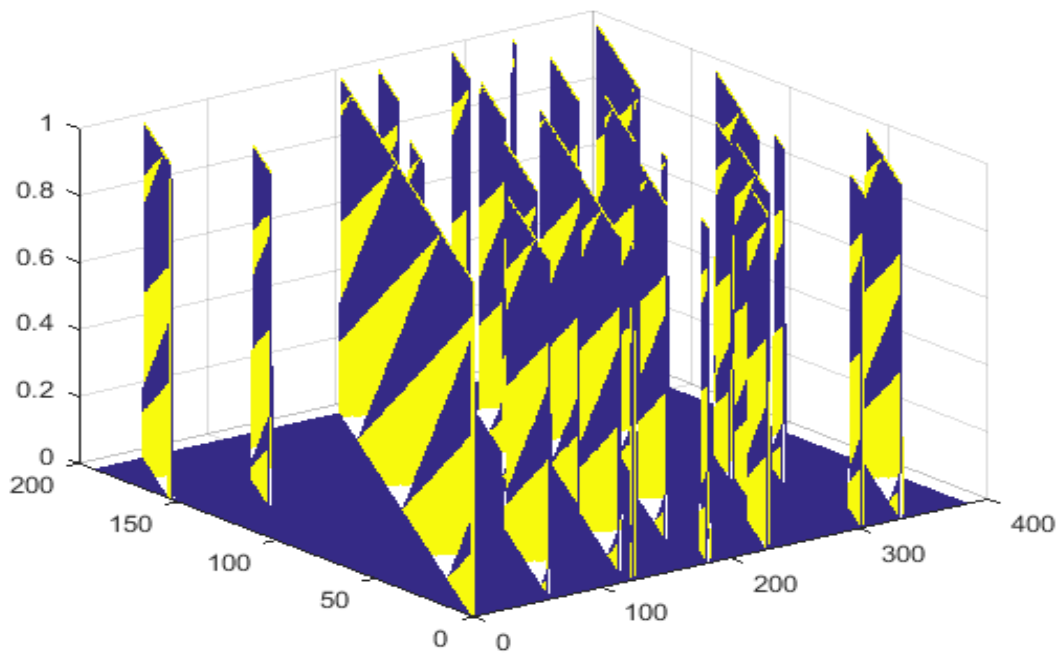


Figure 6.14 Entries of the parity check matrix (192x384) of the QC-MPCGC

**Secondly**, the decoding complexity of layered BP QC-MPCGC has been calculated and the results show that the complexity of the proposed layered BP QC-MPCGC exploited lower decoding complexity when compared with the conventional MPCGC system in terms of iterations and edges as shown in Figures 6.15 and 6.16. The conventional MPCGC is the base of the Gallager codes with SPA only.

Moreover, the advantages of the layered BP QC-MPCGC can be exploited without significant additional complexity but with a trade off in BER performance.

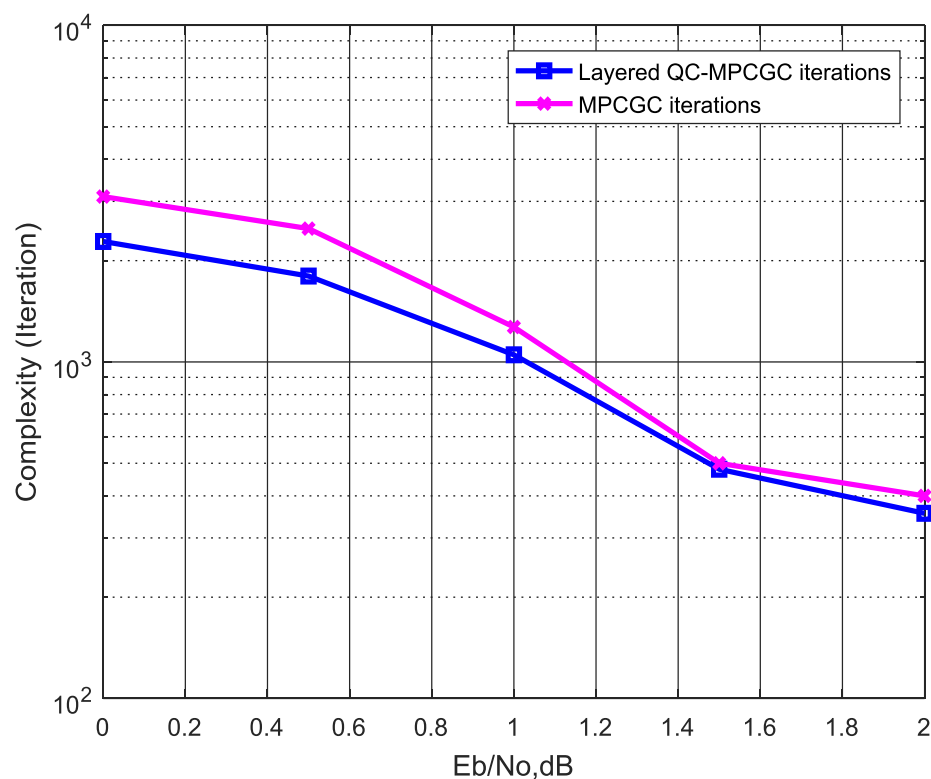


Figure 6.15 Complexity and performance comparison between Layered BP QC-MPCGC and conventional MPCGC.

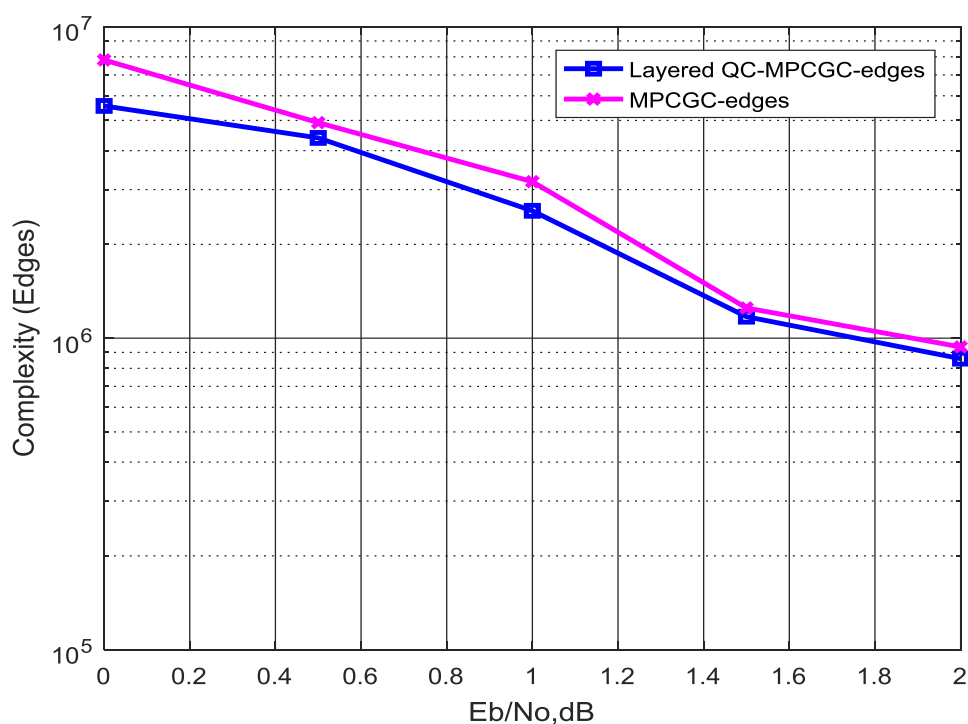


Figure 6.16 Complexity and performance comparison between Layered BP QC-MPCGC and conventional MPCGC.

## 6.7 Summary

In this chapter a further novel exploration is applied to the MPCGC to enhance the system performance with reduced complexity. QC-MPCGC is applied by gathering two Gallager codes and one QC-LDPC code to enhance the BER performance compared to the conventional single LDPC codes. Furthermore, the complexity analysis in terms of number of edges and iterations has shown that the novel proposed QC-MPCGC structure has less complexity compared with the conventional MPCGCs structure. There is benefit from reducing complexity by reducing the memory requirement of QC-MPCGC for decoding than that of the conventional MPCGC. Layered BP decoding has been applied to reduce the complexity of the QC-MPCGC in terms of iterations and edges with a trade off in BER performance.

MIMO technique is applied also to the MPCGC to improve the system performance and enhance the BER performance of MIMO-MPCGC over fading channel compared to the conventional LDPC.

## Chapter 7: Conclusion and future work

### 7.1 Conclusion

The thesis has focused on investigating a new class of concatenated codes based on the parallel concatenation of LDPC codes. MPCGC, which is a good class of parallel-concatenated codes that used to reduce the encoder/decoder complexity and to enhance the communication system performance. The LDPC codes in the MPCGC structure required well design to achieve excellent BER performance with reduced in the overall decoding complexity compared to the conventional LDPC.

For enabling LDPC codes in the MPCGC structure to use the a priori information between the component decoders, they have been modified. Specific LDPC codes with comparable rate and information frame length in both AWGN and flat Rayleigh fading channels have been outperformed by this class of codes,

**Chapter three** has presented a superior MPCGC coding model that consists of three or four LDPC components with different matrix densities when compared with conventional single LDPC component. The MPCGC-BPSK has shown a better BER performance compared to conventional Kim et al reported results by 0.2 dB gain. In addition, the MPCGC-BPSK provides 0.8 dB when compared to the single irregular LDPC at the same parameter. Furthermore, the MPCGC of three LDPC codes outperforms the serial MPCGC by 1.3 dB at the same parameter. Another advantage of the proposed MPCGC in the capacity achievement as it is shown that the MPCGC with different modulation has capacity improvement regarding single LDPC at the same parameter.

For MPCGC of four LDPC components, the BER calculation has been done and shown that it outperforms the equivalent single irregular LDPC by 0.2 dB at the same parameter.

A trade-off in the decoding complexity of the MPCGC has been calculated, a preliminary complexity comparison and analysis have been carried out in terms of the maximum number of iterations and edges inside the decoding process. The results show that the benefit of MPCGC can be exploited without significant additional complexity.

**Chapter four** has proposed a novel punctured MPCGC scheme evaluated over AWGN and flat Rayleigh fading channels. The puncturing process enabled to maximize the code rate and reduced the decoding complexity of the system.

It is also concluded that MPCGCs scheme provides superior coding structure with and without puncturing compared to the original conventional LDPC codes the same parameters.

Three types of punctured MPCGC have been presented and it has been shown that irregular puncturing provides better performance than regular and random puncturing. In addition, the efficient proposed punctured MPCGC has less decoding complexity analysis in terms of a number of iterations and edges compared to the conventional MPCGC structure. The advantage of reducing decoding complexity by reducing the required memory for decoding than that of conventional single LDPC. The proposed punctured MPCGC codes have the ability to be attractive in flexible applications while enhancing coding characteristics with less implementations overheads.

**Chapter five** has presented a novel MPCGC-WiMAX system based on the IEEE 802.16 standard. The proposed well designed MPCGC-WiMAX was based on standard BPSK modulation over AWGN and flat Rayleigh fading channels. The proposed MPCGC-WiMAX has been shown to achieve 0.3 dB improvement over an LDPC-WiMAX with the same parameter. The MPCGC-WiMAX can use the irregular puncturing scheme proposed to enhance and maximize the code rate to be compatible with standard WiMAX system.

**Finally**, chapter six has presented a novel application of QC-LDPC with MPCGC to reduce the decoding complexity and also improve overall system performance. The novel proposed QC-MPCGC is based on combining two Gallager codes and one QC-LDPC code with specific MCW design to enhance the BER performance compared to the conventional LDPC codes at the same parameters.

The proposed QC-MPCGC outperforms the equivalent single irregular LDPC by 0.7 dB with the same parameters. Moreover, the QC-MPCGC performance has a gain of 0.2 dB improvement compared to the Kim et al. reported conventional method with the same parameter.

The main advantage of the proposed QC-MPCGC design is that it has less complexity in terms of iterations and edges of the decoding process compared with the conventional powerful MPCGC. In addition, a Layered BP decoder was incorporated in QC-MPCGC instead of the sum product algorithm (SPA), the result shows that Layered BP QC-MPCGC has less decoding complexity compared with the conventional MPCGC with a trade-off in BER performance.

The MIMO technique was shown to enhance the MPCGC performance over a fading channel with both a 2X2 MIMO and 2X4 MIMO configurations.

To sum up, the MPCGCs are suitable for future wireless applications due to their good performance with higher capacity alongside reduced encoding and decoding complexity. MPCGCs structure is especially attractive for applications where flexibility in forward error control coding is required without significant added complexity.

### 7.2 Future work

There is a recommendation of MPCGC to be further researched so that their potential usage is completely explored alongside the work presented in this thesis. As comparable binary LDPC codes were demonstrated to be outperformed by LDPC codes, the idea of investigating MPCGCs based on non-binary  $GF(q)$  LDPC component codes would be of interest.

Another potential area of research is further investigation of other component codes concatenation by combined the convolutional codes or BCH codes with the concatenation of LDPC codes. There can be the implementation of various combinations of different code rates to match specific applications requirements. The decoding algorithm which is most widely used for LDPC does is the sum-product algorithm, as suggested by Gallager. Nevertheless, reduced complexity implementation of the decoding algorithm through parallel implementation techniques and log-domain arithmetic implementations is the focus of recent research. The investigation of how MPCGCs perform under such alternative decoding algorithm implementations would be of great interest.

The performance of the MPCGC is greatly influenced by the interleaver design in turbo codes. A square identity matrix having randomly permuted columns as per the interleaver sequence can be used to visualize the interleaver. The investigation of the use of a randomly generated rate 1/2 LDPC code as an interleaver between the two component encoders would be of great interest. The input to the next component encoder would be formed by the parity part of the generated LDPC codeword.

Efficient modification to the MPCGC by using only single LDPC component with mean column weight (MCW)  $\geq 2.5$  but the parity bits of the encoder are send it triple times. This procedure enhances the BER performance and reducing the decoding complexity [52][65][124].

Punctured MPCGCs can be further investigated by adding a dummy data before encoding to control on the compatible code rate then remove it later which will make a code rate compatible and enhance the system performance with reduced decoding complexity.

Enhancing the MPCGC-WiMAX application, since the investigation of the performance evaluation was being conducted for perfect CSI at the receiver, the performance analysis supposed that the channel parameters are well known at the receiver. This thesis does not cover the channel estimation practices for MIMO-WiMAX in realistic mobile environments. In addition, thought-provoking outcomes could be achieved by carrying out an investigation of these codes in circumstances where perfect CSI is unavailable.

The hardware implementation of VLSI decoder architecture for MPCGC can be potential research to evaluate and enhance the capacity achieved. The potential proposed architecture is based on the quasi-cyclic (QC-LDPC) codes whose circulant permutation matrix which provide a good performance compared with that of randomly LDPC codes for small to moderate block length [125][126].

A spatially coupled of LDPC code can be incorporated with MIMO-OFDM-SC-MPCGC to enhance the system performance and increased the capacity achieved. Spatially coupled (SC) LDPC codes are based on the construction of convolutional codes. Moreover, the SC-QC-LDPC codes can provide high capacity with reduced decoding complexity [127-129].

The using of MPCGC based on binary LDPC codes needs to be extended to the nonbinary LDPC codes due to their flexibility to cover more enhancing the system performance.

Efficient MPCGC coding performance can be achieved by proposing optimized FFT based on q-ary SPA decoding for (NB-LDPC) component codes with flooding and layered schedules. The (NB-LDPC) are linear block codes provide excellent error correcting codes compared to the binary LDPC codes at the same parameter. High throughput with excellent performance can be achieved from the proposed model [130][131].

## Appendix A

### Signal to noise ratio calculation

The signal to noise ratio in the received samples is defined as:

$$SNR = 10 \log_{10}\left(\frac{2E_b}{N_0}\right) \quad (A_1)$$

Where  $E_b$  is the average energy per transmitted bit, and  $N_0/2$  is the two-sided power spectral density of the additive white Gaussian noise.

The average transmitted energy per bit is given by:

$$E_b = \frac{1}{b} \quad (A_2)$$

Where  $b$  is the number of bits used in the encoding process to produce each of the symbols.

The variance in the real parts of noise samples in the received samples is given by:

$$\sigma^2 = \frac{N_0}{2} \quad (A_3)$$

From equations  $A_1$  to  $A_3$ , the signal to noise ratio (measured in dB) is taken to be:

$$SNR = 10 \log_{10}\left(\frac{1}{b\sigma^2}\right) \quad (A_4)$$

For BPSK the value of  $1/b=1$ .

The information digits are generated with a uniform distribution, and the real parts of the noise sample are generated as the Gaussian random number generator with zero means and a standard deviation  $\sigma$ .

The Monte Carlo method is used to simulate the SNR calculations against bit error rate (BER). The performance of all systems is determined by calculating the BER (bit error rate) at different SNR [132][133].

$$BER = \frac{\text{Number of erroneous bits}}{\text{Number of transmitted bits}} \quad (A_5)$$

---

## References

- [1] R. G. Gallager, "Low-density parity-check codes," *IRE Trans. Inf. Theory*, vol. IT-8, pp. 21–28, 1962.
- [2] R. Tanner, "A recursive approach to low complexity codes," *IEEE Trans. Inf. Theory*, vol. 27, no. 5, pp. 533–547, 1981.
- [3] C. Berrou, A. Glavieux, and P. Thitimajshima, "Near Shannon limit error-correcting coding and decoding: Turbo-codes. 1," in *Communications, 1993. ICC '93 Geneva. Technical Program, Conference Record, IEEE International Conference on*, 1993, vol. 2, pp. 1064–1070 vol.2.
- [4] D. J. C. MacKay and R. M. Neal, "Near Shannon limit performance of low density parity check codes," *Electron. Lett.*, vol. 32, no. 18, p. 1645-, 1996.
- [5] D. J. C. Mackay, D. J. C. Mackay, R. M. Neal, and R. M. Neal, "Good codes based on very sparse matrices," *Cryptogr. Coding, 5th IMA Conf. (Lecture Notes Comput. Sci. C. Boyd, Ed*, vol. 111, no. 1025, p. 1025pp110-111, 1995.
- [6] H. M. Behairy and M. Benaissa, "Multiple Parallel Concatenated Gallager Codes ( MPCGC ): Code Design and Decoding Techniques," 1995.
- [7] T. Brack *et al.*, "Low Complexity LDPC Code Decoders for Next Generation Standards," in *Proceedings of the Conference on Design, Automation and Test in Europe*, 2007, pp. 331–336.
- [8] S.-Y. Chung, G. D. Forney, T. J. Richardson, and R. Urbanke, "On the design of low-density parity-check codes within 0.0045 dB of the Shannon limit," *IEEE Commun. Lett.*, vol. 5, no. 2, pp. 58–60, 2001.
- [9] S. Lin and D. J. Costello, *Error Control Coding, Second Edition*. Upper Saddle River, NJ, USA: Prentice-Hall, Inc., 2004.
- [10] R. W. Hamming, "Error detecting and error correcting codes," *Bell Labs Tech. J.*, vol. 29, no. 2, pp. 147–160, 1950.
- [11] C. E. SHANNON, "A mathematical theory of communication, Part I, Part II," *Bell Syst. Tech. J.*, vol. 27, pp. 623–656, 1948.
- [12] T. J. Richardson and R. L. Urbanke, "Modern Coding Theory," *Sci. York*, p. 572, 2008.
- [13] T. M. Cover and J. A. Thomas, *Elements of Information Theory 2nd Edition (Wiley Series in Telecommunications and Signal Processing)*, 2nd ed. Wiley-Interscience, 2006.
- [14] J. Liu, "Novel LDPC coding and decoding strategies: design, analysis, and algorithms," University of York, 2012.
- [15] A. F. Molisch, *Wireless communications*, vol. 34. John Wiley & Sons, 2012.
- [16] R. G. Gallager, "Low density parity check codes, Research Monograph series." MIT Press, Cambridge, 1963.
- [17] J. C. Á. Moreira and P. G. Farrell, *Essentials of Error-Control Coding*. Wiley, 2006.
- [18] Y. Kou, S. Lin, and M. P. C. Fossorier, "Low-density parity-check codes based on finite geometries: a rediscovery and new results," *IEEE Trans. Inf. Theory*, vol. 47, no. 7, pp. 2711–2736, 2001.
- [19] J. Xu, L. Chen, I. Djurdjevic, S. Lin, and K. Abdel-Ghaffar, "Construction of Regular and Irregular LDPC Codes: Geometry Decomposition and Masking," *IEEE Trans. Inf. Theory*, vol. 53, no. 1, pp. 121–134, 2007.
- [20] S. J. Johnson and S. R. Weller, "Construction of low-density parity-check codes from Kirkman triple systems," in *Global Telecommunications Conference, 2001. GLOBECOM '01. IEEE*, 2001, vol. 2, pp. 970–974 vol.2.

- [21] M. P. C. Fossorier, "Quasicyclic low-density parity-check codes from circulant permutation matrices," *IEEE Trans. Inf. Theory*, vol. 50, no. 8, pp. 1788–1793, 2004.
- [22] R. G. Gallager, "Low-density parity-check codes," *IRE Trans. Information Theory*, vol. IT-8, pp. 21–28, 1962.
- [23] S. Myung, K. Yang, and J. Kim, "Quasi-cyclic LDPC codes for fast encoding," *IEEE Trans. Inf. Theory*, vol. 51, no. 8, pp. 2894–2901, 2005.
- [24] H. Fujita and K. Sakaniwa, "Some Classes of Quasi-Cyclic LDPC Codes: Properties and Efficient Encoding Method\* This paper was presented in part at the 26th Symposium on Information Theory and Its Applications, Higashiura, Hyogo, Japan, December 15--18," in *2003 and at IEEE International Symposium on Information Theory, Chicago, IL USA, June*, pp. 3627–3635.
- [25] L. Lan, L. Zeng, Y. Y. Tai, L. Chen, S. Lin, and K. Abdel-Ghaffar, "Construction of quasi-cyclic LDPC codes for AWGN and binary erasure channels: A finite field approach," *IEEE Trans. Inf. Theory*, vol. 53, no. 7, pp. 2429–2458, 2007.
- [26] L. Chen, J. Xu, I. Djurdjevic, and S. Lin, "Near-Shannon-limit quasi-cyclic low-density parity-check codes," *IEEE Trans. Commun.*, vol. 52, no. 7, pp. 1038–1042, 2004.
- [27] Y. Kou, S. Lin, and M. P. C. Fossorier, "Low density parity check codes based on finite geometries: a rediscovery," in *Information Theory, 2000. Proceedings. IEEE International Symposium on*, 2000, p. 200.
- [28] K. D. Rao, *Channel coding techniques for wireless communications*. Springer, 2015.
- [29] A. C. Al Ghouwayel, A. Nasser, H. Hijazi, and A. Alaeddine, "Simplified representation of the LLR messages in the check node processor for NB-LDPC decoder," in *Microelectronics (ICM), 2013 25th International Conference on*, 2013, pp. 1–4.
- [30] V. A. Chandrasetty and S. M. Aziz, "A reduced complexity message passing algorithm with improved performance for LDPC decoding," in *Computers and Information Technology, 2009. ICCIT'09. 12th International Conference on*, 2009, pp. 19–24.
- [31] A. Anastopoulos, "A comparison between the sum-product and the min-sum iterative detection algorithms based on density evolution," in *Global Telecommunications Conference, 2001. GLOBECOM'01. IEEE*, 2001, vol. 2, pp. 1021–1025.
- [32] S. Ten Brink, "Convergence behavior of iteratively decoded parallel concatenated codes," *IEEE Trans. Commun.*, vol. 49, no. 10, pp. 1727–1737, 2001.
- [33] T. J. Richardson, M. A. Shokrollahi, and R. L. Urbanke, "Design of capacity-approaching irregular low-density parity-check codes," *IEEE Trans. Inf. Theory*, vol. 47, no. 2, pp. 619–637, 2001.
- [34] M. G. Luby, M. Mitzenmacher, M. A. Shokrollahi, and D. A. Spielman, "Improved low-density parity-check codes using irregular graphs," *IEEE Trans. Inf. Theory*, vol. 47, no. 2, pp. 585–598, 2001.
- [35] R. Paul, S. Lally, and L. Trajkovic, "Simulation and performance evaluation of WiFi and WiMAX using OPNET," 2011.
- [36] M. Weiss, "WiMAX general information about the standard 802.16," *Rohde Schwarz Appl. Note, Munich, Ger.*, 2006.
- [37] S. Song and B. Issac, "Analysis of Wifi and Wimax and Wireless Network Coexistence," *arXiv Prepr. arXiv1412.0721*, 2014.
- [38] G. Ofori-Dwumfuo and S. Salakpi, "WiFi and WiMAX deployment at the Ghana Ministry of Food and Agriculture," *Res. J. Appl. Sci.*, vol. 3, 2011.
- [39] B. Tahir, S. Schwarz, and M. Rupp, "BER comparison between Convolutional, Turbo,

- LDPC, and Polar codes,” in *Telecommunications (ICT), 2017 24th International Conference on*, 2017, pp. 1–7.
- [40] K. Singh and R. Talwar, “MIMO-OFDM in Rayleigh Fading Channel with LDPC,” *Eur. J. Adv. Eng. Technol.*, vol. 1, no. 1, pp. 54–60, 2014.
- [41] P. Dambacher, “COFDM combined encoder modulation for digital broadcasting sound and video with PSK, PSK/AM, and QAM techniques.” Google Patents, 1996.
- [42] G. Tsoulos, *MIMO system technology for wireless communications*. CRC press, 2006.
- [43] A. Goldsmith, *Wireless communications*. Cambridge university press, 2005.
- [44] S. A. Joshi, T. S. Rukmini, and H. M. Mahesh, “Performance analysis of MIMO technology using V-BLAST technique for different linear detectors in a slow fading channel,” in *Computational Intelligence and Computing Research (ICCIC), 2010 IEEE International Conference on*, 2010, pp. 1–4.
- [45] B. Ahmed, M. A. Matin, and others, *Coding for MIMO-OFDM in future wireless systems*. Springer, 2015.
- [46] C. Berrou, A. Glavieux, and P. Thitimajshima, “Near Shannon Limit Error - Correcting Coding and Decoding: Turbo-Codes (1),” *Commun. 1993. ICC '93 Geneva. Tech. Program, Conf. Rec. IEEE Int. Conf.*, vol. 2, no. 1, pp. 1064–1070, 1993.
- [47] D. J. C. MacKay and R. M. Neal, “Near Shannon limit performance of low density parity check codes,” *Electron. Lett.*, vol. 33, no. 6, p. 457, 1997.
- [48] H. Behairy and S. C. Chang, “Parallel concatenated Gallager codes,” *Electron. Lett.*, vol. 36, no. 24, pp. 2025–2026, 2000.
- [49] S. ten Brink and G. Kramer, “Design of repeat-accumulate codes for iterative detection and decoding,” *IEEE Trans. Signal Process.*, vol. 51, no. 11, pp. 2764–2772, 2003.
- [50] A. Abbasfar, D. Divsalar, and K. Yao, “Accumulate repeat accumulate codes,” in *Information Theory, 2004. ISIT 2004. Proceedings. International Symposium on*, 2004, p. 505.
- [51] G. Yue, X. Wang, and M. Madhian, “Design of rate-compatible irregular repeat accumulate codes,” *IEEE Trans. Commun.*, vol. 55, no. 6, pp. 1153–1163, 2007.
- [52] R. P. Kumar and R. S. Kshetrimayum, “An efficient methodology for parallel concatenation of LDPC codes with reduced complexity and decoding delay,” *2013 Natl. Conf. Commun.*, pp. 1–5, Feb. 2013.
- [53] C. Condo, “Concatenated turbo/LDPC codes for deep space communications: performance and implementation,” 2013.
- [54] D. Morero and M. Hueda, “Novel serial code concatenation strategies for error floor mitigation of low-density parity-check and turbo product codes,” *Can. J. Electr. Comput. Eng.*, vol. 36, no. 2, pp. 52–59, 2013.
- [55] H. Futaki and T. Ohtsuki, “Low-density parity-check (LDPC) coded MIMO systems with iterative turbo decoding,” in *Vehicular Technology Conference, 2003. VTC 2003-Fall. 2003 IEEE 58th*, 2003, vol. 1, pp. 342–346.
- [56] J. C. Serrato and T. O’Farrell, “Structured Parallel Concatenated LDPC Codes,” in *Proceedings of London Communication Symposium (LCS2006)*, 2006.
- [57] H. M. Behairy and M. Benaissa, “Multiple parallel concatenated gallager codes: Code design and decoding techniques,” *IETE J. Res.*, vol. 59, no. 6, pp. 659–664, 2013.
- [58] B. Oudjani, H. Tebbikh, and N. Doghmane, “Modification of extrinsic information for parallel concatenated Gallager/Convolutional code to improve performance/complexity trade-offs,” *AEU-International J. Electron. Commun.*, vol. 83, pp. 484–491, 2017.
- [59] G. P. Aswathy and N. K. Haneefa, “Non zero syndrome parallel concatenated gallager

- codes,” in *Circuit, Power and Computing Technologies (ICCPCT), 2017 International Conference on*, 2017, pp. 1–6.
- [60] G. D. Forney, “Concatenated Codes, Cambridge, Massachusetts.” USA: MIT Press, 1966.
- [61] D. J. C. MacKay, “Good error-correcting codes based on very sparse matrices,” *IEEE Trans. Inf. Theory*, vol. 45, no. 2, pp. 399–431, 1999.
- [62] H. Behairy and S.-C. Chang, “On the design, simulation and analysis of parallel concatenated Gallager codes,” in *Communications, 2002. ICC 2002. IEEE International Conference on*, 2002, vol. 3, pp. 1850–1854.
- [63] H. Behairy, S. Chang, and A. T. Encoder, “On the Design , Simulation and Analysis of Parallel Concatenated Gallager Codes,” pp. 1850–1854, 2002.
- [64] W. Ryan and S. Lin, *Channel codes: classical and modern*. Cambridge University Press, 2009.
- [65] S. J. Johnson, “Introducing Low-Density Parity-Check Codes.”
- [66] V. Branka and Y. Jinhong, “Turbo Codes: Principles and Applications.” Kluwer Academic Publisher, Boston, 2000.
- [67] D. Fan, “Multiple Parallel Concatenated Gallager Codes: High Throughput Architecture Design and Implementation,” University of Sheffield, 2016.
- [68] D. Divsalar, S. Dolinar, and F. Pollara, “Iterative turbo decoder analysis based on density evolution,” *IEEE J. Sel. areas Commun.*, vol. 19, no. 5, pp. 891–907, 2001.
- [69] M. Ardakani, “Efficient Analysis, Design and Decoding of Low-Density Parity-Check Codes//Ph. D. dissertation, University of Toronto, 2004.,” 2004.
- [70] K. S. Kim, S. H. Lee, Y. H. Kim, and J. Y. Ahn, “Design of binary LDPC code using cyclic shift matrices,” *Electron. Lett.*, vol. 40, no. 5, pp. 325–326, 2004.
- [71] H. M. Behairy, “Parallel concatenated gallager codes and their applications in CDMA wireless networks.”
- [72] H. Pishro-Nik and F. Fekri, “Results on punctured low-density parity-check codes and improved iterative decoding techniques,” *IEEE Trans. Inf. Theory*, vol. 53, no. 2, pp. 599–614, 2007.
- [73] H. Y. Park, J. W. Kang, K. S. Kim, and K. C. Whang, “Efficient puncturing method for rate-compatible low-density parity-check codes,” *IEEE Trans. Wirel. Commun.*, vol. 6, no. 11, 2007.
- [74] H. Pishro-Nik and F. Fekri, “Results on punctured LDPC codes,” *Inf. Theory Work.*, pp. 215–219, 2004.
- [75] D. G. M. Mitchell, M. Lentmaier, A. E. Pusane, and D. J. Costello, “Approximating decoding thresholds of punctured LDPC code ensembles on the AWGN channel,” in *Information Theory (ISIT), 2015 IEEE International Symposium on*, 2015, pp. 421–425.
- [76] J. Ha and S. W. McLaughlin, “Optimal puncturing of irregular low-density parity-check codes,” in *Communications, 2003. ICC’03. IEEE International Conference on*, 2003, vol. 5, pp. 3110–3114.
- [77] I. Sason and G. Wiechman, “On achievable rates and complexity of LDPC codes for parallel channels with application to puncturing,” *arXiv Prepr. cs/0508072*, 2005.
- [78] I. Sason and G. Wiechman, “On Achievable Rates and Complexity of LDPC Codes for Parallel Channels: Information-Theoretic Bounds and Applications,” in *Information Theory, 2006 IEEE International Symposium on*, 2006, pp. 406–410.
- [79] J. Hagenauer, “Rate-compatible punctured convolutional codes (RCPC codes) and their applications,” *IEEE Trans. Commun.*, vol. 36, no. 4, pp. 389–400, 1988.
- [80] K. ElMahgoub and M. Nafie, “Symbol based log-map in concatenated LDPC-

- convolutional codes,” in *Consumer Communications and Networking Conference (CCNC), 2010 7th IEEE*, 2010, pp. 1–4.
- [81] P. Matthias, “Mobile fading channels: modelling, analysis & simulation.” S. 1.]= John Wiley, 2002.
- [82] M. K. Simon and M.-S. Alouini, *Digital communication over fading channels*, vol. 95. John Wiley & Sons, 2005.
- [83] U. D. Dalal and Y. P. Kosta, “Adaptive Parameters Based Transmission Control and Optimization in Mobile WiMAX at Physical Layer,” in *WiMAX New Developments*, InTech, 2009.
- [84] B. P. Salmon and J. C. Olivier, “Performance analysis of low density parity-check codes on a WiMAX platform,” in *Wireless Communications and Networking Conference, 2007. WCNC 2007. IEEE*, 2007, pp. 569–571.
- [85] M. Samsuzzaman, M. S. Uddin, T. Islam, S. Bappi, and S. Sulaiman, “Comparison Wimax and other technology for broad band wireless access (Bwa),” *Aust. J. Basic Appl. Sci.*, vol. 6, no. 9, pp. 605–615, 2012.
- [86] A. R. Shankar, N. Kumari, D. Bhagat, P. Raddy, and others, “Analysis of Mobile WiMAX 802.16 e Physical Layer Performance for Multimedia Communication,” in *IJCA Special Issue on International Conference on Electronic Design and Signal Processing*, 2013, no. 2, pp. 32–35.
- [87] Y. Zhang, *WiMAX network planning and optimization*. CRC Press, 2009.
- [88] K. Lu, Y. Qian, H.-H. Chen, and S. Fu, “WiMAX networks: from access to service platform,” *IEEE Netw.*, vol. 22, no. 3, 2008.
- [89] L. Liang, H. Peng, G. Y. Li, and X. Shen, “Vehicular communications: A physical layer perspective,” *IEEE Trans. Veh. Technol.*, vol. 66, no. 12, pp. 10647–10659, 2017.
- [90] F. Wang, A. Ghosh, C. Sankaran, and P. Fleming, “WiMAX overview and system performance,” in *Vehicular Technology Conference, 2006. VTC-2006 Fall. 2006 IEEE 64th*, 2006, pp. 1–5.
- [91] N. T. Awon, M. Islam, M. Rahman, A. Z. M. Islam, and others, “Effect of AWGN & Fading (Rayleigh & Rician) channels on BER performance of a WiMAX communication System,” *arXiv Prepr. arXiv1211.4294*, 2012.
- [92] M. A. Hasan and others, “Performance evaluation of WiMAX/IEEE 802.16 OFDM physical layer,” 2007.
- [93] L. Korowajczuk, *LTE, WiMAX and WLAN network design, optimization and performance analysis*. John Wiley & Sons, 2011.
- [94] K. H. Teo, Z. Tao, and J. Zhang, “The mobile broadband WiMAX standard [standards in a nutshell],” *IEEE Signal Process. Mag.*, vol. 24, no. 5, pp. 144–148, 2007.
- [95] R. Orzechowski, “Performance Analysis of LDPC Coded OFDM System,” in *XIV Poznań Telecommunications Workshop--PWT 2010*, pp. 50–53.
- [96] Y. Sun and J. R. Cavallaro, “A flexible LDPC/turbo decoder architecture,” *J. Signal Process. Syst.*, vol. 64, no. 1, pp. 1–16, 2011.
- [97] X.-M. Wang, Y. Zhang, J. Fu, and Y. Wang, “Design and implementation of WIMAX LDPC code decoder based on FPGA,” *J. Dalian Univ. Technol.*, vol. 52, no. 4, pp. 594–598, 2012.
- [98] T. Ferrett and M. C. Valenti, “LDPC code design for noncoherent physical layer network coding,” in *Communications (ICC), 2015 IEEE International Conference on*, 2015, pp. 2054–2059.
- [99] M. WiMAX-Part, “I: A technical overview and performance evaluation,” in *WiMAX forum*, 2006, vol. 1, no. 7.

- [100] K. Elmahgoub and M. Nafie, "On the Enhancement of LDPC Codes Used in WiMAX," no. 4, pp. 19–24, 2011.
- [101] M. Daud, A. B. Suksmono, and others, "Comparison of decoding algorithms for LDPC codes of IEEE 802.16 e standard," in *Telecommunication Systems, Services, and Applications (TSSA), 2011 6th International Conference on*, 2011, pp. 280–283.
- [102] B. Sahoo, R. R. Prasad, and P. Samundiswary, "BER Analysis of Mobile WiMAX System using LDPC Coding and MIMO System under Rayleigh Channel," pp. 514–518, 2013.
- [103] Y. S. Cho, J. Kim, W. Y. Yang, and C. G. Kang, *MIMO-OFDM wireless communications with MATLAB*. John Wiley & Sons, 2010.
- [104] M. A. Kadhim and W. Ismail, "Implementation of WIMAX IEEE 802.16 e Baseband Transceiver on Multi-Core Software Defined Radio Platform," *Int. J. Comput. Theory Eng.*, vol. 2, no. 5, p. 820, 2010.
- [105] T. B. Iliev, G. V. Hristov, P. Z. Zahariev, and M. P. Iliev, "Application and evaluation of the LDPC codes for the next generation communication systems," in *Novel Algorithms and Techniques In Telecommunications, Automation and Industrial Electronics*, Springer, 2008, pp. 532–536.
- [106] Y.-C. He, S.-H. Sun, and X.-M. Wang, "Fast decoding of LDPC codes using quantisation," *Electron. Lett.*, vol. 38, no. 4, pp. 189–190, 2002.
- [107] H. Fujita and K. Sakaniwa, "Some classes of quasi-cyclic LDPC codes: Properties and efficient encoding method," *IEICE Trans. Fundam. Electron. Commun. Comput. Sci.*, vol. 88, no. 12, pp. 3627–3635, 2005.
- [108] Y. Dai, Z. Yan, and N. Chen, "Optimal overlapped message passing decoding of quasi-cyclic LDPC codes," *IEEE Trans. Very Large Scale Integr. Syst.*, vol. 16, no. 5, pp. 565–578, 2008.
- [109] B. K. Butler, "Minimum Distances of the QC-LDPC Codes in IEEE 802 Communication Standards," *arXiv Prepr. arXiv/1602.02831*, 2016.
- [110] B. Zhou, J. Kang, S. W. Song, S. Lin, K. Abdel-Ghaffar, and M. Xu, "Construction of non-binary quasi-cyclic LDPC codes by arrays and array dispersions-[transactions papers]," *IEEE Trans. Commun.*, vol. 57, no. 6, 2009.
- [111] M. Cheema and S. A. Kulkarni, "Analysis of MIMO OFDM Based WiMAX system with LDPC," in *Advances in Computing and Communications (ICACC), 2015 Fifth International Conference on*, 2015, pp. 223–226.
- [112] M. Bakhmutsky, "Multi-code-book variable length decoder." Google Patents, 1997.
- [113] P. H. Tan and L. K. Rasmussen, "Belief propagation for coded multiuser detection," in *Information Theory, 2006 IEEE International Symposium on*, 2006, pp. 1919–1923.
- [114] D.-S. Shin, "Iterative decoding for layered space-time codes," in *Communications, 2000. ICC 2000. 2000 IEEE International Conference on*, 2000, vol. 1, pp. 297–301.
- [115] J. Zhang and M. Fossorier, "Shuffled belief propagation decoding," in *Signals, Systems and Computers, 2002. Conference Record of the Thirty-Sixth Asilomar Conference on*, 2002, vol. 1, pp. 8–15.
- [116] R. Wesel, M.-C. F. Chang, Y.-M. Chang, and A. I. V. Casado, "Lower-complexity layered belief propagation decoding LDPC codes." Google Patents, 2013.
- [117] D. E. Hocevar, "A reduced complexity decoder architecture via layered decoding of LDPC codes," in *Signal Processing Systems, 2004. SIPS 2004. IEEE Workshop on*, 2004, pp. 107–112.
- [118] T. Deepa and R. Kumar, "Performance evaluation of LDPC coded MIMO transceiver with equalization," in *Recent Trends in Information Technology (ICRTIT), 2013 International Conference on*, 2013, pp. 147–151.

- [119] A. G. D. Uchoa, C. T. Healy, and R. C. de Lamare, "Iterative detection and decoding algorithms for MIMO systems in block-fading channels using LDPC codes," *IEEE Trans. Veh. Technol.*, vol. 65, no. 4, pp. 2735–2741, 2016.
- [120] X. Zhang and S.-Y. Kung, "Capacity analysis for parallel and sequential MIMO equalizers," *IEEE Trans. Signal Process.*, vol. 51, no. 11, pp. 2989–3002, 2003.
- [121] W. Ullah, Y. Fengfan, and A. Yahya, "QC LDPC Codes for MIMO and Cooperative Networks using Two Way Normalized Min-Sum Decoding," *Indones. J. Electr. Eng. Comput. Sci.*, vol. 12, no. 7, pp. 5448–5457, 2014.
- [122] M. P. C. Fossorier, M. Mihaljevic, and H. Imai, "Reduced complexity iterative decoding of low-density parity check codes based on belief propagation," *IEEE Trans. Commun.*, vol. 47, no. 5, pp. 673–680, 1999.
- [123] L. XI, X. ZHAO, and K. Wang, "VLSI decoding design of low-density parity-check codes based on circulant matrices," *J. Zhejiang Univ. (Engineering Sci.)*, vol. 2, p. 14, 2009.
- [124] G. P. Aswathy and N. K. Haneefa, "Efficient implementation of parallel concatenated gallager codes with single encoder," in *Communication Systems and Networks (ComNet), International Conference on*, 2016, pp. 39–43.
- [125] M. Beermann, T. Breddermann, and P. Vary, "Rate-compatible LDPC codes using optimized dummy bit insertion," in *Wireless Communication Systems (ISWCS), 2011 8th International Symposium on*, 2011, pp. 447–451.
- [126] Y. Sun, M. Karkooti, and J. R. Cavallaro, "VLSI decoder architecture for high throughput, variable block-size and multi-rate LDPC codes," in *Circuits and Systems, 2007. ISCAS 2007. IEEE International Symposium on*, 2007, pp. 2104–2107.
- [127] M. Hagiwara, K. Kasai, H. Imai, and K. Sakaniwa, "Spatially coupled quasi-cyclic quantum LDPC codes," in *Information Theory Proceedings (ISIT), 2011 IEEE International Symposium on*, 2011, pp. 638–642.
- [128] B. Lu, G. Yue, and X. Wang, "Performance analysis and design optimization of LDPC-coded MIMO OFDM systems," *IEEE Trans. Signal Process.*, vol. 52, no. 2, pp. 348–361, 2004.
- [129] S. Kudekar, T. J. Richardson, and R. L. Urbanke, "Threshold saturation via spatial coupling: Why convolutional LDPC ensembles perform so well over the BEC," *IEEE Trans. Inf. Theory*, vol. 57, no. 2, pp. 803–834, 2011.
- [130] Z. Liu, R. Liu, Y. Hou, H. Peng, and L. Zhao, "Efficient GPU-based implementation for decoding non-binary LDPC codes with layered and flooding schedules," *Concurr. Comput. Pract. Exp.*
- [131] M. C. Davey and D. MacKay, "Low-density parity check codes over GF (q)," *IEEE Commun. Lett.*, vol. 2, no. 6, pp. 165–167, 1998.
- [132] L. Dong, W. Wenbo, and L. Yonghua, "Monte Carlo simulation with error classification for multipath Rayleigh Fading channel," in *Telecommunications, 2009. ICT'09. International Conference on*, 2009, pp. 223–227.
- [133] C. M. Collins, "Fundamentals of Signal-to-Noise Ratio (SNR)," *Electromagn. Magn. Reson. Imaging Phys. Princ. Relat. Appl. Ongoing Dev.*, 2016.